Distribution Agreement

In presenting this thesis or dissertation as a partial fulfillment of the requirements for an advanced degree from Emory University, I hereby grant to Emory University and its agents the non-exclusive license to archive, make accessible, and display my thesis or dissertation in whole or in part in all forms of media, now or hereafter known, including display on the world wide web. I understand that I may select some access restrictions as part of the online submission of this thesis or dissertation. I retain all ownership rights to the copyright of this thesis or dissertation. I also retain the right to use in future works (such as articles or books) all or part of this thesis or dissertation.

Signature:

_____ _____

Nicolle Baird Date

Influenza virus reassortment in the absence of segment mismatch

By

Nicolle Baird
Doctor of Philosophy

Graduate Division of Biological and Biomedical Sciences
Microbiology and Molecular Genetics

_____
Anice Lowen, Ph.D.
Advisor

_____
Richard Compans, Ph.D.
Committee Member

_____
Jackie Katz, Ph.D.
Committee Member

_____
Sam Speck, Ph.D.
Committee Member

_____
John Steel, Ph.D.
Committee Member

_____
Dave Steinhauer, Ph.D.
Committee Member

Accepted:

_____
Lisa A. Tedesco, Ph.D.
Dean of the James T. Laney School of Graduate Studies

_____

Date

Influenza virus reassortment in the absence of segment mismatch

By

Nicolle Baird
B.S., West Virginia University, 2008

Advisor: Anice Lowen, Ph.D.

An abstract of
A dissertation submitted to the Faculty of the
James T. Laney School of Graduate Studies of Emory University
in partial fulfillment of the requirements for the degree of
Doctor of Philosophy
in Microbiology and Molecular Genetics
2015

Abstract

Influenza virus reassortment in the absence of segment mismatch
By Nicolle Baird

Influenza A virus (IAV) carries an eight-segmented genome which allows for reassortment when two different strains co-infect the same cell. Reassortment can lead to the generation of novel IAV, contributing to the development of epidemics and pandemics. A better understanding of the conditions that favor reassortment in nature would aid the development of public health measures aimed at limiting the impact of emerging IAV. It has been previously shown that reassortment is restricted by segment mismatch, including functional incompatibilities at the RNA or protein level. Due to this potent effect, additional factors that affect reassortment efficiency have been difficult to characterize. To study IAV reassortment in the absence of genetic incompatibilities, we have developed a system in which parental and progeny virus are of equal fitness, eliminating selection bias. A pair of phenotypically identical, yet genetically different viruses was generated using influenza A/Panama/2007/99 (H3N2) virus. Silent mutations introduced into each of the eight gene segments allowed our variant (var) virus to be differentiated from the wild-type virus by high resolution melt analysis. Using this system, we determined baseline frequencies of reassortment in cell culture and *in-vivo*. We further evaluated the effects of dosage, time and defective particles on this baseline frequency. The potential for reassortment declined quickly with increasing time intervals between two infections. Our results show that this effect is due to super-infection interference, which results from removal of sialic acids from the host cell surface by the viral neuraminidase and induction of interferon responses by the host cell. We demonstrated, using both computational and experimental methods, that semi-infectious (SI) particles promote diversification through reassortment. The introduction of defective interfering (DI) particles, by contrast, was found to potently suppress detectable reassortment, most likely due to the known interfering effects of segments carrying large deletions. These data suggest that semi-infectious, but not defective-interfering, particles may accelerate the evolution of IAV. Taken together, the work described has established a powerful new method for studying reassortment and exploited this method to reveal novel insights in to the potential for reassortment to occur within a cell and within an intact host.

Influenza virus reassortment in the absence of segment mismatch

By

Nicolle Baird
B.S., West Virginia University, 2008

Advisor: Anice Lowen, Ph.D.

A dissertation submitted to the Faculty of the
James T. Laney School of Graduate Studies of Emory University
in partial fulfillment of the requirements for the degree of
Doctor of Philosophy
in Microbiology and Molecular Genetics
2015

Table of Contents

Abstract

Table of Contents

List of Figures and Tables

Chapter 1: Introduction **1**

Organization and Classification of Influenza A Viruses 1

Influenza A Virus Life Cycle 2

Influenza A Virus Natural and Model Hosts 5

Human Influenza Disease 7

Influenza A Virus Epidemiology 8

Influenza A Virus Transmission 12

Influenza A Virus Evolution 13

Introduction to Thesis Project 18

Chapter 2: Influenza virus reassortment occurs with high frequency in the absence of segment mismatch **20**

Abstract 21

Introduction 22

Results 25

Discussion 31

Materials and Methods 37

References 45

Figure Legend 50

Tables and Figures 53

Chapter3: Influenza virus reassortment is enhanced by semi-infectious particles but can be suppressed by defective interfering particles **62**

Abstract 63

Introduction 64

Results 68

Discussion 83

Materials and Methods 89

References 103

Figure Legends 108

Tables and Figures 115

Chapter 4: Mechanisms of influenza A virus super-infection interference 130

Abstract 131

Introduction 132

Materials and Methods 134

Results 141

Figure Legends 145

Figures 148

Discussion 154

References 158

Chapter 5: Discussion 162

References 166

List of Figures and Tables

Chapter 2: Influenza virus reassortment occurs with high frequency in the absence of segment mismatch

Figure 1. . rPan/99 wt and var viruses show similar growth phenotypes in MDCK cells and guinea pigs.

Figure 2. Identification of wild-type and variant virus gene segments by high resolution melt analysis.

Figure 3. Reassortment in cultured cells is efficient under unbiased conditions.

Figure 4. Frequency of reassortment increases exponentially with frequency of co-infection.

Figure 5. Super-infection delayed by up to 12 h allowed robust co-infection and by up to 8 h allowed robust reassortment in cell culture.

Figure 6. Infections separated by less than 18 h led to robust reassortment in vivo.

Figure 7. Viral spread in cell culture leads to increased frequency of co-infected cells when super-infection is delayed by 8 or 12 hours.

Table 1. The frequency of reassortment in vivo is dependent on inoculum dose

Table 2. Super-infection up to 12 h after primary infection leads to robust reassortment in vivo.

Chapter 3: Influenza virus reassortment is enhanced by semi-infectious particles but can be suppressed by defective interfering particles

Figure 1. Relationships between % infection and % reassortment or % co-infection, as predicted by computational simulation of co-infection with viruses of two types.

Figure 2. Impact on % infection, % co-infection, and % reassortment of introducing semi-infectious particles into the model.

Figure 3. Measurement of HA positive cells, dually HA positive cells and reassortment following co-infection of MDCK cells with Pan/99wt and Pan/99var viruses.

Figure 4. Modeled outcomes do not match the observed relationship between HA positive and dually HA positive cells when P_P is constant among the eight segments.

Figure 5. Varying P_P by segment yields good fit between modeled and observed relationships among HA positive cells, dually HA positive cells and reassortment.

Figure 6. Increasing semi-infectious particle content by UV irradiation of virus stocks augments observed % reassortment.

Figure 7. Results observed with UV treated Pan/99wt and Pan/99var viruses match simulated co-infections in which each virus carries an average of 2.0 UV hits per genome.

Figure 8. Semi-infectious particles increase reassortment at a given MOI by increasing the proportion of infected cells that are co-infected.

Figure 9. Impact on % reassortment of introducing defective interfering particles into the model.

Figure 10. Production of virus stocks with high levels of DI particles: ratio of RNA copy number to PFU increases with serial passage at high MOI.

Figure 11. Virus populations dominated by DI particles give rise to a higher proportion of dually HA positive cells but a lower proportion of reassortant progeny viruses compared to virus populations with low DI content.

Figure 12. Comparison of modeled and experimentally determined relationships among % HA positive cells, % dually HA positive cells and % reassortment.

Figure 13. Theoretical interplay among P_P, P_I and DIX in determining reassortment outcomes.

Table 1. Proportion of polymerase segments intact in P3 and P4 viruses, relative to P0 viruses.

Table 2. Terminology used herein to identify different types of infected cells and virus particles.

Chapter 4: Mechanisms of influenza A virus super-infection interference

Figure 1. Infection with influenza virus inhibits attachment by a second influenza virus ex-vivo.

Figure 2. Treating with bacterial NA is sufficient to markedly reduce infection of MDCK cells.

Figure 3. Super-infection experimental design.

Figure 4. SA receptors remain intact late after infection with NA mutant virus.

Figure 5. Neuraminidase deficient virus elicits incomplete super-infection interference.

Figure 6. A decrease in co-infection correlates temporally with an increase in IFN-β induction.

Chapter 1: Introduction

Organization and Classification of Influenza A Viruses

Influenza A virus (IAV) belongs to the virus family Orthomyxoviridae, which includes six genera: Influenzavirus A, Influenzavirus B, Influenzavirus C, Isavirus, Thogotovirus and Quaranjavirus. Recently a seventh genus was suggested, Influenzavirus D, after the isolation of a novel virus among cattle and swine with 50% homology to Influenza C virus [1]. The principle reservoir for IAV is wild birds, though it can infect and establish lineages within the human, porcine, equine, canine and other mammalian populations. Recently, IAV strains have been identified in bats, suggesting these animals as a possible reservoir, although the strains discovered in bats are highly divergent from those found in avian and other mammalian hosts [2-4].

IAV is an enveloped, eight-segmented, negative sense RNA virus, which encodes a minimum of 10 proteins. IAV is classified into subtypes based on the antigenic differences of the surface glycoproteins: hemagglutinin (HA) and neuraminidase (NA). Presently, there are 18 HA subtypes and 11 NA subtypes, of which H17N10 and H18N11 are exclusive to bats [4,5]. The remaining 16 HA and 9 NA subtypes are all known to circulate within the avian reservoir. Only H1N2, H2N2 and H3N2 viruses have caused pandemics and become established within the human population. In addition, avian IAVs of the subtypes H5N1, H9N2, H7N3, H7N7, H7N9 and H10N8 have crossed species and caused limited zoonotic infections in humans [2, 6, 7].

Influenza A Virus Life Cycle

The influenza virus life cycle begins when the virion attaches to a host cell. The viral HA protein binds sialic acid (SA), which is attached to the penultimate galactose of surface sialyloligosaccharides in one of two different conformations. Each conformation is important in determining the specificity of the HA that can bind in different host species [8, 9]. HA proteins of avian IAVs bind SA attached to galactose by an α-2,3 linkage, which is the primary sialic acid found on epithelial cells in the avian gut. In contrast, HA proteins of human IAVs preferentially bind SA attached to galactose by an α-2,6 linkage. This SA is predominantly found on epithelial cells in the human upper respiratory tract, though α-2,3 SAs have been detected on ciliated epithelial cells in respiratory tract as well. Both α-2,3 and α-2,6 SAs are found in the swine respiratory tract, and as such, these animals are susceptible to infection by both avian and human influenza viruses [10-14].

Following attachment of the virion to host cell SAs, the virion is endocytosed. IAV enters the cell in an endosome via different mechanisms: clathrin-mediated pathways, non-clathrin-mediated pathways and macropinocytosis [15-20].

The endosome traffics toward the nucleus, and along the way, two distinct acidification steps occur. During the first step, occurring in early endosomes, acidification of the viral lumen occurs via the M2 protein, a transmembrane proton channel, resulting in the dissociation of the ribonucleoprotein (RNP) complex from the M1 matrix protein [21, 22]. The second acidification step takes place in late endosomes. Here, a conformational change in the virion-associated HA occurs, exposing the fusion peptide and driving it into

the opposing host cell endosomal membrane. A further conformational change in the HA occurs which then brings the opposing membranes together, forming a stalk. Eventually, the stalk ruptures, becoming a fusion pore, allowing the eight viral ribonucleoprotein (vRNP) segments to disseminate into the cytoplasm [23-26].

Influenza viral transcription and replication occur in the host cell nucleus. Entry of viral RNPs into the nucleus is an active process involving nuclear-localization signals (NLS) on the vRNA-associated nucleoprotein (NP) and the polymerase complex proteins (PB2, PB1, PA) and the importin-mediated pathway [27-30]. Mammalian RNPs require binding of the cellular adapter protein importin-α7 to the NLS for nuclear entry, while avian RNPs depend on importin-α3. The protein-importin-α complex in turn binds to importin-β, which then directs the complex through the nucleopore [27, 31].

Once inside the nucleus, the negative sense vRNAs serve as templates for transcription and replication, carried out by the viral RNA polymerase. Transcription is the predominant process carried out early in the viral life cycle and produces a partial (+) sense copy of the vRNA template (mRNA) that is capped, polyadenylated and translated into viral protein. The accumulation of viral mRNA and protein is necessary for the generation of new virions, however because only a partial (+) sense copy of the vRNA is produced during transcription, a molecular "switch" to replication activity must occur in order to produce the full-length (+) sense copy of vRNA (cRNA) necessary for genomic synthesis [32-34]. Several different mechanisms have been proposed that mediate the switch between transcription and replication [35-38]. A recent study suggests that the switch is triggered by accumulation of small viral RNAs (svRNA) corresponding to the genomic termini. These svRNAs were suggested to interact with the viral polymerase

machinery, allowing for full replication of the genomic ends, though the precise mechanism remains unclear [39].

To initiate transcription, the RNA-dependent RNA polymerase (RdRp), comprised of the PB2, PB1 and PA proteins, is involved in a "cap-snatching" mechanism that provides the necessary primer. The PB2 protein binds the cap on the host pre-mRNA transcripts. The PA protein has endonuclease activity and consequently cleaves the mRNA ~10-13 bases downstream from the 5' cap, while PB1 contains the polymerase activity necessary for activation and elongation of the transcript [40-46]. Transcription continues until the polymerase "stutters" along a string of terminal U sequences, forming a 3' poly-A tail [47,48]. Once transcribed, the mRNA is exported from the nucleus to the cytoplasm, where the host cell translation machinery translates the mRNA into viral proteins. Some of the newly synthesized proteins, specifically NP and the polymerase complex, are transported back into the nucleus through the importin pathway. NP encapsidates developing cRNA and associates with the polymerase complex to form the template for replication of genomic vRNA. Genomic vRNA is then coated with free NP, which associates with the polymerase complex to form a new vRNP complex. As the infection progresses, cytoplasmic M1 and NEP (NS2) proteins enter the nucleus where they bind to vRNPs and transport them through nuclear pore complexes via the Crm1-dependent pathway [21, 32, 33, 49-52]. Exported RNPs interact with the GTP-ase Rab11 on recycling endosomes and are able to move through the cytoplasm to the membrane along the microtubule network using the vesicular transport system [53-56]. Following synthesis in the rough ER, HA, NA and M2 are transported to the apical plasma membrane via the Golgi complex, where HA and NA associate with cholesterol and

sphingolipid-rich lipid rafts and M2 accumulates on the boundaries of lipid rafts. Here, the membrane proteins' cytoplasmic tails bind to the vRNP-associated M1 [51, 57-61]. The HA, NA, M1 and M2 proteins have all been associated with budding; however the precise details of this event are still unclear. M2 facilitates membrane scission of the budding virion and prepares it for release [62-68]. Finally, the receptor-destroying enzyme, NA, cleaves the sialic acids on the surface of the virus and the host cell resulting in the release the progeny virus [69,70].

The IAV life cycle can be interrupted by the host innate immune system to prevent infection and/or dissemination of the virus. The host cell has a variety of pattern recognition receptors (PRRs) that recognize structurally conserved molecules derived from microbes. Of particular importance in IAV infections are the RIG-I-like receptors (RLRs). RIG-I recognizes the 5'-triphosphorylated viral RNA of an incoming influenza virus. Upon ligand binding, RIG-I interacts with the cellular protein, TRIM25, leading to a signaling cascade that results in the induction of type I IFN and interferon stimulating genes (ISGs). Type I IFNs can act in an autocrine and paracrine manner to trigger ISG expression and thereby eliciting a robust innate immune response in infected and surrounding cells, arresting the viral infection at many different stages of the life cycle [71-73].

Influenza A Virus Natural and Model Hosts

Natural Hosts

Wild aquatic birds are the primary, natural reservoir for influenza A viruses, though there is increasing evidence for bats as a reservoir as well [3,4]. Aquatic birds are the source of

all influenza A viruses that have established distinct, persistent lineages in other hosts, such as domestic poultry, swine, horses, dogs and humans [2-4, 74, 75]. In addition to the circulating lineages, IAV has been known to infect other mammals, including seals, whales, tigers, cats, leopards, and mink [76-80].

Animal Models

In-vitro models alone cannot accurately assess the complexity of an influenza virus infection, thus most investigations are supplemented with animal models. Mice are the most common animal model for IAV studies given their low cost, small size, availability, ease of manipulation, and availability of immunological reagents. However, prior adaptation through serial passage is usually necessary for replication of IAV strains in this model, and even when replicating to high titers, IAV does not readily transmit between mice [81-83]. For this reason, other animal models are frequently used to study IAV more effectively.

The ferret was the first animal model devised for the study of influenza virus [84]. They are highly susceptible to several human influenza virus strains without prior adaptation and the virus is readily transmitted between this species [83]. The pattern of viral attachment in the human respiratory tract closely resembles that of the ferret for both human and avian viruses [85]. In addition, upon infection with IAV, the ferret exhibits similar clinical symptoms of infection to those witnessed in humans. Despite these advantages, there are several limitations to using the ferret model, including its limited availability, high cost, and greater husbandry requirements than smaller mammals [83,86].

Guinea pigs are a smaller, more cost effective alternative to the ferret model. They are more commercially available and easier to handle and house than ferrets. In addition, they are susceptible to infection with IAV without prior adaptation, and are highly efficient in transmitting the virus via direct contact and aerosol amongst other guinea pigs. A drawback of using the guinea pig model includes the lack of overt clinical symptoms upon infection, making them a poor model to examine the pathogenicity of IAV infections; however this feature has no effect on reassortment studies. IAV growth is primarily restricted to the upper respiratory tract and therefore nasal washes and nasal turbinate tissues from infected animals generally yield high titers of virus, while virus is usually not found or detected at very low titers in the lower respiratory tract [123-126]. Therefore, viral specimen collection can occur simply by obtaining multiple nasal wash samples, rather than whole tissue and /or organ collection. Similarly, seasonal influenza virus infections in both humans and ferrets are generally limited to the upper respiratory tract, rather than the lower respiratory tract [87-89]. Consequently, the tropism for human seasonal IAVs in guinea pigs seems to correspond well with that in both humans and ferrets. All of the reasons stated above make guinea pigs an ideal animal model for reassortment studies.

Human Influenza Disease

IAV infections are responsible for a significant amount of morbidity and mortality every year in the United States, affecting approximately 5-20% of the population [90]. Human IAV infections present with a respiratory infection that is typically self-limiting, but has the potential to be fatal. Responses can range from asymptomatic to severe viral pneumonia with typical, uncomplicated symptoms including cough, fever, headache, sore

throat, sneezing, congestion and body aches. Symptoms can appear as early as 24h, with the incubation period ranging from 1 to 5 days [91]. For most individuals, the infection wanes after 7-10 days. Severe viral infection can occur if the virus travels to and replicates in the lower respiratory tract, causing pneumonia [92,93].

Disease severity is dependent on a combination of viral and host factors, including: viral virulence, differences in host genetic and immunological background, host immune response and the presence of pre-existing conditions [94,95].

Influenza A Virus Epidemiology

Pandemics

The H1N1 influenza pandemic of 1918 was very severe, killing approximately 50 million people worldwide. Phylogenetic evidence suggests that the virus may have been the product of reassortment between an avian and human H1N1 virus that transmitted within the human population [96]. Typical influenza outbreaks display a "U"-shape mortality curve, exhibiting a higher degree of mortality in the very young and the very old. However, the 1918 pandemic exhibited a "W"-shape mortality curve, reflecting higher mortality rates among young adults, aged about 20-40 years. In fact, this group had 20% higher death rates during the 1918 pandemic than in the previous year [97,98]. Most deaths were the result of pneumonia due to secondary bacterial infections, however mortality due to an abnormal immune response ("cytokine storm") played a significant role as well [99].

The second influenza pandemic of the 20th century, known as the "Asian influenza pandemic", occurred in 1957 with the introduction of a novel H2N2 virus into the human

population. The pandemic virus first emerged in China and was derived from reassortment between the previously circulating human H1N1 virus and an avian H2N2 virus, which contributed its PB1, HA and NA gene segments to the human strain [100]. The mortality rate from this pandemic was significantly less than that of the 1918 pandemic, with the number of influenza-associated deaths estimated at approximately 70,000 people in the United States [101].

In 1968, a novel H3N2 virus emerged in Southeast Asia, initiating the third documented influenza pandemic, the "Hong Kong influenza pandemic". The HA and PB1 segments from an avian H3 subtype virus were introduced into the circulating human H2N2 virus through reassortment [101,102]. Similar to the 1957 pandemic, death rates were significantly lower than those of the 1918 pandemic [101].

In 2009, a novel H1N1 virus emerged in Mexico and quickly circulated in humans, killing approximately 280,000 people globally, producing the most recent influenza pandemic [97, 103]. Interestingly, the emergence of the virus occurred in the spring, a deviation from the typical seasonality associated with influenza viruses [104]. The virus was generated through multiple reassortment events from avian, human and swine viruses: the PB2 and PA genes originated from a North American avian virus, the PB1 from a human H3N2 virus, the HA, NP and NS genes from a classical swine virus and the NA and M genes from a Eurasian avian-like swine virus [97, 105]. The pandemic H1N1 virus became endemic by replacing the previously circulating human seasonal H1N1 virus.

Epidemics

On average, 5-20% of the population in the United States is affected with an influenza virus infection each year, with the highest attack rate seen in young children [106]. The highest transmission rates seem to occur during the winter months, which appears to be due to lower temperature and humidity conditions during this season [107, 108]. Intrinsic viral fitness and host factors, such as the level of pre-existing immunity within the population, affects the spread of IAV. About 50,000-100,000 hospitalizations are estimated each year, with most of those occurring in young children and the elderly [109].

The unusually severe epidemic of 1947 can be attributed to intra-subtype reassortment, in which the A/H1N1 virus acquired novel PB2 and HA genes from a different strain of the same subtype. This virus was so significantly different antigenically from other IAVs, that initially it was difficult to establish it as the cause of the epidemic. Although disease was global, relatively few deaths occurred [102,110]. Similarly, the 1951 influenza epidemic has been connected to intra-subtype reassortment between A/H1N1 viruses [110]. Though the epidemic was not particularly severe in the United States, the death toll in other countries, such as Canada and England, was unusually high [111]. Additionally, intra-subtype reassortment has been documented for the A/H3N2 virus. The A/Fujian/411/2002-like virus that was the source of the influenza epidemic of 2003-2004, was generated through reassortment events between co-circulating Clade A and Clade B H3N2 viruses [112].

Zoonosis

H5N1 subtype highly pathogenic avian influenza (HPAI) viruses have posed a public health threat and socio-economic challenge in Southeast Asia. It is thought that the precursor virus was a low pathogenic avian influenza (LPAI) that was circulating in wild aquatic birds, though the actual origin is unclear [113]. The virus was first detected in poultry in 1996 in China and since has undergone several genetic reassortment events and spread to other countries. This virus has caused repeated human zoonotic infections throughout the area since 2003, resulting 784 human cases with 429 deaths in 16 different countries as of March, 2015 [114]. Infections generally present with cough, fever and pneumonia, leading to respiratory failure, with the highest number of cases reported predominantly in children and young adults [115].

A similar zoonotic infection occurred with the novel LPAI H7N9 virus that first emerged in the spring of 2013, causing rapid human disease and death, with 602 confirmed cases and 227 deaths as of March 2015 [114]. To date, no cases have been identified outside the mainland of China, though possible spread outside this region in the future cannot be excluded. This virus may have evolved from several different origins, including duck, migratory birds and chickens and through several reassortment events [116]. Clinical presentation of H7N9 infection is similar to that for H5N1 infections, however the highest number of cases are predominantly in persons around 58 years of age, with only mild cases reported in children [115, 117].

Influenza A Virus Transmission

Influenza A virus can be transmitted among humans by either contact or respiratory droplet transmission. Contact transmission can occur either by direct contact with another infected individual or by indirect contact with a contaminated object, or fomite. Respiratory droplet transmission occurs through the direct inhalation of respiratory droplets or aerosol droplets from an infected individual, which can be generated through normal breathing, coughing, sneezing and talking. The distinction between respiratory and aerosol droplets is determined by the time that these droplets can remain suspended in air after they are expelled, which in turn is dependent upon the droplet size. Larger droplets (>5-10um) are involved in short-range transmission, as they descend from the air at a faster rate than smaller droplets, or droplet nuclei, (<5um), which are able to spread over greater distances and are therefore capable of airborne transmission [83,108,118]. The size of the particle also determines how efficiently it is deposited in the respiratory tract after inhalation and therefore determines the infection site. Larger particles are trapped predominantly in the upper respiratory tract, while smaller particles have the potential to travel and be deposited in the upper and lower respiratory tracts [118,119]. It has been revealed that environmental conditions influence influenza virus transmission. Cold and dry conditions (temperature = 5˚C with humidity levels between 20-35%) have been shown to be the most favorable for aerosol transmission between infected and naïve guinea pigs. These conditions are in accord with the natural seasonality of influenza virus transmission [107,108].

In addition to the features of human-to-human transmission described above, there are other factors that must be taken into consideration for animal-to-human transmission to

occur. Occasionally, human infections with influenza A viruses of non-human origin transpire. Most of these infections are self-limiting; however some establish sustained human-to-human transmission, leading to pandemics. For a zoonotic IAV to successfully transmit to humans, several barriers must be overcome. First, humans must have direct exposure to the animal to contract the virus, whether the exposure is directly with waterfowl through shared aquatic habitats, such as swimming in contaminated waters, or through contact with an intermediate host such as poultry or swine through markets or fairs. In addition, a zoonotic IAV needs to transmit via the respiratory droplet or aerosol route to spread among humans, making the route of transmission a component of cross-species transmission [120]. Other barriers include viral factors including: the cooperative efforts of both the HA and NA proteins in determining the effectiveness of host specificity and subsequent viral entry into, fusion with and exit from the host cell [10, 11, 58, 119, 121-134]; the PB2 protein with its ability to affect viral replication within the host cell [135-139]; and finally the M segment, though the mechanism behind this has yet to be fully determined [140, 141].

Influenza A Virus Evolution

The accumulation of mutations over time, along with the shuffling of gene segments between two or more distinct IAVs within an infected cell (reassortment), contribute to the evolution of IAV. There is a discernable difference between the evolutionary rates of IAVs that infect wild aquatic birds and those that infect terrestrial poultry, swine or humans. IAVs that infect wild aquatic birds seem to have reached an evolutionary stasis, characterized by relatively low rates of change, particularly at the amino acid level, indicating that these viruses are well adapted to their hosts [109, 142, 143]. Conversely,

mutations at the amino acid level in human IAV strains are continually accumulating. The rates of change vary amongst the individual proteins as a result of the strength of the immune selection pressure on that protein, with HA and NA accepting the most pressure [109].

Antigenic Drift

The IAV has a low-fidelity polymerase, as it lacks proofreading capabilities and is therefore highly error prone. This leads to random mutations that accumulate predominantly in the antigenic sites of the surface HA and NA glycoproteins due to immune selection pressure. These mutations accumulate over time, generating new variants and confer selective advantages by allowing the variants to escape pre-existing immunity, leading to repetitive influenza outbreaks and epidemics [144-146]. For each round of replication, the IAV mutation rate is in the range of 1×10^{-5} substitutions per nucleotide per round of replication. A subset of the resulting mutations becomes fixed in the viral genome [142,143,147-150]. The process of viral evolution due to accumulated mutations over time is termed antigenic drift.

Reassortment

Viral evolution can also occur through the more rapid process of reassortment. The segmented nature of IAV promotes viral diversity through reassortment, or the exchange of gene segments between two different IAV strains upon co-infection of the same cell. A co-infection with just two influenza viruses, each with eight gene segments, can yield 2^8=256 different progeny genotypes, illustrating the potential for reassortment to generate significant viral diversity. Reassortment among IAVs adapted to human and non-human

hosts can pose a threat to public health when novel gene constellations, along with selection pressure for the reassortant virus to adapt to its new host, accelerate the evolution of an antigenically novel, transmissible and pathogenic virus, as was seen with the pandemic viruses of 1918, 1957, 1968 and 2009 [151-153].

It has been well demonstrated that reassortment is responsible for the emergence of pandemic influenza viruses. The 1918, 1957 and 1968 pandemics arose from reassortment events between human and avian influenza viruses that introduced and transmitted antigenically novel HAs within the human population [154, 155]. Similarly, multiple reassortment events occurred to generate the human H1N1 virus responsible for the 2009 pandemic [156,157] . Furthermore, reassortment played a role in the generation of zoonotic events, such as the H5N1 and H7N9 viruses that are currently circulating in poultry in Southeast Asia [116,158]. It is clear from these cases that reassortment plays a significant role in IAV diversity and can contribute to interspecies transmission.

Phylogenetic evidence has indicated that reassortment between strains of the same subtype (intra-subtype) occurs more frequently than between those of differing subtypes (inter-subtype) [159]. In fact, the unusually severe epidemics of 1947 and 1951 can be attributed to intra-subtype reassortment between A/H1N1 viruses [110]. Additionally, intra-subtype reassortment has been documented for the A/H3N2 virus in 2003-2004 [112]. In addition to the emergence of epidemics, intra-subtype reassortment is responsible for the worldwide increase in adamantane resistance between the years 2004-2006, as the S31N resistance mutation in the M2 protein was combined with other advantageous mutations through reassortment events between two H3N2 viruses [160].

Since 1977, A/H1N1 and A/H3N2 viruses have co-circulated in humans, providing sufficient opportunity for inter-subtype reassortment between these subtypes, as evidenced by reports describing A/H1N2 viruses. Nishikawa et al. reported the isolation of the first human H1N2 virus from a patient that was co-infected with A/H3N2 and A/H1N1 influenza viruses [161], while Xu et al. isolated a human H1N2 virus during the 2001-2002 influenza season, wherein the HA from the A/New Caledonia/20/99 (H1N1) strain was coupled with the NA from the A/Moscow/10/99 (H3N2) strain [162]. Finally, an H1N2 virus was isolated from a human and was proven to be the product of a reassortment event between the 2009 pandemic H1N1 virus and an H3N2 virus [163].

To date, there have been numerous, beneficial reassortment studies conducted that focus on three main areas of study. The first examines the topic of mapping viral genotypes and phenotypes. Inoculating a substrate with two different influenza virus subtypes and then evaluating the RNA patterns via polyacrylamide gel of the recombinant and parental viruses permitted the mapping of the viral genome before the more common use of reverse-genetics [164, 165]. In addition, determining the genotypes of the resulting progeny viruses after a mixed co-infection, one can determine the potential for reassortment between the two parental viruses. This feature is particularly important in risk assessment studies, or uncovering the potential for variants with increased virulence or transmissibility to arise after co-infection with an avian and human virus [130,166-168]. Second, since 1969, reassortment experiments between specific circulating strains and the lab-adapted A/Puerto Rico/8/34 (PR8) have been performed in order to generate high-yield vaccine viruses in embryonated chicken eggs. Co-infecting eggs with the two viruses and negatively selecting against the HA and NA of the PR8 virus with antiserum

produces reassortant viruses with the HA and NA of the target circulating strain while retaining the internal segments of the high-growth PR8 virus [169-171]. This process continues to be optimized and used today. Finally, the phenomenon of segment mismatch has been routinely investigated. Segment mismatch, or the inability for gene segments from two different IAV strains to come together in a random manner due to functional incompatibilities either at the RNA or protein level, resulting in specific gene pairs appearing more frequently than others [172]. Segment mismatch is a major obstacle in obtaining non-attenuated progeny from a reassortment event. This was illustrated in the 1977 work by Scholtissek et al. in which replacement of one gene segment from a highly pathogenic strain of IAV with that from a different IAV strain resulted in the attenuation of the original virus [173]. One reason for this is RNA packaging signal incompatibility. One of the final steps in the viral replication process is the packaging of the viral genome. A fully infectious virus must contain a full complement of all eight gene segments. Though the precise mechanism by which vRNA are packaged has been debated, there is increasing evidence demonstrating that vRNA are packaged selectively via interactions between segment-specific packaging signal sequences that are located in both the untranslated regions (UTR's) and terminal coding regions at both the 3' and 5' ends of the vRNA. The packaging signals are unique for each of the eight gene segments and are not highly conserved among different strains, suggesting the role of packaging signals in limiting the formation of reassortant viruses between genetically diverse influenza strains [174-177].

Incompatibilities that restrict the fitness and generation of reassortant viruses can also occur at the level of viral proteins and functions that are important throughout the life

cycle. The viral RNP complex is composed of three proteins, PB2, PB1 and PA, and is essential for viral replication and transcription. Therefore, production of reassortant progeny viruses is dependent upon a combination of polymerase proteins from the parental viruses able to form a functional RNP complex [178]. In addition to direct protein-protein interactions, indirect functional interactions can also be susceptible to genetic mismatch. One requirement for efficient replication of influenza viruses is the functional balance of the receptor binding protein (HA) and the receptor destroying enzyme (NA). Experimental co-infection studies with an avian and a human influenza virus revealed that the human NA protein was unable to fully cleave the sialic acids to which progeny reassortant viruses containing the avian HA protein bind, thus constraining the isolation of these viruses [179].

Introduction to Thesis Project

In the following chapters, we investigate influences other than genetic mismatch on the frequency of reassortment of influenza A virus. We have developed a system that allows us to perform co-infections using a pair of phenotypically identical, yet genetically different viruses in both cell culture and guinea pig models. Using this system, we performed simultaneous co-infections at a high multiplicity of infection and determined the baseline frequency of reassortment. We found that in the absence of segment mismatch, reassortment efficiency is quite high and directly dependent on dosage. However, we reveal that as a delay is introduced between co-infections, reassortment efficiency decreases both *in-vitro* and *in-vivo* as a result of some mechanism of super-infection interference. We suggest that in our system, host innate immune responses seem to be the most potent source of super-infection interference, with the removal of sialic

acid receptors from the host cell surface by the viral neuraminidase protein also playing a role. Finally, we investigate the role of semi-infectious particles and defective-interfering particles on reassortment frequency. We generated semi-infectious particles and defective-interfering particles by 1) exposing our viruses to low dose UV and 2) serial passage of viruses at a high multiplicity of infection in cell culture, respectively. We discovered that while semi-infectious particles enhance reassortment, defective-interfering particles suppress reassortment. Our results suggest that although segment mismatch is a dominant feature of reassortment, several other factors do contribute to reassortment frequency.

Chapter 2: Influenza virus reassortment occurs with high frequency in the absence of segment mismatch

Nicolle Marshall, Lalita Priyamvada, Zachary Ende, John Steel and Anice C. Lowen*

The work of this chapter was published in 2013 in *PLoS Pathogens*

Article citation:

Marshall N, Priyamvada L, Ende Z, Steel J, Lowen AC (2013) Influenza Virus Reassortment Occurs with High Frequency in the Absence of Segment Mismatch. PLoS Pathog 9(6): e1003421. doi:10.1371/journal.ppat.1003421

Abstract

Reassortment is fundamental to the evolution of influenza viruses and plays a key role in the generation of epidemiologically significant strains. Previous studies indicate that reassortment is restricted by segment mismatch, arising from functional incompatibilities among components of two viruses. Additional factors that dictate the efficiency of reassortment remain poorly characterized. Thus, it is unclear what conditions are favorable for reassortment and therefore under what circumstances novel influenza A viruses might arise in nature. Herein, we describe a system for studying reassortment in the absence of segment mismatch and exploit this system to determine the baseline efficiency of reassortment and the effects of infection dose and timing. Silent mutations were introduced into A/Panama/2007/99 virus such that high-resolution melt analysis could be used to differentiate all eight segments of the wild-type and the silently mutated variant virus. The use of phenotypically identical parent viruses ensured that all progeny were equally fit, allowing reassortment to be measured without selection bias. Using this system, we found that reassortment occurred efficiently (88.4%) following high multiplicity infection, suggesting the process is not appreciably limited by intracellular compartmentalization. That co-infection is the major determinant of reassortment efficiency in the absence of segment mismatch was confirmed with the observation that the proportion of viruses with reassortant genotypes increased exponentially with the proportion of cells co-infected. The number of reassortants shed from co-infected guinea pigs was likewise dependent on dose. With 106 PFU inocula, 46%-86% of viruses isolated from guinea pigs were reassortants. The introduction of a delay between infections also had a strong impact on reassortment and allowed definition of time windows during which super-infection led to reassortment in culture and in vivo. Overall,

our results indicate that reassortment between two like influenza viruses is efficient but also strongly dependent on dose and timing of the infections.

Author Summary

Reassortment is the process by which influenza viruses, which carry RNA genomes comprising eight segments, exchange genetic material. Reassortment of the genome segments of two differing influenza strains has the potential to vastly increase the diversity of circulating influenza viruses. Despite its importance to influenza virus evolution, the frequency with which reassortment occurs in a cell or an animal infected with two or more variant viruses is unclear. Toward determining how readily reassortment can occur, we assessed the incidence of reassortment during experimental infection in cultured cells and in guinea pigs. We found that reassortment can occur with high efficiency in both systems, but that that efficiency is dependent on i) the dose of each virus added to the cells or taken up by the host and ii) the relative timing with which each virus infects. These results suggest that influenza A virus reassortment may be more prevalent in nature than one might expect based on the results of surveillance studies.

Introduction

Reassortment is the process by which viruses carrying segmented genomes exchange gene segments. The reshuffling of genetic material achieved through reassortment supports rapid production of variant viruses that can be markedly different, genotypically and phenotypically, from the parental strains. The more gradual process of genetic drift, resulting from errors in genome replication, and the process of reassortment come

together to generate vast genomic diversity among influenza A viruses. It is this diversity that, in turn, permits the rapid evolution of influenza viruses and the generation of novel pandemic and epidemic strains.

The contribution of reassortment to the emergence of pandemic influenza viruses is well established: the 1957 and 1968 pandemics arose following reassortment events between avian and human influenza viruses that allowed novel HA subtypes to gain widespread circulation in the human population [1,2,3]. Reassortment furthermore played a prominent role in the creation of the H5N1 viruses that continue to circulate in poultry of Southeast Asia [4], and in the H1N1 swine influenza viruses that emerged in humans in April 2009 [5,6]. Thus, epidemiological studies indicate that reassortment is an important means of viral diversification and often facilitates inter-species transmission.

In addition to its role in pandemic influenza, phylogenetic studies have revealed the importance of reassortment between co-circulating viruses of the same subtype in generating a diverse pool of seasonal influenza viruses [7,8,9,10,11,12,13,14]. This diversity in turn allows for the selection of variants that escape pre-existing immunity in the population and thereby cause widespread epidemics: evidence suggests that the unusually severe epidemics of 2003, 1951 and 1947 were each caused by strains generated through intra-subtype reassortment among co-circulating clades [8,10].

Previous efforts to study influenza virus reassortment in the lab have been of three main types. First, beginning with the work of Lubeck et al. in 1979, several research groups have examined the phenomenon of segment mismatch, in which the gene segments of two differing strains are found to assort in a non-random fashion due to functional

incompatibilities between the viral proteins or RNA segments [15,16,17,18]. It is clear from this literature that strain differences between parental viruses limit the fitness of many reassortant progeny and thereby restrict the number of different genotypes that arise, or are detected, following co-infection. Thus, segment mismatch is a potent determinant of reassortment efficiency. Second, a number of risk assessment type studies have addressed the potential for variants with increased virulence or transmissibility to arise through reassortment between two strains of epidemiologic importance [19,20,21,22,23,24,25,26,27]. Third, since reassortment between circulating strains and the egg-adapted A/Puerto Rico/8/34 virus has been used since 1969 to generate vaccine seed strains that grow well in embryonated chicken's eggs, significant research effort has been put into optimizing this procedure [28,29].

Research to date is lacking on the conditions of co-infection that are most favorable for reassortment, and it is therefore unclear under what circumstances we can expect to see novel influenza A viruses arising in nature. In part, this knowledge gap has arisen because, when one studies reassortment between two dissimilar strains, the effects of other parameters are confounded by those of segment mismatch. Herein, we report a novel method for the study of reassortment in the absence of segment mismatch and the application of this method to determine the baseline frequency of reassortment under unbiased conditions, and the impacts of infection dose and timing on this baseline.

Results

A system for the study of unbiased reassortment. In order to obtain data that are not confounded by segment mismatch, we have designed an approach that employs a pair of phenotypically identical but genotypically distinct influenza viruses. Reverse genetics was used to introduce silent mutations into each gene segment of A/Panama/2007/99 (H3N2) [Pan/99] virus such that the segments of the resultant variant, or rPan/99var, virus can be distinguished from those of the rPan/99wt virus using molecular techniques (described below). The mutations introduced were selected carefully such that the rPan/99var viruses were not attenuated in growth relative to the rPan/99wt strain (Figure 1). As a result, all 256 different progeny that might arise following co-infection with rPan/99wt and rPan/99var viruses are expected to be of equal fitness. Because there are no selective pressures acting differentially on the various progeny strains, co-infection with rPan/99wt and rPan/99var viruses constitutes an unbiased system in which to study reassortment.

As shown in Figure 2, the silent mutations differentiating rPan/99wt and rPan/99var viruses allow the full genotypes of progeny arising from mixed infections to be determined using high resolution melt (HRM) analysis [30]. This method exploits the fact that sequence differences between two double stranded DNA (dsDNA) molecules confer differences in melting properties. These differences in melting properties can in turn be detected as changes in fluorescence when dsDNAs labelled with a saturating fluorescent dye are heated (e.g. from 65˚C to 95˚C), since the dye will cease to fluoresce as the DNA melts into single strands. As described in more detail in the methods section, we have

applied HRM analysis to clonal virus isolates derived from co-infection in order to identify each gene segment as either wt or var in origin.

Reassortment occurs with high efficiency under unbiased conditions. We have defined the baseline frequency of reassortment as the percentage of progeny viruses with reassortant genotypes that arises after a single cycle of replication, given high levels of co-infection at the cellular level and an absence of segment mismatch or other selection pressures that would promote parental genotypes over reassortant ones. To determine this baseline value, rPan/99wt-HIS and rPan/99var-HA viruses were used to co-infect MDCK cells at a multiplicity of infection of 10 PFU/cell of each virus. Epitope tagged versions of the wt and var strains were used so that the number of cells infected with each virus and the number of cells co-infected could be determined by flow cytometry. Co-infection rates of 99.4% were achieved in each of two independent samples. As shown in Figure 3, the resultant frequencies of reassortment were 87.6% and 89.2% (average = 88.4%). While this result indicates that reassortant viruses arise with high frequency under the unbiased conditions described, the theoretically optimal efficiency of 254/256, or 99.2%, was not achieved: parental progeny viruses were over-represented relative to the expected frequency of 0.8% ($p<0.001$, exact test). This discrepancy could be suggestive of incomplete mixing between genomes in co-infected cells, but also may be the result of a small differences in the input of wt and var viruses into individual cells, due either to a slight skewing of the inoculum or to the Poisson distribution (with MOIs of 10, a sizable proportion of cells would be expected to receive, for example, 10 copies of the wt virus but 9 or 11 copies of the var virus).

The frequency of reassortant progeny shows an exponential relationship with the frequency of co-infected cells. Co-infection at the cellular level is a necessary precursor to reassortment. To determine the quantitative relationship between the frequency of co-infected cells and frequency of reassortant progeny viruses, we examined both co-infection and reassortment levels following inoculation of MDCK cells at a range of multiplicities from 10 PFU/cell to 0.01 PFU/cell. Twelve hours after infection with rPan/99wt and rPan/99var viruses, supernatant was collected to determine the frequency of reassortant viruses therein. At the same time, cells were harvested and used to determine the numbers of uninfected, singly infected and doubly infected cells by flow cytometry. As shown in Figure 4, co-infection of MDCK cells was seen with all four MOI conditions but spanned a wide range, with about 13% of infected cells harboring both wt and var viruses at the lowest MOI to about 90% at the highest MOI. Reassortment was also seen following infection at all four multiplicities and, as predicted, occurred with the highest frequency (average 78.5%) at the highest MOI and the lowest frequency (average 9.5%) at the lowest MOI. In particular, reductions in the proportion of reassortant progeny were significant when the MOI was reduced from 10 to 0.1 or 0.01 PFU/cell ($p<0.0001$, Fisher's exact test). Rather than a simple linear relationship, however, the data suggest that reassortment levels increased exponentially with the proportion of cells that were co-infected (Figure 4).

The frequency of reassortant progeny arising in vivo is dependent on inoculum dose. The results obtained following co-infection of cultured cells at a range of MOIs indicated that, as expected, reassortment levels are acutely dependent on co-infection rates. In an animal host, one might expect co-infection and therefore reassortment rates to be low

since the number of epithelial cells available for viral infection within the respiratory tract is presumably high. To address this hypothesis, guinea pigs were co-infected intranasally with rPan/99wt and rPan/99var viruses at two doses: 10^3 PFU or 10^6 PFU of each strain. At 48 h post-infection nasal lavage was collected from each guinea pig and viruses therein were genotyped. As reported in Table 1, robust reassortment levels were detected under both conditions (averages of 30% and 59% following infection with 10^3 PFU and 10^6 PFU, respectively). The difference between the two dosage groups was found to be significant ($p=0.03$, Student's t-test), indicating that the level of reassortment in vivo is dependent on inoculum dose.

Super-infection up to 8 hours after primary infection led to robust reassortment in cell culture. In nature, the probability of an individual being co-infected with two distinct strains (as opposed to a quasi-species) of influenza virus simultaneously is expected to be quite low; rather, most co-infections are likely to arise from sequential infection events. We therefore sought to determine the window of time during which a second infection can result in reassortment. To this end, experiments were performed in which inoculation of MDCK cells with rPan/99var virus was followed at a range of time points by inoculation with rPan/99wt virus. MDCK cells were infected with either rPan/99var2-HA virus and rPan/99wt-HIS virus together (0 h) or with rPan/99var2-HA virus alone, followed by sequential infections with rPan/99wt-HIS virus 2, 4, 8, 12, 16 or 24 h later. Following each addition of virus, a 1 h attachment period at 4°C was used to synchronize infections; since the viral neuraminidase would not be active at this temperature, it is important to note that any stripping of sialic acids from infected cell surfaces would occur up to the point when the second virus was added, but not during the attachment period. At

12 h post-infection with rPan/99wt-HIS virus, supernatant was collected for genotyping of released virus and cells were harvested to determine co-infection rates by flow cytometry. The results show (Figure 5) that a delay of up to 8 h between the primary and secondary infection led to a 5-16% decrease in the proportion of infected cells that were co-infected when compared to a simultaneous infection. These moderate decreases in the number of co-infected cells were accompanied by larger decreases in the amount of reassortment (41% reduction in the 8 h group relative to the 0 h group, $p=0.003$, Fisher's exact test). Nevertheless, up to an 8 h time interval between additions of rPan/99wt and rPan/99var viruses allowed for robust reassortment: 47.5% of virus isolates sampled from the 8 h infections carried a mixed genotype. In contrast, a delay of 12 h between primary and secondary infections resulted in just 4.75% of isolates showing reassortment. This low level of reassortment with the 12 h interval occurred despite the fact that 43% of infected cells were doubly infected under these conditions.

Super-infection up to 12 hours after primary infection led to robust reassortment in the guinea pig model. To determine how the introduction of a time interval between two influenza virus infections would impact reassortment in an animal host, we set up a similar series of infections in the guinea pig model. Groups of three guinea pigs were infected intranasally either with rPan/99var and rPan/99wt viruses together (0 h group) or with rPan/99var virus alone, followed by rPan/99wt virus 6, 12, 18 or 24 h later. Nasal washings were collected 48 h after the rPan/99wt virus infection. Since the induction of an antiviral response following primary infection has the potential to block secondary infection, we first evaluated whether the rPan/99wt virus infection was productive by quantifying wt and var HA vRNA in each nasal wash sample. In all groups, rPan/99wt

virus was found to infect productively (Table 2); in the 24 h group, however, Ct values for HAwt were found to be markedly higher than in the other groups, indicating a less robust rPan/99wt virus infection in these animals. In a separate experiment, infection with rPan/99wt virus 48 or 72 h after rPan/99var virus did not result in productive infection (HAwt Ct >35 in 5/6 guinea pigs). Progeny virus isolates obtained from the nasal wash samples were then genotyped and scored as wt, var or reassortant. The results indicate that a delay of up to 12 hours between primary and secondary infections with rPan/99 virus does not reduce reassortment frequency (Table 2). In fact, higher levels of reassortment were seen in guinea pigs with a 12 h interval between infections than in those infected with both viruses simultaneously ($p=0.02$, Student's t-test; Figure 6). In contrast, secondary infection 18 h after primary infection resulted in a low frequency of reassortant progeny (6.7% on average), whereas no reassortants were detected when the two infections were staggered by 24 h. Thus, while a brief delay between primary and secondary influenza virus infections may actually increase the potential for reassortment, no reassortment was seen with a delay of 24 h or more.

Viral spread over time leads to increased numbers of co-infected cells.

We had expected co-infection rates in cell culture and in vivo to decline with increasing time interval between infections. While this was found to be the case at high MOI in MDCK cells, co-infection was increased in guinea pigs with the introduction of a 12 h delay prior to super-infection. To explain this observation, we hypothesized that the delay allows the first virus to undergo one round of replication and then spread, thereby increasing the probability that the second infection will result in doubly infected cells. We tested this hypothesis by performing an MDCK cell based co-infection experiment

from a low MOI (0.01 PFU/cell) in the presence of trypsin. Under these conditions that allow for viral spread, the proportion of infected cells that were co-infected increased with an 8 or 12 h interval between inoculations ($p<0.0001$, chi-squared test). A decline in co-infected cells was then seen with 16 and 24 h intervals, indicating that super-infection interference has taken effect at these times after the primary infection (Figure 7).

Discussion

We have evaluated, to our knowledge for the first time, the efficiency with which influenza A viruses undergo reassortment in the absence of fitness differences among parental and progeny genotypes. Our results show that reassortment is very efficient: where high rates of co-infection are achieved, high frequencies of reassortant genotypes are seen. These findings demonstrate that compartmentalization within the cell does not prevent extensive mixing of gene segments from two co-infecting viruses. It remains unclear whether this mixing occurs in the cytoplasm upon virus uncoating, in the nucleus during replication, during nuclear export and trafficking to the cell membrane, during the assembly process or throughout the virus life cycle. It is clear, however, that at least one stage of the life cycle allows for unrestricted exchange of gene segments.

The efficiency of reassortment was decreased when inoculation with var and wt viruses was staggered by 12 h in cell culture: despite the fact that an appreciable number of cells were co-infected under these conditions, reassortment levels were near the limit of detection. This observation suggests that reassortment is limited when the life cycles of co-infecting viruses are at markedly asynchronous. Given that released virus was sampled

12 h after the second inoculation, however, there was enough time for the second virus to undergo a full cycle of replication [31], sampling all stages of the life cycle. Thus, perhaps the predominance of progeny carrying full var genotypes was simply due to a predominance of var genomes within the co-infected cells. Higher intracellular levels of var gene segments compared to wt would be expected, given that their replication began several hours before the first wt genomes entered the cell.

A system for the study of influenza virus co-infection rates in cell culture was recently described by Bodewes et al. [32]. Two similar recombinant influenza viruses that encoded different fluorescent proteins in the place of neuraminidase (NA) were generated. Using these viruses, co-infection of MDCK cells at an MOI of 3 PFU/cell resulted in double infections in about 10% of cells. In contrast, at an MOI of approximately 1 PFU/cell, we observed that about 65% of MDCK cells were co-infected with rPan/99wt and rPan/99var viruses. Variation in experimental design most likely accounts for these differences: the efficiency of infection with the fluorescein encoding viruses may have been decreased by the absence of NA on the virions [33] and also may have differed from that seen with the rPan/99 viruses due to the H5 subtype background that was used. Deviations of our own co-infection rates from those predicted by the Poisson distribution most likely result from antiviral factors present in undiluted virus stocks used for MOI=10 infections, the contribution of gene segments from non-infectious particles (especially important at lower MOIs), and routine experimental error.

The proportion of progeny viruses with reassortant genotypes was found to increase exponentially with the proportion of cells that were co-infected. This relationship may reflect the relative likelihood at each MOI of an individual cell receiving equal doses of

wt and var. At low MOI, those cells that are co-infected are highly likely to have only one copy of each genome and therefore a 1:1 ratio of wt and var. At intermediate MOI, in contrast, the probability of two wt and one var virus (or vice versa) entering a given cell is appreciable. At high MOI, virtually all cells are expected to have several copies of each genome so that the wt:var ratios are likely to be close to 1:1 (e.g. under MOI=10 conditions, 9 wt and 11 var viruses might enter the same cell). Thus, the data suggest that discordant doses at the level the individual co-infected cell decrease the efficiency of reassortment.

The rates of reassortment observed in co-infected guinea pigs were markedly higher than those seen previously in a ferret model [19], but comparable to those obtained in a swine based experiment [26]. In a risk assessment study in ferrets, Jackson et al. examined the progeny arising from simultaneous co-infection with 105.7 PFU each of an H3N2 seasonal strain (A/Wyoming/03/03) and a highly pathogenic avian H5N1 influenza virus (A/Thailand/16/06). On average, 8.7% of the isolates (n=360) obtained from ferret nasal washings were reassortants [19]. Similarly, Ma et al. evaluated reassortment following simultaneous co-infection of pigs with 10^6 PFU each of classical H1N1 and triple-reassortant H3N2 swine influenza viruses. In this case, 84.5% of virus isolates (n=71) carried mixed genomes [26]. The relatively low frequency of reassortant progeny resulting from A/Wyoming/03/03 + A/Thailand/16/06 virus co-infection might be accounted for by i) functional incompatibilities between the gene products ii) mismatch among packaging sequences [17], and/or iii) low co-infection rates resulting from differing receptor binding specificities [34]. Each of these aspects of functional mismatch may have been diminished in the swine experiment since the viruses used were both

adapted to this host and the NS, M and NP genes were of classical swine origin in each case [35].

In guinea pigs infected with 10^6 PFU of each virus, reassortment rates were similar to those obtained in cell cultures infected at individual MOIs of approximately 1 PFU/cell. The two situations should not be compared directly, however, since the MDCK based experiments were limited to a single cycle of replication (both by the absence of trypsin and the early time point at which samples were collected), while multiple rounds of replication occurred in vivo. Amplification of both the input viruses (leading to more opportunity for co-infection) as well as the reassortant progeny viruses may have contributed to the high frequency of reassortant genotypes. It should be noted, however, that the reassortant genotypes identified in vivo were, in general, diverse. In other words, the reassortant isolates identified were not members of one or a few clonal populations.

Influenza virus infection triggers a number of effects that disfavor super-infection. These include the induction of cellular and host antiviral responses [36], the stripping of sialic acid receptors from the cell surface by viral neuraminidase [37], and the destruction of potential target cells through lysis. Since the potency or extent of each of these effects increases over time, we predicted that the opportunity for co-infection and reassortment would decrease over time after a primary infection. In cell culture, under high multiplicity conditions, this hypothesis was found to be correct. In guinea pigs inoculated with 1000 PFU, however, infections staggered by 12 h led to a higher level of reassortment than did simultaneous co-infection. A 12 h delay between first and second infections in vivo may allow for the first virus to undergo one round of replication and then spread, thereby increasing the probability that the second infection will result in

doubly infected cells. This hypothesis is supported by our observation that, following low MOI infection in cell culture, time intervals of 8 and 12 h between infections increased the number of co-infected cells compared to simultaneous infection. That fewer co-infected cells and reassortant viruses were produced from infections staggered by 16 h or 18 h in MDCK cells and guinea pigs, respectively, suggests that at these times after primary infection one or more of the mechanisms of super-infection exclusion has begun to take effect.

Recent progress in the field on the mechanisms of influenza virus genome packaging have led to the hypothesis that sequence-specific interactions between RNA segments drive their selective incorporation during virion assembly [17,38,39,40,41,42,43,44,45]. It follows that, if packaging signals vary between strains of influenza A virus, a requirement for such RNA-RNA interactions would limit reassortment between divergent viruses. The regions of each segment thought to be important for packaging [41,43,46] were avoided in the mutagenesis of rPan/99var virus; thus, rPan/99wt and rPan/99var viruses most likely carry identical packaging signals. For this reason, our data are not expected to, and do not, reveal linkages between the segments at the RNA level. Our results do offer some insight into packaging specificity, however, in that HRM analyses of clonal isolates allowed the typing of each segment as wt or var. We did not see clear examples of isolates that carried both a wt and a var copy of a given segment. This result is in agreement with recent publications by Chou et al. and Inagaki et al., which showed respectively that eight distinct segments are packaged into one virion [40] and that homologous gene segments compete for incorporation [47].

For the experiments described, we chose to use a seasonal influenza virus representative of the human H3N2 lineage. We would, however, expect influenza viruses of other strains and subtypes to behave similarly to the Pan/99 virus. The reason is that we are essentially studying the reassortment of a virus with itself; any strain should reassort well with itself under the "baseline" conditions described. When conditions are altered from the baseline, however, certain strain specific effects would be expected to arise. Two such effects relevant to the results herein are i) the role of receptor binding specificity and other host-adaptive traits in determining the efficiency of infection and therefore co-infection in a given host species or target cell type; and ii) the precise timing with which super-infection interference takes effect. The latter will most likely vary with the rate of viral growth and may hinge on the efficiency of IFN suppression or stripping of cellular sialic acids, depending on the mechanism(s) at play.

Much remains to be done to gain a comprehensive understanding of influenza virus reassortment and the conditions under which it occurs. In addition to the effects of dose and timing described herein, cell tropism, host species, pre-existing immunity in the host, relative rates of viral growth and a wide range of strain specific factors that contribute to the phenomenon of segment mismatch will each come into play in determining the outcome of mixed influenza virus infections. In turn, the number of virus particles transmitted from a co-infected host to a recipient will be important in determining the epidemiological significance of reassortment events. Comparison of intra- and inter-host genetic diversity in equine and swine influenza suggests that the transmission bottleneck is loose; in other words, the diversity of genotypes transmitted was similar to that present

in the initial host [48,49,50]. Under these conditions, a reassortant virus present even as a minor population would frequently be passed on to additional hosts.

In sum, our findings indicate that influenza virus reassortment is an efficient process in a co-infected cell and in a co-infected host, and that the frequency of reassortment both at the level of individual cells as well as that of the animal host is dependent on dose and timing of infection. In establishing a simplified and well-controlled system to examine reassortment, we have laid the groundwork for future studies that will focus on virus and host-specific factors. By systematically varying individual parameters within our system, we hope to quantify the impact of a wide range of factors such that the complexity of influences determining natural reassortment rates can be evaluated for a given situation.

Materials and Methods

Ethics statement

This study was performed in accordance with the recommendations in the Guide for the Care and Use of Laboratory Animals of the National Institutes of Health. Animal husbandry and experimental procedures were approved by the Emory University Institutional Animal Care and Use Committee (IACUC protocol #2000719).

Cells

Madin-Darby Canine Kidney (MDCK) cells were maintained in minimum essential medium (MEM) supplemented with 10% FBS and penicillin-streptomycin. 293T cells were maintained in Dulbecco's MEM supplemented with 10% FBS.

Guinea pigs

Female, Hartley strain, guinea pigs weighing 300-350 g were obtained from Charles River Laboratories. Prior to intranasal inoculation, nasal lavage or CO2 euthanasia, guinea pigs were sedated with a mixture of ketamine and xylazine (30 mg/kg and 2 mg/kg, respectively). Inoculation and nasal lavage were performed as described previously [51], with PBS as the diluent / collection fluid in each case.

Viruses

rPan/99wt and variant viruses were recovered by reverse genetics following standard procedures [52,53]. Briefly, a 12 plasmid rescue system based on pPOL1 and pCAGGS vectors and co-culture of 293T and MDCK cells were used. Plaque isolates derived from rescue supernatants were amplified in 11-day-old embryonated chicken eggs to generate virus stocks and stock titers were determined by plaque assay on MDCK cells.

Four rPan/99 based viruses were used in the research described: rPan/99wt, rPan/99var6, rPan/99wt-HIS and rPan/99var2-HA. The first is a reverse genetics derived version of the wild-type A/Panama/2007/99 virus. The second, rPan/99var6, contains the following silent mutations relative to rPan/99wt virus (nucleotide numbering is from the 5' end of the cRNA): NS C329T, C335T, and A341G; M C413T, C415G and A418C; NA C418G, T421A and A424C; NP C537T, T538A and C539G; HA T308C, C311A, C314T, A464T, C467G and T470A; PA A342G and G333A; PB1 C288T and T297C; and PB2 C354T and C360T. The third, rPan/99wt-HIS, differs from rPan/99wt virus only in that it encodes a HIS tag within the HA open reading frame (inserted immediately after the sequence encoding the signal peptide [54]). The fourth, rPan/99var2-HA, encodes an HA

tag within the HA open reading frame (again, inserted after the signal peptide) as well as the following silent mutations: NS C329T, C335T, and A341G; M C413T, C415G and A418C; NA C418G, T421A and A424C; NP C537T, T538A and C539G; HA T308C, C311A, C314T, A464T, C467G and T470A; PA G603A, T604A and C605G; PB1 C346T, T348G and A351G; and PB2 T621C, T622A and C623G. The rPan/99wt-HIS and rPan/99var2-HA viruses were used in the MDCK cell base experiments described, whereas the rPan/99wt and rPan/99var6 viruses were used in the guinea pig experiments.

Our rationale for the above-described mutagenesis is as follows. The mutations were selected to allow differentiation of wt and var viruses by HRM analysis of ~100 bp amplicons containing the mutation sites. In addition, we wished to avoid attenuation of the var viruses and therefore used a minimal number of mutations and avoided any known cis-acting signals. Two or three mutations were found to be sufficient to obtain clear HRM results, and C/T and A/G mutations were preferred since they confer the greatest change in melting properties. In addition, a second set of three mutations was introduced into the var HA segment such that the two mutated regions could be used as primer binding sites unique to wt or var so that these segments could be quantified in a standard qPCR assay (as reported in Table 2).

Determination of reassortment frequency in vitro following simultaneous co-infection

rPan/99wt-HIS and rPan/99var2-HA viruses were mixed in equal proportions and then diluted with PBS to the appropriate titer for inoculation at MOI 10, 1, 0.1 or 0.01 PFU/cell of each virus. For the calculation of MOI, each well of a 6-well dish was

assumed to have $1x10^6$ cells. Prior to inoculation of MDCK cells, growth medium was removed, monolayers were washed with PBS three times and the 6-well dish was placed on ice. Each well was inoculated with a 250ul volume and cells were incubated at 4˚C for one hour to allow equal binding of all virus. Unattached virus was removed by aspirating inoculum and washing three times with PBS. After the addition of virus medium (MEM supplemented with 3% BSA, Penicillin Streptomycin, and 1 ug/ml trypsin where indicated), cells were transferred to 33˚C. At 12 hours post-infection, supernatant was collected and stored at -80˚C for subsequent genotyping of released virus. MDCK-infected cells were harvested and prepared for flow cytometry (see below). To determine the gene constellations of viruses present in the supernatant, 121 (Figure 3) or 21 (Figure 4) clones per sample were isolated by plaque assay of the supernatant and all 8 vRNA segments from each was typed by HRM analysis.

Determination of reassortment frequency in vitro following super-infection

Seven 6-well plates of MDCK cells were infected in triplicate for this experiment. For the first plate ("0 h" time point), MDCK cells were infected with rPan/99wt-HIS and rPan/99var2-HA viruses as described above for the simultaneous co-infection at MOI 10 of each virus. The remaining plates were each infected at MOI 10 of rPan/99var2-HA virus alone at time = 0 h and then infected subsequently (2, 4, 8, 12, 16, or 24 h after the var virus infection) with rPan/99wt-His virus at MOI 10. In each case, infections were carried out on ice and with a 1 h attachment period at 4°C, as described above. Supernatant was collected from each plate at 12 h following infection with rPan/99wt-His virus and stored at -80˚C. Cells were harvested at this same time point and prepared for flow cytometry (see below). The frequency of reassortant progeny in the supernatant was

determined by typing all 8 gene segments of 21 plaque isolates from each sample by HRM analysis.

Enumeration of infected and co-infected cells

To determine the number of infected and co-infected cells, MDCK cells were harvested 12 h after either wt/var virus co-infection or 12 h after wt virus infection by trypsinizing the monolayer and collecting with serum-supplemented medium. The cells were then washed 3 times with PBS-2% fetal calf serum (FBS) and incubated with Penta HIS Alexa Fluor 647 conjugated antibody (5ug/ml; Qiagen) and Anti-HA-FITC Clone HA-7 (7ug/ml; Sigma Aldrich) for 45 minutes, on ice. Cells were then washed 2 times with PBS-2% FBS and re-suspended with 200ul of PBS-2% FBS and 5ul/sample (0.25ug) of 7-Amino Actinomycin D (7-AAD), a dead cell excluder (BD Biosciences). Flow cytometry was performed using a FACSVerse flow cytometer (Becton Dickinson) and analyzed with FlowJo software.

Determination of reassortment frequency in vivo following simultaneous co-infection

rPan/99wt and rPan/99var6 viruses were mixed in equal proportions and then diluted in PBS to the appropriate titer ($6.6x10^3$ or $6.6x10^6$ total PFU/ml for inoculation with 10^3 or 10^6 PFU of each virus, respectively). A total of five guinea pigs per dose were inoculated intranasally with 300 ul and unused inoculum was stored at -80˚C. At 48 h post-infection nasal washings were collected and stored at -80˚C. To determine the ratio of wt and var viruses present in the inoculum, 25-30 clones were isolated by plaque assay of the unused inoculum and two vRNA segments from each was typed by HRM analysis. Similarly, the

frequency of reassortant progeny shed into nasal washings was determined by typing all eight gene segments of 19-24 plaque isolates derived from each nasal wash sample by HRM analysis. The data shown in Table 1 are the products of three different experiments: animals 1, 2, 3, 6, 7, and 8 comprised one experiment; animals 4 and 5 comprised a second; and animals 9 and 10 comprised a third.

Determination of reassortment frequency in vivo following super-infection

Five groups of three guinea pigs were used in this experiment. The first group (the "0 h" group) was infected with rPan/99wt and rPan/99var6 viruses as described above for the simultaneous co-infection with 10^3 PFU of each virus. The remaining guinea pigs were each infected with 10^3 PFU of rPan/99var6 virus alone at time = 0 h and then infected subsequently (6, 12, 18 or 24 h after the var virus infection) with 10^3 PFU of rPan/99wt virus. Nasal washings were collected from each guinea pig 48 h following infection with the rPan/99wt strain and stored at -80˚C. The frequency of reassortant progeny shed into nasal washings was determined by typing all eight gene segments of 19-22 plaque isolates derived from each nasal wash sample by HRM analysis.

Determination of virus genotypes by high resolution melt analysis

To screen virus released from co-infected cell cultures or guinea pigs, the following steps were performed. 1) Plaque isolates were obtained by plaque assay of cell culture supernatants or guinea pig nasal wash fluids in 10 cm cell culture dishes. Agar plugs above well separated (>0.5 cm apart) plaques were picked using 5 ml serological pipettes, ejected into 160 ul of PBS in 1.5 ml tubes, and then stored at -80˚C. 2) RNA was extracted from the agar plugs using the Qiagen QiaAmp Viral RNA kit, with the

following modifications to the manufacturer's protocol: carrier RNA was not used, agar plugs in PBS were heated at 65˚C for 5 min prior to mixing with AVL lysis buffer, and 40 ul water was used for the elution step. 3) Twelve microliters of RNA was reverse transcribed using Maxima reverse transcriptase (Fermentas) according to the manufacturer's instructions. 4) cDNA was used as template in qPCR reactions. Four microliters of 1:4 diluted cDNA were combined with the appropriate primers (0.4 uM final concentration; see Supplementary Table 1 for primer sequences) and Precision Melt Supermix (BioRad) in wells of a white, thin wall, 384 well plate (BioRad). qPCR and melt analyses were carried out in a CFX384 Real-Time PCR Detection System, as per the instructions provided with the Precision Melt Supermix. Data were analyzed using Precision Melt Analysis software (BioRad). Viruses were scored as reassortant if the genome comprised a mixture of wt and var gene segments in any proportion (e.g. both 7:1 reassortants and 4:4 reassortants were treated in the same way). Occasionally, one gene segment from a given isolate could not be typed as wt or var with high confidence (this was the case with approximately 2.5% of segments); such isolates were scored as wt or var parental viruses if all other gene segments were wt or var, respectively. If greater than one segment could not be typed, the isolate was excluded from the analysis.

Quantification of HA segment in bulk nasal wash fluids

The HA segments of rPan/99 wt and rPan/99var6 viruses differ by 6 nucleotides in two clusters: T308C / C311A / C314T and A464T / C467G / T470A. Forward and reverse primers encompassing these mutation clusters were designed: HAwt 295F / HAwt 481R and HAvar 295F / HAvar 481R. These primers specifically amplify the wt or var HA segments, respectively, allowing their quantification by conventional qPCR methods.

Thus, RNA extracted directly from nasal lavage fluids was subjected to reverse transcription followed by qPCR using SsoFast Evagreen Supermix (BioRad), according to the manufacturer's instructions. qPCR was performed with a CFX384 Real-Time PCR Detection System and results were analyzed using CFX Manager software (BioRad).

Statistical analyses

A one-sided exact test was applied to the data shown in Figure 3 to determine whether the proportion of isolates with parental genotypes was statistically greater than 2/256, or 0.008 (the expected value if reassortment occurred with full efficiency). Two-sided Fisher's exact tests were used to compare proportions of reassortant vs. parental progeny for data shown in Figures 4 and 5, while chi-squared tests were applied to compare proportions of singly vs. doubly infected cells for flow cytometric data shown in Figures 4, 5 and 7. Finally, unpaired, two-sided Student's t-tests were applied to data shown in Figure 6 and Tables 1 and 2.

Acknowledgements

We would like to thank Anshante Jones and Shamika Danzy for technical assistance and Fred Souret and Jacob Kohlmeier for helpful discussions. We are also indebted to Robert Lyles of the Biostatistics, Epidemiology and Research Design (BERD) program at Emory University for help with statistical analyses.

References

1. Scholtissek C (1994) Source for influenza pandemics. Eur J Epidemiol 10: 455-458.

2. Wright PF, Neumann G, Kawaoka Y (2006) Orthomyxoviruses. In: Knipe DM, Howley PM, editors. Fields Virology. 5 ed. pp. 1691-1740.

3. Scholtissek C, Rohde W, Von Hoyningen V, Rott R (1978) On the origin of the human influenza virus subtypes H2N2 and H3N2. Virology 87: 13-20.

4. Li KS, Guan Y, Wang J, Smith GJD, Xu KM, et al. (2004) Genesis of a highly pathogenic and potentially pandemic H5N1 influenza virus in eastern Asia. Nature 430: 209-213.

5. Trifonov V, Khiabanian H, Greenbaum B, Rabadan R (2009) The origin of the recent swine influenza A(H1N1) virus infecting humans. Euro Surveill 14.

6. Smith GJ, Vijaykrishna D, Bahl J, Lycett SJ, Worobey M, et al. (2009) Origins and evolutionary genomics of the 2009 swine-origin H1N1 influenza A epidemic. Nature 459: 1122-1125.

7. Schweiger B, Bruns L, Meixenberger K (2006) Reassortment between human A(H3N2) viruses is an important evolutionary mechanism. Vaccine 24: 6683-6690.

8. Nelson MI, Viboud C, Simonsen L, Bennett RT, Griesemer SB, et al. (2008) Multiple reassortment events in the evolutionary history of H1N1 influenza A virus since 1918. PLoS Pathog 4: e1000012.

9. Nelson MI, Simonsen L, Viboud C, Miller MA, Taylor J, et al. (2006) Stochastic processes are key determinants of short-term evolution in influenza a virus. PLoS Pathog 2: e125.

10. Holmes EC, Ghedin E, Miller N, Taylor J, Bao Y, et al. (2005) Whole-genome analysis of human influenza A virus reveals multiple persistent lineages and reassortment among recent H3N2 viruses. PLoS Biol 3: e300.

11. Rambaut A, Pybus OG, Nelson MI, Viboud C, Taubenberger JK, et al. (2008) The genomic and epidemiological dynamics of human influenza A virus. Nature 453: 615-619.

12. Simonsen L, Viboud C, Grenfell BT, Dushoff J, Jennings L, et al. (2007) The genesis and spread of reassortment human influenza A/H3N2 viruses conferring adamantane resistance. Mol Biol Evol 24: 1811-1820.

13. Lindstrom SE, Cox NJ, Klimov A (2004) Genetic analysis of human H2N2 and early H3N2 influenza viruses, 1957-1972: evidence for genetic divergence and multiple reassortment events. Virology 328: 101-119.

14. Ghedin E, Sengamalay NA, Shumway M, Zaborsky J, Feldblyum T, et al. (2005) Large-scale sequencing of human influenza reveals the dynamic nature of viral genome evolution. Nature 437: 1162-1166.

15. Lubeck MD, Palese P, Schulman JL (1979) Nonrandom association of parental genes in influenza A virus recombinants. Virology 95: 269-274.

16. Greenbaum BD, Li OT, Poon LL, Levine AJ, Rabadan R (2012) Viral reassortment as an information exchange between viral segments. Proc Natl Acad Sci U S A 109: 3341-3346.

17. Gao Q, Palese P (2009) Rewiring the RNAs of influenza virus to prevent reassortment. Proc Natl Acad Sci U S A 106: 15891-15896.

18. Li C, Hatta M, Watanabe S, Neumann G, Kawaoka Y (2008) Compatibility among polymerase subunit proteins is a restricting factor in reassortment between equine H7N7 and human H3N2 influenza viruses. J Virol 82: 11880-11888.

19. Jackson S, Van Hoeven N, Chen LM, Maines TR, Cox NJ, et al. (2009) Reassortment between avian H5N1 and human H3N2 influenza viruses in ferrets: a public health risk assessment. J Virol 83: 8131-8140.

20. Maines TR, Chen LM, Matsuoka Y, Chen H, Rowe T, et al. (2006) Lack of transmission of H5N1 avian-human reassortant influenza viruses in a ferret model. Proc Natl Acad Sci U S A 103: 12121-12126.

21. Imai M, Watanabe T, Hatta M, Das SC, Ozawa M, et al. (2012) Experimental adaptation of an influenza H5 HA confers respiratory droplet transmission to a reassortant H5 HA/H1N1 virus in ferrets. Nature 486: 420-428.

22. Banbura MW, Kawaoka Y, Thomas TL, Webster RG (1991) Reassortants with equine 1 (H7N7) influenza virus hemagglutinin in an avian influenza virus genetic background are pathogenic in chickens. Virology 184: 469-471.

23. Octaviani CP, Ozawa M, Yamada S, Goto H, Kawaoka Y (2010) High level of genetic compatibility between swine-origin H1N1 and highly pathogenic avian H5N1 influenza viruses. J Virol 84: 10918-10922.

24. Schrauwen EJ, Herfst S, Chutinimitkul S, Bestebroer TM, Rimmelzwaan GF, et al. (2011) Possible increased pathogenicity of pandemic (H1N1) 2009 influenza virus upon reassortment. Emerg Infect Dis 17: 200-208.

25. Kiseleva I, Dubrovina I, Bazhenova E, Fedorova E, Larionova N, et al. (2012) Possible outcomes of reassortment in vivo between wild type and live attenuated influenza vaccine strains. Vaccine 30: 7395-7399.

26. Ma W, Lager KM, Lekcharoensuk P, Ulery ES, Janke BH, et al. (2010) Viral reassortment and transmission after co-infection of pigs with classical H1N1 and triple-reassortant H3N2 swine influenza viruses. J Gen Virol 91: 2314-2321.

27. Qiao C, Liu Q, Bawa B, Shen H, Qi W, et al. (2012) Pathogenicity and transmissibility of reassortant H9 influenza viruses with genes from pandemic H1N1 virus. J Gen Virol 93: 2337-2345.

28. Fulvini AA, Ramanunninair M, Le J, Pokorny BA, Arroyo JM, et al. (2011) Gene constellation of influenza A virus reassortants with high growth phenotype prepared as seed candidates for vaccine production. PLoS One 6: e20823.

29. Baez M, Palese P, Kilbourne ED (1980) Gene composition of high-yielding influenza vaccine strains obtained by recombination. J Infect Dis 141: 362-365.

30. Wittwer CT, Reed GH, Gundry CN, Vandersteen JG, Pryor RJ (2003) High-resolution genotyping by amplicon melting analysis using LCGreen. Clin Chem 49: 853-860.

31. Emma P, Kamen A (2013) Real-time monitoring of influenza virus production kinetics in HEK293 cell cultures. Biotechnol Prog 29: 275-284.

32. Bodewes R, Nieuwkoop NJ, Verburgh RJ, Fouchier RA, Osterhaus AD, et al. (2012) Use of influenza A viruses expressing reporter genes to assess the frequency of double infections in vitro. J Gen Virol 93: 1645-1648.

33. Matrosovich MN, Matrosovich TY, Gray T, Roberts NA, Klenk HD (2004) Neuraminidase is important for the initiation of influenza virus infection in human airway epithelium. J Virol 78: 12665-12667.

34. van Riel D, Munster VJ, de Wit E, Rimmelzwaan GF, Fouchier RA, et al. (2007) Human and avian influenza viruses target different cells in the lower respiratory tract of humans and other mammals. Am J Pathol 171: 1215-1223.

35. Vincent AL, Ma W, Lager KM, Janke BH, Richt JA (2008) Swine influenza viruses a North American perspective. Adv Virus Res 72: 127-154.

36. Garcia-Sastre A (2011) Induction and evasion of type I interferon responses by influenza viruses. Virus Res 162: 12-18.

37. Huang IC, Li W, Sui J, Marasco W, Choe H, et al. (2008) Influenza A virus neuraminidase limits viral superinfection. J Virol 82: 4834-4843.

38. Marsh GA, Hatami R, Palese P (2007) Specific residues of the influenza A virus hemagglutinin viral RNA are important for efficient packaging into budding virions. J Virol 81: 9727-9736.

39. Marsh GA, Rabadan R, Levine AJ, Palese P (2008) Highly conserved regions of influenza a virus polymerase gene segments are critical for efficient viral RNA packaging. J Virol 82: 2295-2304.

40. Chou YY, Vafabakhsh R, Doganay S, Gao Q, Ha T, et al. (2012) One influenza virus particle packages eight unique viral RNAs as shown by FISH analysis. Proc Natl Acad Sci U S A 109: 9101-9106.

41. Fujii K, Fujii Y, Noda T, Muramoto Y, Watanabe T, et al. (2005) Importance of both the coding and the segment-specific noncoding regions of the influenza A virus NS segment for its efficient incorporation into virions. J Virol 79: 3766-3774.

42. Fujii Y, Goto H, Watanabe T, Yoshida T, Kawaoka Y (2003) Selective incorporation of influenza virus RNA segments into virions. Proc Natl Acad Sci U S A 100: 2002-2007.

43. Muramoto Y, Takada A, Fujii K, Noda T, Iwatsuki-Horimoto K, et al. (2006) Hierarchy among viral RNA (vRNA) segments in their role in vRNA incorporation into influenza A virions. J Virol 80: 2318-2325.

44. Fournier E, Moules V, Essere B, Paillart JC, Sirbat JD, et al. (2012) A supramolecular assembly formed by influenza A virus genomic RNA segments. Nucleic Acids Res 40: 2197-2209.

45. Hutchinson EC, Curran MD, Read EK, Gog JR, Digard P (2008) Mutational analysis of cis-acting RNA signals in segment 7 of influenza A virus. J Virol 82: 11869-11879.

46. Palese P, Shaw ML (2006) Orthomyxoviridae: The Viruses and Their Replication. In: Knipe DMH, P. M., editor. Fields Virology. Philidelphia: Lippincott-Raven. pp. 1647-1690.

47. Inagaki A, Goto H, Kakugawa S, Ozawa M, Kawaoka Y (2012) Competitive incorporation of homologous gene segments of influenza A virus into virions. J Virol 86: 10200-10202.

48. Hughes J, Allen RC, Baguelin M, Hampson K, Baillie GJ, et al. (2012) Transmission of equine influenza virus during an outbreak is characterized by frequent mixed infections and loose transmission bottlenecks. PLoS Pathog 8: e1003081.

49. Murcia PR, Baillie GJ, Daly J, Elton D, Jervis C, et al. (2010) Intra- and interhost evolutionary dynamics of equine influenza virus. J Virol 84: 6943-6954.

50. Murcia PR, Hughes J, Battista P, Lloyd L, Baillie GJ, et al. (2012) Evolution of an Eurasian avian-like influenza virus in naive and vaccinated pigs. PLoS Pathog 8: e1002730.

51. Lowen AC, Mubareka S, Tumpey TM, Garcia-Sastre A, Palese P (2006) The guinea pig as a transmission model for human influenza viruses. Proc Natl Acad Sci U S A 103: 9988-9992.

52. Fodor E, Devenish L, Engelhardt OG, Palese P, Brownlee GG, et al. (1999) Rescue of influenza A virus from recombinant DNA. J Virol 73: 9679-9682.

53. Steel J, Lowen AC, Mubareka S, Palese P (2009) Transmission of influenza virus in a mammalian host is increased by PB2 amino acids 627K or 627E/701N. PLoS Pathog 5: e1000252.

54. Li ZN, Mueller SN, Ye L, Bu Z, Yang C, et al. (2005) Chimeric influenza virus hemagglutinin proteins containing large domains of the Bacillus anthracis protective antigen: protein characterization, incorporation into infectious influenza viruses, and antigenicity. J Virol 79: 10003-10012.

Figure Legends

Figure 1. rPan/99 wt and var viruses show similar growth phenotypes in MDCK cells and guinea pigs. A) MDCK cells were infected at an MOI of 0.001 PFU/cell with the indicated viruses. For rPan/99wt-HIS virus, n=6 dishes; for rPan/99var2-HA virus, n=3 dishes. B) Groups of three guinea pigs were inoculated intranasally with 1000 PFU of the indicated virus. Virus titers in nasal washings are plotted vs. day post-infection. Average values +/- standard deviations are shown.

Figure 2. Identification of wild-type and variant virus gene segments by high resolution melt analysis. Examples of the Difference RFU (relative fluorescence units) curves generated by the Precision Melt Analysis software are shown for each vRNA segment. Curves colored red clustered with the rPan/99wt control and curves colored green clustered with the rPan/99var control.

Figure 3. Reassortment in cultured cells is efficient under unbiased conditions. The results are shown of HRM genotyping analysis of 121 plaque isolates obtained from each of two culture dishes of MDCK cells co-infected at high MOI (10 PFU/cell). In A, 108/121 (89.3%) had reassortant genotypes and in B, 106/121 (87.6%) had reassortant genotypes. This experiment was done in the presence of trypsin. Green coloring indicates a segment derived from rPan/99var virus; red coloring indicates a segment derived from Pan/99wt virus; white indicates a segment that was untyped. The right-most column in each chart shows the overall genotype: green for var, red for wt and blue for reassortant.

Figure 4. Frequency of reassortment increases exponentially with frequency of co-infection. MDCK cells were infected simultaneously at the indicated MOIs with rPan/99wt and rPan/99var viruses carrying His and HA tags, respectively. At 12 h post-infection, cells were collected for flow cytometric analysis to determine co-infection frequency and cell culture medium was collected for genotyping of released virus. To prevent multiple cycles of replication, infections were performed in the absence of trypsin. Average values (n=2 cell culture dishes) +/- standard deviation are shown. The coefficient of determination (R2) value indicates how well the exponential trend line fits the data.

Figure 5. Super-infection delayed by up to 12 h allowed robust co-infection and by up to 8 h allowed robust reassortment in cell culture. MDCK cells were infected at MOI 10 PFU/cell with rPan/99var2-HA virus at 0 h and then super-infected at MOI 10 PFU/cell with rPan/99wt-HIS virus after the indicated time interval. Clonal isolates from supernatant collected 12 h after the wt virus infection were obtained and genotyped to determine the % reassortment. Flow cytometry was performed on the harvested cells to determine % co-infection. To prevent multiple cycles of replication, infections were performed in the absence of trypsin. Average values (n=2 cell culture dishes) +/- standard deviations are shown.

Figure 6. Infections separated by less than 18 h led to robust reassortment in vivo. Groups of three guinea pigs were infected with 1000 PFU rPan/99var virus and, either at the same time (0 h group), or after the indicated time interval, infected with 1000 PFU rPan/99wt virus. Plaque isolates derived from nasal washings collected 48 h after wt virus infection were genotyped by HRM analysis. The average +/- standard deviation of the percentage of isolates with reassortant genotypes is shown.

Figure 7. Viral spread in cell culture leads to increased frequency of co-infected cells when super-infection is delayed by 8 or 12 hours. MDCK cells were infected in the presence of trypsin at an MOI of 0.01 PFU/cell with each virus, simultaneously (0 h), or first with the var virus and then with the wt virus at the times indicated. Cell monolayers were collected and processed for flow cytometry 12 h after the wt virus infection. The average (n=3) percentage of infected cells that were co-infected is plotted. Error bars indicate standard deviation.

Table S1. Nucleotide sequences of primers used for HRM analysis.

Virus[1]	Segment	Silent mutations	Forward Primer	Reverse Primer
rPan/99var	NS	C329T, C335T, A341G	acctgcttcgcgatacataac	aggggtccttccacttttg
rPan/99var	M	C413T, C415G, A418C	gcactcagttattctgctggtg	aatgccacttcggtggttac
rPan/99var	NA	C418G, T421A, A424C	tcatgcgatcctgacaagtg	tgtcatttgaatgcctgttg
rPan/99var	NP	C537T, T538A, C539G	caacataccagaggacaagagc	accttctagggagggtcgag
rPan/99var	HA	T308C, C311A, C314T, A464T, C467G, T470A	ccttgatggagaaaactgcac	caacaaaaaggtcccattcc
rPan/99var-2-HA	PA	G603A, T604A, C605G	caagaaatggccaacagagg	tgcgcatagttcctgagattt
rPan/99var-2-HA	PB1	C346T, T348G, A351G	gctatggccttccttgaaga	tgtccacccttgtttgttga
rPan/99var-2-HA	PB2	T621C, T622A, C623G	aaagaagaactccgagattgc	ttgttccgccagcaactg
rPan/99var-6	PA	A342G, G333A	tgcaacactactggagctgag	ctccttgtcactccaatttcg
rPan/99var-6	PB1	C288T, T297C	aacccaattgatggaccact	gatccctgggtgggattc
rPan/99var-6	PB2	C354T, C360T	tggaatagaaatggacctgtga	ggttccatgttttaacctttcg

Primers were used to differentiate the segments of the indicated var virus from those of the wt virus. Since the NS, M, NA, NP and HA segments of rPan/99var2-HA and rPan/99var6 viruses are identical, the generalized term rPan/99var is used.

Table 1. The frequency of reassortment in vivo is dependent on inoculum dose

Guinea pig	Inoculum dose	Input mixture[2]		Genotypes of virus isolates (%)[3]		
no.	(log_{10}PFU/ml)	% wt	% var	Reassortant	wt	var
1	3	60	40	24	67	9
2	3	60	40	53	47	0
3	3	60	40	10	86	5
4	3	52	48	20	70	10
5	3	52	48	42	32	26
6	6	50	50	65	5	30
7	6	50	50	46	0	54
8	6	50	50	86	0	14
9	6	54	46	48	48	5
10	6	54	46	48	48	5

1 The difference in % reassortants between 103 and 106 groups was found to be significant, with p=0.03 (Student's T-test)
2 n was 30 for 1, 2, 3, 6, 7, and 8; n was 25 for 4 and 5; n was 26 for 9 and 10.
3 n ranged from 19 to 24

Table 2. Super-infection up to 12 h after primary infection leads to robust reassortment in vivo.

Guinea pig no.	Time interval (h)	Prevalence of HA RNA in bulk nasal wash fluid (Ct value)[1]		Genotypes of virus isolates (%)[2]		
		HAwt	HAvar	Reassortant	wt	var
1	0[3]	25.0	24.6	14	52	33
2	0	26.0	25.6	18	27	55
3	0	25.3	26.4	33	57	10
4	6	28.1	27.1	29	29	43
5	6	26.2	26.8	14	64	23
6	6	24.8	25.2	19	62	19
7	12	25.4	25.6	42	33	26
8	12	27.2	26.7	45	23	32
9	12	26.2	24.6	57	0	43
10	18	29.1	23.3	10	5	86
11	18	25.7	23.0	5	24	71
12	18	29.8	23.2	5	0	95
13	24	31.5	22.7	0	0	100
14	24	33.7	26.0	0	0	100
15	24	32.5	25.8	0	0	100
[4]wt	n/a	27.9	>40	n/a	n/a	n/a
[4]var6	n/a	>40	25.9	n/a	n/a	n/a

[1] Quantitative PCR was performed using primers specific for wild-type or var virus HA segments. Average of two replicates is shown. Ct values < 35 were considered indicative of productive infection.
[2] n=19-22 virus isolates from each guinea pig
[3] The proportion of wt and var viruses present in the inoculum for the 0h group was 61% and 39%, respectively (n=25).
[4] wt and var6 controls are nasal washes collected from guinea pigs singly infected with each virus.

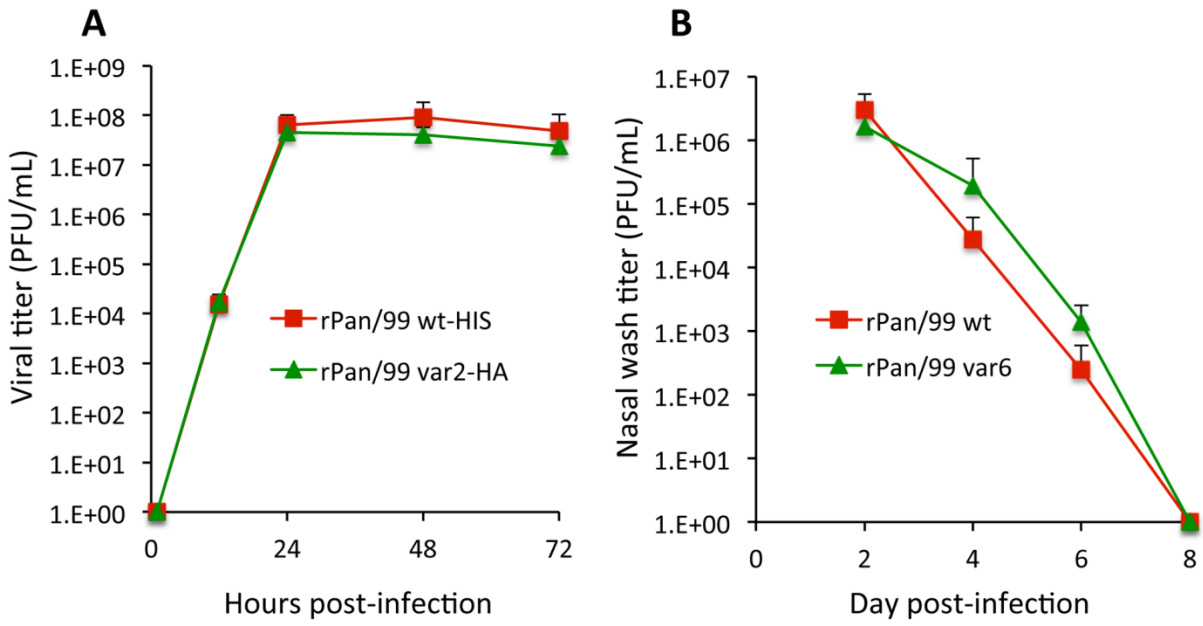
A
1.E+09
1.E+08
1.E+07
1.E+06
1.E+05
1.E+04
1.E+03
1.E+02
1.E+01
1.E+00
Viral titer (PFU/mL)
0
24
48
72
Hours post-infection
rPan/99 wt-HIS
rPan/99 var2-HA
B
1.E+07
1.E+06
1.E+05
1.E+04
1.E+03
1.E+02
1.E+01
1.E+00
Nasal wash titer (PFU/mL)
0
2
4
6
8
Day post-infection
rPan/99 wt
rPan/99 var6

Figure 1

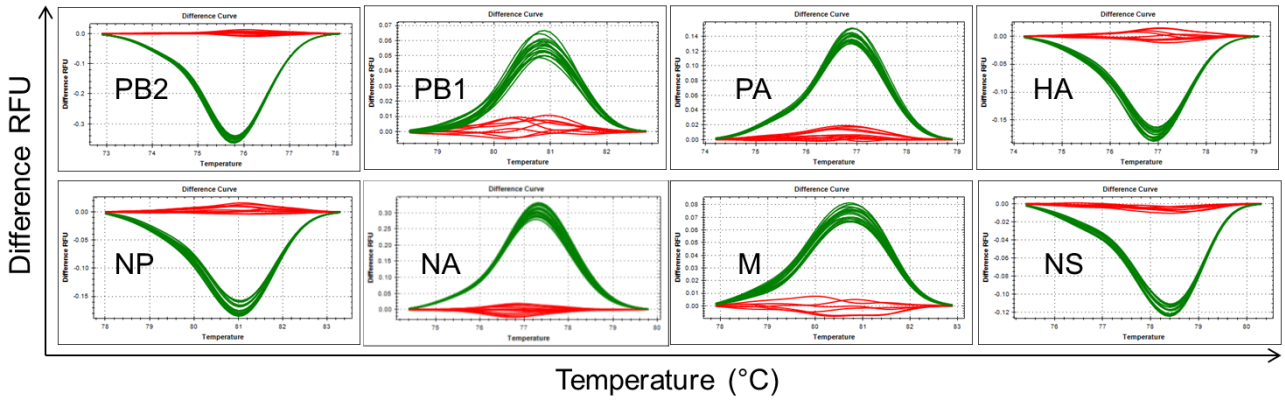

Figure 2

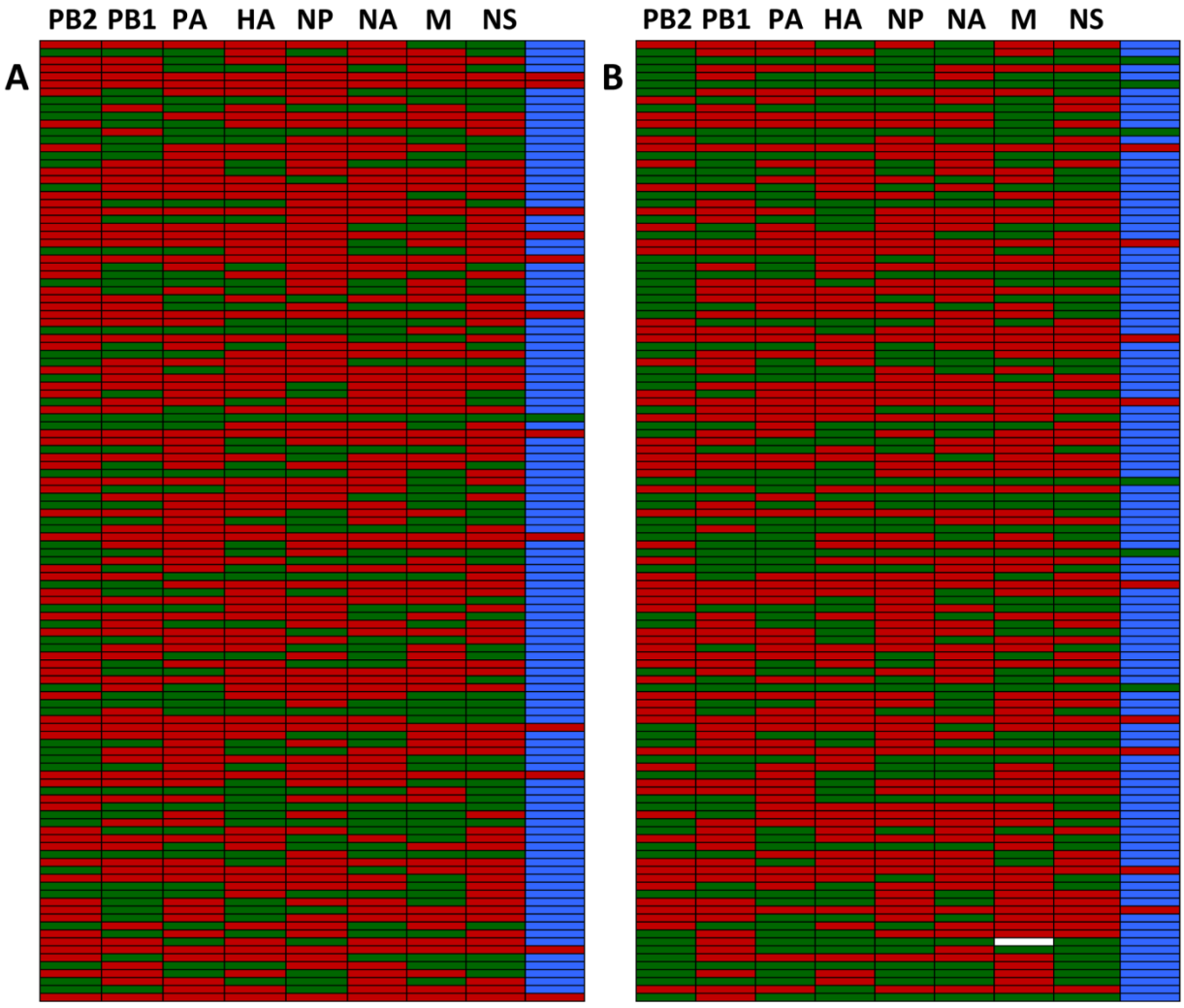

Figure 3

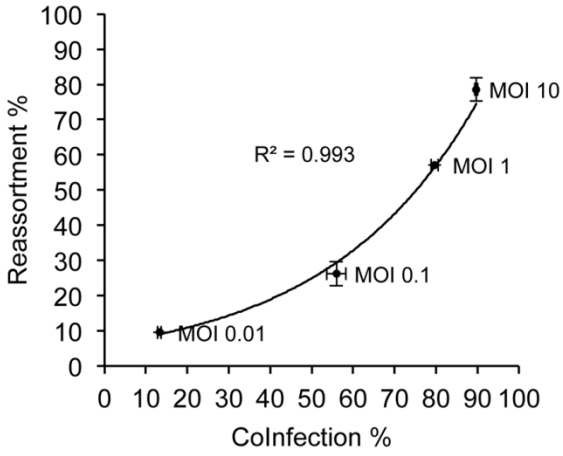
100
90
80
70
60
50
40
30
20
10
0
Reassortment %
0 10 20 30 40 50 60 70 80 90 100
CoInfection %
R² = 0.993
MOI 10
MOI 1
MOI 0.1
MOI 0.01

Figure 4

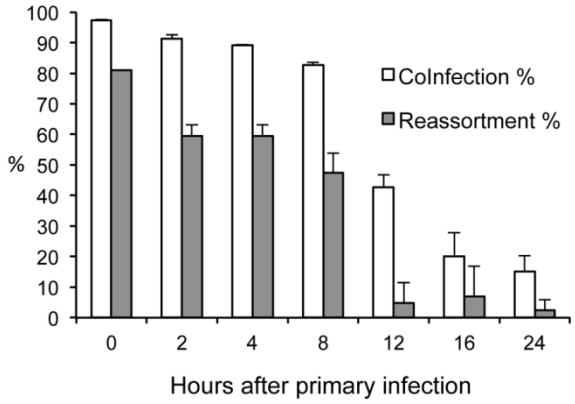
100
90
80
70
60
%
50
40
30
20
10
0
CoInfection %
Reassortment %
0
2
4
8
12
16
24
Hours after primary infection

Figure 5

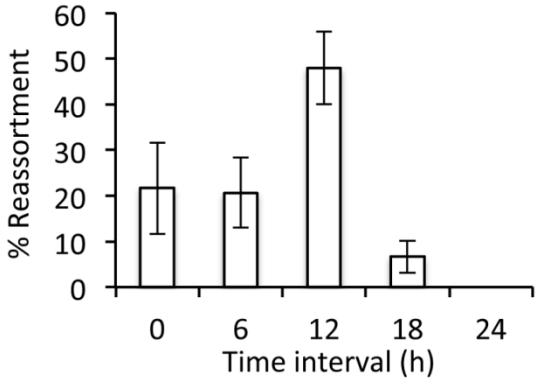

Figure 6

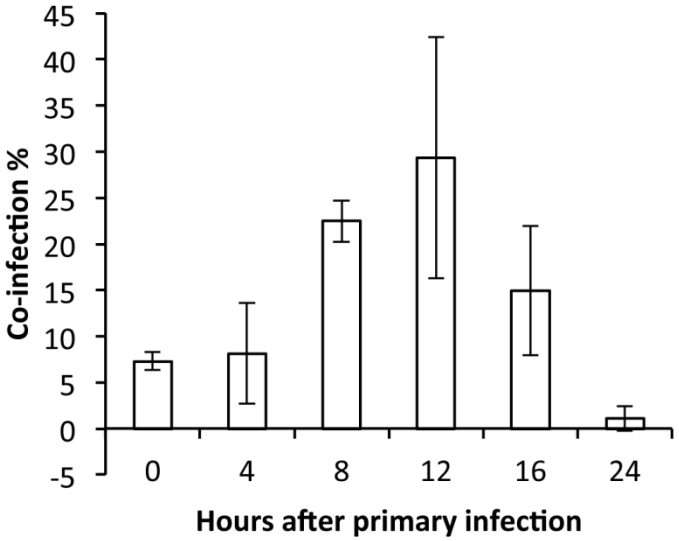
45
40
35
30
25
20
15
10
5
0
-5
Co-infection %
0
4
8
12
16
24
Hours after primary infection

Figure 7

Chapter 3: Influenza virus reassortment is enhanced by semi-infectious particles but can be suppressed by defective interfering particles

Judith M. Fonville#1, Nicolle Marshall#2, Hui Tao, John Steel and Anice C. Lowen*

#These authors contributed equally to the work described

The work of this chapter was published in 2015 in *PLoS Pathogens*

Article citation:

Fonville JM, Marshall N, Tao H, Steel J, Lowen AC (2015) Influenza Virus Reassortment is Enhanced by Semi-Infectious Particles but Can Be Suppressed by Defective-Interfering Particles. PLoS Pathog 11(10): e1005204.

doi:10.1371/journal.ppat.1005204

Abstract

A high particle to infectivity ratio is a feature common to many RNA viruses, with ~90-99% of particles unable to initiate a productive infection under low multiplicity conditions. A recent publication by Brooke et al. revealed that, for influenza A virus (IAV), a proportion of these seemingly non-infectious particles are in fact semi-infectious. Semi-infectious (SI) particles deliver an incomplete set of viral genes to the cell, and therefore cannot support a full cycle of replication unless complemented through co-infection. In addition to SI particles, IAV populations often contain defective-interfering (DI) particles, which actively interfere with production of infectious progeny. With the aim of understanding the significance to viral evolution of these incomplete particles, we tested the hypothesis that SI and DI particles promote diversification through reassortment. Our approach combined computational simulations with experimental determination of infection, co-infection and reassortment levels following co-inoculation of cultured cells with two distinct influenza A/Panama/2007/99 (H3N2)-based viruses. Computational results predicted enhanced reassortment at a given % infection or multiplicity of infection with increasing semi-infectious particle content. Comparison of experimental data to the model indicated that the likelihood that a given segment is missing varies among the segments and that most particles fail to deliver ≥1 segment. To verify the prediction that SI particles augment reassortment, we performed co-infections using viruses exposed to low dose UV. As expected, the introduction of semi-infectious particles with UV-induced lesions enhanced reassortment. In contrast to SI particles, inclusion of DI particles in modeled virus populations could not account for observed reassortment outcomes. DI particles were furthermore found experimentally to

suppress detectable reassortment, relative to that seen with standard virus stocks, most likely by interfering with production of infectious progeny from co-infected cells. These data indicate that semi-infectious particles increase the rate of reassortment and may therefore accelerate adaptive evolution of IAV.

Author Summary

Since the genome of influenza A virus has eight non-contiguous segments, two influenza A viruses can exchange genes readily when they infect the same cell. This process of reassortment is important to the evolution of the virus and is one reason why this pathogen is constantly changing. It has long been known that a large proportion of the virus particles that influenza and many other RNA viruses produce are not fully infectious, but the biological significance of these particles has remained unclear. Here we show that virus particles that deliver incomplete genomes to the cell enhance the rate of reassortment. Thus, despite their limited potential to produce progeny viruses, these incomplete particles may play an important role in viral evolution.

Introduction

The influenza A virus (IAV) genome comprises eight segments of negative sense RNA, each of which encode at least one essential viral protein [1,2]. This genome structure supports the generation of viral diversity through two major mechanisms: genetic drift due to an error prone viral polymerase, and exchange of gene segments between viruses through reassortment [3]. While drift allows the accumulation of small changes over time, reassortment allows substantial genetic change to occur quickly. Reassortment is highly prevalent among avian and swine IAVs and has been implicated repeatedly in the

emergence of epidemically significant human strains [reviewed in 4]. The 1957, 1968 and 2009 pandemic strains arose through reassortment involving seasonal human strains and viruses adapted to avian and/or swine hosts [5-7]. In addition, reassortment among co-circulating human IAVs facilitated the spread worldwide of adamantane resistant H3N2 viruses and has brought about unusually severe seasonal epidemics including the Fujian-like outbreak in 2003/2004 [8-11]. The potential for reassortment to purge the viral genome of deleterious changes and bring together multiple beneficial mutations makes it a powerful catalyst of viral evolution [12].

The ratio of total particles to plaque forming units for influenza and other RNA viruses is on the order of 10:1 to 100:1 [13-17]. Thus, only ~1-10% of virions are thought to initiate productive infection of a cell under low multiplicity conditions of infection. The precise make up of the remaining virus particles is not clear but is likely a mixture of virions carrying qualitatively different defects [18,19]. Some may be non-infectious in that they fail to deliver viral RNA to the site of replication due to the lack of a genome, defects at the protein level, or a stochastic failure to initiate infection. Some may be classical defective-interfering (DI) particles, which carry one or more segments with a large internal deletion and act as parasites, hindering the production of fully infectious progeny [20-23]. Some will harbor a lethal point mutation in one or more segments [24,25]. Finally, some virions may be semi-infectious particles, which deliver fewer than eight segments to the nucleus [26,27]. Like DI particles and those with a lethal point mutation, SI particles cannot complete the viral life cycle. In contrast to these other particle types, however, SI virions do not carry a defective gene and are therefore not expected to interfere with the production of infectious progeny in the context of co-infection. Support

for the existence of semi-infectious particles was recently gleaned through a careful analysis of viral protein expression in individual infected cells [27]. The majority of cells infected at low multiplicity failed to express one or more viral proteins, suggesting that the corresponding genes were disrupted or missing entirely from the viral genome. In that study, the probability of any segment being present and functional was estimated to be 0.781, which suggests that semi-infectious particles outnumber fully infectious particles by 6:1 [27].

In terms of their potential biological significance, there is an important difference between non-infectious and DI or SI particles. Any genetic material packaged into non-infectious particles will not be replicated. In contrast, under high multiplicity conditions, the genomes of DI and SI particles can be propagated through complementation by a co-infecting virus. This phenomenon of complementation, termed multiplicity reactivation, yields a greater number of infected and co-infected cells than would be predicted based on infectious titers determined at limiting dilution [28,29]. In addition, fully infectious viral progeny emerging from cells co-infected with only DI and/or SI viruses would necessarily be reassortant. Due to the anticipated increase in co-infected cells and the requirement for reassortment to yield fully infectious progeny from two incomplete parents, we hypothesized that the presence of DI or SI particles in an influenza virus population would promote genetic diversification through reassortment.

We tested this hypothesis using a combination of computational and experimental approaches. Our previously described system [30] for studying reassortment in the absence of fitness differences among parental and progeny strains was central to the experimental work and allowed the development of a relatively simple and robust model.

Viral infection of cultured cells with two phenotypically identical viruses was simulated computationally at a range of multiplicities of infection. The model was then used to indicate expected relationships among infection, co-infection and reassortment in the absence and presence of increasing levels of semi-infectious particles. We tested the model by comparing co-infection with standard virus stocks to that with viruses that were UV irradiated to artificially increase SI particle content. By comparing experimental outcomes to the model, we were able to estimate semi-infectious particle content of non-irradiated virus stocks and obtained results in agreement with those of Brooke et al. indicating a high proportion of SI particles in IAV populations [27]. Our results furthermore suggest that the frequency with which each of the eight segments is missing from a virion varies among the segments. When the effect of DI segments was tested in the model, we found that their presence could promote or suppress reassortment relative to theoretical "perfect" virus stocks, depending on the potency with which a modeled DI segment interfered with infectious progeny production. To test the effect of DI particles experimentally, we used serial passage at high MOI to enrich for DI particles and studied co-infection with these virus stocks. The results indicated that DI segments reduce measured reassortment efficiency relative to standard virus stocks. Reassortment levels observed with DI-rich viruses were, however, higher than those predicted in the absence of any type of defective particle. In sum, we show herein that delivery of incomplete or defective genomes to target cells promotes reassortment by increasing the proportion of productively infected cells that are co-infected.

Results

Computational modeling of influenza virus infection, co-infection and reassortment.

To determine the expected relationships between infection, co-infection and reassortment, we performed simulations where a 1:1 mixture of viruses of type A and B were randomly distributed over a computational set of cells (see Methods for details). Multiplicity of infection (MOI) was varied. For each MOI, we evaluated all cells and determined which were infected (defined as cells infected with A, B or A and B) and which were co-infected (with A and B). We calculated the % reassortment expected for each infected cell, taking into account the number of virions of each virus type present and allowing the segments to assort at random [30]. For example, cells that are infected with only a single virus type will produce 0% reassortant progeny, while cells infected with one of each type are expected to produce 99.22% reassortant progeny. The average % reassortment for all cells was then calculated to reflect the pool of progeny viruses released from all infected cells.

The results, shown in Fig. 1, indicate that % co-infection and % reassortment depend in a non-linear, but monotonically increasing fashion, on the % infection. For low levels of infection, the likelihood of infections with multiple virus types is small; hence the % co-infection is low. To illustrate the interrelationship among % infection, % co-infection and % reassortment, we offer an example: at a low level of co-infection of 3.3%, where infection was 32.87%, the average expected % reassortment is calculated to be 9.899%. This result makes sense because ~10% of infected cells are co-infected and these co-infected cells are expected to produce nearly 100% reassortant viruses, while the infected cells that are not co-infected will produce only parental (type A or B) progeny.

Impact on predicted co-infection and reassortment levels of introducing semi-infectious particles into the model.

Because they deliver an incomplete genome to the site of replication, semi-infectious particles (SI particles) are expected to affect levels of reassortment. To evaluate how the relationships among reassortment, infection and co-infection are impacted by incomplete virions, we introduced SI particles into the simulated A and B virus populations and varied their prevalence using the parameter P_P. The value assigned to P_P indicates the probability that a given segment is present in a virus particle. (Note that a segment that is not "present" could be physically missing from the particle or, alternatively, could fail to be delivered to the site of replication.) We initially assigned the same P_P value to all eight segments and explored a range of values between 0.3 (where the probability that a virion has all eight segments is $0.3^8=6.5x10^{-5}$) and 1 (where all virions contain eight segments). The presence of SI particles in a virus population gives rise to different types of infected cells: those that express HA and those that do not, and those that produce virus and those that do not. Thus, to allow meaningful discussion of the impact of SI particles on infection, co-infection and reassortment, we have generated the lexicon presented in Table 1. Within a simulated co-infection we are able to monitor all infected cells; that is, all cells into which a virus enters. For the purposes of comparing results of the simulation to those of the experimental co-infections described below, however, it is useful to also monitor cells that are expected to express HA protein on their surface. In the model, we defined an HA positive cell as an infected cell that has at least one copy of PB2, PB1, PA, NP and HA gene segments [31,32]. Given that some semi-infectious particles may lack one or more of these segments, a cell can be infected but be HA negative. To count

as dually HA positive (i.e. expressing HAs of both type A and B viruses), a cell must have copies of both HA segments and at least one copy of PB2, PB1, PA and NP segments. Thus, a cell can be co-infected (at least one virus A and one virus B entered the cell), but only express one (or none) of the HA types, depending on the segments present in the type A and B viruses.

Fig. 2A monitors the cells that were infected and co-infected, regardless of the presence of segments needed for HA expression, and shows that the results are insensitive to parameter P_P. This outcome is as expected since the absence of segments does not alter infection status. However, when studying HA positive cells and dually HA positive cells, the results vary with P_P (Fig. 2B). For a given % HA positive cells, the % dually HA positive cells increases as more viral genomes become incomplete (lower P_P). This observation can be explained as follows. To achieve a given percentage of HA positive cells with more incomplete genomes, the number of virions per cell must increase to allow sufficient complementation. If the number of virions per cell (i.e. the MOI) is increased, the percentage of cells that are dually HA positive will also rise.

Similarly, missing segments will affect reassortment: a cell infected with one virion of type A and one virion of type B, both missing a different segment and thus complementing the other, will by definition produce 100% reassortant progeny. However, missing segments can also prevent progeny from being made, as at least one copy of each of the 8 segments is required to produce progeny in the model. In Fig. 2C, reassortment levels expected under various conditions of P_P were calculated by averaging the expected % reassortment across all cells that were able to produce progeny. The results show that average % reassortment readily increases as P_P is lowered and more

viral genomes are incomplete. This observation reflects the requirement for complementation, achieved via multiple infections, for infected cells to produce progeny viruses when viral populations are characterized by lower values of P_P.

Testing of the model: co-infection and reassortment observed following co-inoculation of cells with standard virus stocks.

We performed a series of co-infections in Madin Darby canine kidney (MDCK) cells at a range of MOIs and monitored reassortment outcomes. To avoid fitness differences among parental and reassortant progeny viruses that could complicate the interpretation of results, we used our previously described A/Panama/2007/99 (H3N2) wild-type (Pan/99wt) and variant (Pan/99var) viruses. These viruses differ by silent mutations introduced into each gene segment of Pan/99var virus and by the insertion of a His epitope tag in the Pan/99wt virus vs. an HA tag in the Pan/99var virus [30]. Infections were performed in triplicate, synchronized by allowing virus attachment at 4^oC and limited to a single cycle by the addition of ammonium chloride at 3 h post-infection [33]. At 12 h post-infection, supernatants were collected to genotype released virus and cells were processed for flow cytometry to enumerate cells with surface expression of the Pan/99wt and Pan/99var HA proteins (using the His and HA epitope tags). The resultant data were analyzed by examining the relationship between i) % cells positive for any HA and % cells dually HA positive and ii) % cells positive for any HA and % reassortment (Fig. 3). The results show that both % dually HA positive cells and % reassortment increase monotonically with % HA positive cells, but with differing patterns. The % dually HA positive cells shows a nearly linear relationship with % HA positive cells. In

contrast, % reassortment increases quickly at lower levels of % HA positive cells, but plateaus at higher levels of % HA positive cells (Fig. 3).

Refinement of the model: varying P_P among the segments was necessary to achieve a fit with the experimental data.

Initial comparisons of the experimental data with the model revealed a poor match for the relationship between % HA positive cells and % dually HA positive cells, regardless of the values assigned to P_P (Fig. 4). We hypothesized that the assumption that P_P is constant among the eight segments might account for the discrepancy. We therefore modified the model to allow P_P to differ among the segments. Specifically, P_P was varied between 0.25 and 1.0 in increments of 0.25 and all possible combinations were tested, taking into account the redundancy of PB2, PB1, PA and NP as well as that of NA, M and NS in our readouts. A total of 2800 possible P_P combinations were evaluated. We quantified the fit for each of the 2800 combinations of P_P values as the sum of the distances between each experimental data point and the lines plotted using modeled results. This sum of errors was calculated for i) % HA positive cells vs. % dually HA positive cells; ii) % HA positive cells vs. % reassortment; and iii) % dually HA positive cells vs. % reassortment. The modeled results for the top 1% of P_P combinations are shown in Fig. 5 together with the experimental data. These analyses highlighted that several P_P combinations gave results that matched the experimental data well. Given the uncertainty in the experimental measurements, the lines plotted in Fig. 5 cannot be said to be meaningfully different. Additionally, the error between the experimental data and computational model varied slightly as a result of small stochastic variations in the

outcome of the computational model when the same settings were repeated, resulting in small changes and uncertainties of the rank order of the top runs. Finally, note again that there are redundancies among certain segments (PB2, PB1, PA and NP are equivalent, as are NA, M and NS). Therefore, we do not consider the parameters giving the best fit with the data (as follows for segments 1 - 8, respectively: 0.25, 0.5, 0.75, 0.75, 1, 1, 1, 1), to be the final answer. Instead, we investigated which features the top 1% of P_P combinations had in common: each included at least one segment among PB2, PB1, PA and NP with P_P=0.25; HA with P_P=0.75; and at least 3 and up to 8 segments with P_P<1.0. Taking the product of all eight P_P values yields the proportion of virions with all eight segments present, which for the best fit was 7.0%. When this proportion was determined from all sets of eight P_P values shown in Fig. 5, the range obtained was 2.2 – 9.4%. In sum, comparison of the experimental data obtained with standard virus stocks to the model revealed that, for the model to fit the data, P_P must be less than 1.0 for multiple segments and P_P of the eight segments cannot be equivalent.

Testing of the model: predicted and observed impact of UV treated particles on co-infection and reassortment outcomes.

To test the validity of our model and more rigorously evaluate the hypothesis that semi-infectious particles augment reassortment, we generated Pan/99wt and Pan/99var virus populations with increased semi-infectious particle content. This increase was achieved by exposing each virus to a low dose of UV irradiation. Since polymerase read-through of pyrimidine dimers is not possible, viral segments carrying UV lesions will not be replicated or transcribed and will behave similarly to missing segments. A UV dose

sufficient to decrease PFU titers by approximately 10-fold was used. Co-inoculation of MDCK cells with Pan/99wt and Pan/99var viruses that had been UV treated was then performed at a range of MOIs (in parallel with co-infections using standard virus stocks, described above). Again, results were analyzed by assessing the relationships among % HA positive cells, % dually HA positive cells and % reassortment. As predicted by the model, co-inoculation with UV treated viruses yielded similar levels of dually HA positive cells, but higher reassortment frequencies at intermediate levels of HA positivity, compared to co-inoculation with mock treated viruses (Fig. 6). To evaluate whether UV treatment has a statistically significant impact on % reassortment, we performed a multiple linear regression analysis of % reassortment vs. $\log_{10}$ (% HA positive), treating UV as a categorical variable. The results showed that, for every increase of 1 $\log_{10}$ (% HA positive), the % reassortment goes up by 40% ($P=3.9x10^{-16}$). Having UV treatment further increases % reassortment by 16%, and is a significant categorical variable ($P=6.6x10^{-6}$). These data support the validity of the model and specifically verify the model's prediction that increasing semi-infectious particles in a virus population enhances the production of reassortant progeny.

We also assessed whether the increase in reassortment seen with UV treatment was quantitatively related to the observed difference in infectivity between UV treated and untreated virus stocks. Analysis of results with the UV treated virus stocks indicated that the levels of reassortment and co-infection observed best matched those predicted for a virus population that had suffered 2.0 hits per genome on average (Fig. 7). Based on a Poisson distribution of UV hits per virus, this UV dose would be expected to reduce PFU titer by 7.4-fold. The observed knock-down in PFU titers with UV treatment was 11-fold.

These results are comparable, particularly when one considers the typical range of error of a plaque assay (approximately 2-fold) [34], and therefore further support the validity of the model.

Deciphering the mechanism by which SI particles promote reassortment.

We hypothesized that SI particles could augment reassortment through one of three, non-mutually exclusive, mechanisms: i) by simply increasing the number of particles entering each cell (i.e. the MOI) given a constant number of productively infected cells; ii) by increasing the frequency of reassortant viruses emerging from productively co-infected cells at a given MOI; and/or iii) by increasing the proportion of productively infected cells that are co-infected at a given MOI. To distinguish among these possibilities, we used the model to examine the impact of varying P_P *and* MOI on levels of reassortment and co-infection. To simplify this theoretical analysis, we assigned the same P_P value to all segments. When MOI was held constant and % reassortment, averaged across all productively infected cells, was plotted as a function of P_P, the result clearly showed increasing reassortment with declining P_P (Fig. 8a). This result indicates that SI particles do not act on reassortment solely by increasing MOI (item i above). When MOI was held constant and average % reassortment for only productively co-infected cells was analyzed as a function of P_P, the model indicated that levels of reassortment were high across the full range of P_P (Fig. 8b). This result reflects the high efficiency of IAV reassortment in co-infected cells and excludes item ii above as an important mechanism driving enhanced reassortment with increasing SI content. Lastly, when MOI was held constant and the ratio of productively co-infected to productively singly infected cells

was plotted as a function of P_P, the results indicated that decreasing P_P leads to an increase in the proportion of cells that are potential vessels for reassortment (Fig. 8c; note the log scale on the Y-axis). This last result reveals that mechanism iii above is functional: addition of SI particles to a virus population increases the likelihood that productively infected cells will produce reassortant viruses by changing this population of cells to be more often co-infected, even when the number of virus particles is not changed.

Modeling the impact of defective interfering particles on co-infection and reassortment outcomes.

We undertook analysis of the impact of DI particles on influenza virus reassortment to confirm that the semi-infectious particles detected in our previous analyses were not, in fact, DI particles, and to determine the potential for these naturally occurring deletion mutants to contribute to viral evolution. Similar to SI particles, DI particles deliver an incomplete genome to the site of replication. DI particles differ from SI particles, however, in that they carry one or more segments with a large internal deletion [35-38]. Importantly, these internally deleted segments have been shown to interfere with the production of infectious progeny and to accumulate over multiple rounds of replication so that they quickly outnumber the corresponding standard genome segments [22,39-43]. Thus, DI particles are expected to affect levels of reassortment in two ways: by delivering an incomplete genome and by interfering with production of infectious progeny. To evaluate how the relationships among reassortment, infection and co-infection are impacted by DI virions, we introduced DI particles into the simulated A and B virus

populations and varied their prevalence using the parameter P_I. The value assigned to P_I indicates the probability that a given segment in a virus particle is intact (i.e. does not have an internal deletion or other lethal mutation). Since the polymerase segments of DI particles are more commonly found to be defective than the remaining five segments, we assigned P_I values < 1.0 to PB2, PB1 and PA, while maintaining $P_I = 1.0$ for HA, NP, NA, M and NS segments. The interfering behavior of defective segments was controlled with the parameter DIX, the fold change in infectious progeny production attributed to each single DI segment in a productively infected cell. When DIX=0.5, a DI segment and the corresponding standard segment have equivalent likelihoods of being incorporated into progeny virions and thus half of the progeny produced will be non-infectious (carrying the DI) while half will be infectious (carrying the standard segment). Since the total number of virus particles produced by a given cell is held constant, a DI with DIX=0.5 reduces infectious progeny by half. To account for the experimental observation that DI particles accumulate over multiple passages [23,41-44], we reasoned that DIX must be less than 0.5. The true value of DIX for a given DI segment is not, however, clear from the literature, may be variable depending on the context, and may vary among differing DI segments. In our analyses, we therefore varied DIX over a range of 0.05 to 0.5 or evaluated three disparate settings of 0.01, 0.1 and 0.45. With the aim of evaluating whether DI segments (rather than missing segments) could account for the reassortment outcomes shown in Fig. 3, our initial analysis was performed with $P_P = 1.0$ for all segments.

The results of this computational analysis are shown in Fig. 9. The results obtained for P_I values of 0.25 – 1.0, independently varied among PB2, PB1 and PA in increments of

0.25, are displayed, with DIX set to 0.01 (very potently interfering), 0.1 (potently interfering) and 0.45 (mildly interfering) in panels A, B and C, respectively. Note that stochastic effects occur in the simulations at low values of P_I and/or P_P due to a low "n" of computational cells producing the computational virus that is analyzed. These stochastic effects give rise to the noisy peaks seen in Fig. 9 and later figures. The results with DIX of 0.01 reveal that very potently interfering DI segments are expected to suppress the production of infectious reassortant progeny viruses. When DIX was set to a more moderate value of 0.1, predicted levels of reassortment fell either above or below those for virus stocks in which all particles are complete, depending on the P_I values used. In contrast, regardless of P_I, virus stocks carrying mildly interfering DI segments (represented with DIX=0.45) were predicted to result in higher reassortment levels than virus stocks with only complete genomes. To test whether the reassortment outcomes observed experimentally with Pan/99wt and Pan/99var standard virus stocks could be accounted for by the presence of mildly interfering DI segments, we overlaid the experimental data with the modeled predictions for DIX=0.45 and the broad range of P_I value combinations analyzed previously (Fig. 9D). All conditions tested yielded % reassortment values lower than those seen experimentally. This result indicates that DI particles do not underlie the relatively high levels of reassortment observed with our standard virus stocks, and furthermore provides a theoretical prediction that DI particles will suppress reassortment relative to standard virus populations. We also evaluated a potential role for defective segments that carry a lethal point mutation rather than a deletion. Such mutations can arise in all eight segments and do not confer a competitive advantage upon the segment carrying them [40]. We therefore varied P_I for all eight

segments in the model and assigned DIX=0.5. These parameters also did not allow a good match between modeled and experimental results (S1 Fig.). Thus, the presence of defective segments is not sufficient to explain the levels of reassortment as a function of % HA positive cells seen in Pan/99wt and Pan/99var virus co-infection.

Testing of the model: observed impact of defective interfering particles on co-infection and reassortment outcomes.

To test the model of IAV reassortment in the presence of DI particles, and differentiate among the outcomes predicted for differing values of DIX, we evaluated reassortment and HA positivity following co-infection with virus stocks that carried high levels of DI particles. Virus stocks rich in DI particles were generated by serial passage of Pan/99wt and Pan/99var viruses at high MOI in MDCK cells. As expected, an increase in the ratio of genome copy number to PFU, relative to the standard virus stocks, was observed with increasing passage number (Fig. 10). We selected passage 3 (P3) and P4 virus stocks for further experiments since both wt and var viruses at these passage numbers showed >10-fold increases in the ratio of genome copy number to PFU, while the very low titers of the P5 viruses precluded their use. To confirm the presence of DI segments, we used an RT qPCR assay in which RNA copy number (relative to standard "P0" stocks) detected with primers binding near the 3' end of the vRNA was compared to that obtained with primers binding internally, in a region typically deleted within DI segments [37,38]. The proportion of viral gene segments that were intact (P_I), relative to P0 stocks, was calculated as described in the Methods and is reported in Table 2. The results reveal low

P_I values for PB2, PB1 and/or PA segments of the P3 and P4 viruses, confirming that high proportions of these segments carried internal deletions (Table 2).

To evaluate the consequences of DI particles for co-infection and reassortment frequencies, we co-inoculated MDCK cells with standard Pan/99wt (P0wt) and Pan/99var (P0var) viruses, P3wt and P3var viruses, or P4wt and P4var viruses at a range of MOIs. To allow comparison among P0, P3 and P4 viruses on a per particle level, multiplicities of infection were based on RNA copy number of the three shortest segments (NS, M and NA) rather than infectious titers. Infections were performed in triplicate and synchronized by allowing virus attachment at 4^{o}C. At 12 h post-infection, supernatants were collected to genotype released virus and cells were processed for flow cytometry to enumerate Pan/99wt and Pan/99var infected cells. Trypsin was excluded but, in contrast to the infections described above, we did not add ammonium chloride at 3 h post-infection. Data were analyzed by examining the relationships between i) % HA positive cells and % HA dually positive cells, ii) % HA positive cells and % reassortment and iii) the proportion of HA positive cells that were dually HA positive and % reassortment (Fig. 11). The results show enhanced frequencies of dually HA positive cells at a given % HA positive for the P3 and P4 virus stocks relative to P0 stocks (Fig. 11A). This observation likely reflects the need for complementation to support the expression of an HA gene carried by a DI particle. Despite the occurrence of such complementation and detection of abundant dually HA positive cells, relatively few reassortant progeny viruses emerged from P3 and P4 virus co-infections (Fig. 11B). This result is very clear when % reassortment is plotted against the proportion of HA positive cells that were dually HA positive (Fig. 11C). Even when a high proportion of cells (up to 0.9) were dually HA

positive and therefore infected with both wt and var viruses, co-infection with the P3 or P4 viruses stocks yielded <25% reassortment. As suggested by the model, this reduction in reassortant progeny relative to that produced by the P0 viruses is likely due to the interfering effects of short, DI, segments [45]. In other words, the predominance of progeny viruses with a parental genotype suggests that cells within the P3 or P4 co-infected dishes that are singly infected with a fully infectious virus produce the majority of the infectious progeny, even when such cells represent a small proportion of HA positive cells (Fig. 11C). In sum, these data demonstrate that, as predicted by the model, the DI rich P3 and P4 virus stocks gave rise to fewer reassortant viruses compared to standard virus stocks.

Comparison of experimental and theoretical reassortment outcomes suggests that $P_P \approx 1.0$ for DI rich virus stocks.

We next compared the experimental results obtained with the P3 and P4 virus stocks to the model directly by overlaying the observed data points with the modeled predictions for % HA positive cells vs. % reassortment and % HA positive cells vs. % dually HA positive cells. In each case, P_I parameters measured for the P3 and P4 viruses stocks (Table 2) were used and DIX was varied from 0.05 to 0.5 in increments of 0.05. Since our results indicated that P_P was less than 1.0 for the standard Pan/99wt and Pan/99var virus stocks, we set P_P within the model to those values found above to yield the best fit between modeled and experimental data (Fig. 5). The results, shown in Fig. 12A-D, indicated that, when combined with P_P values of 0.25, 0.5, 0.75, 0.75, 1.0, 1.0, 1.0, 1.0 for segments 1-8, respectively, the presence of DI particles at levels seen in the P3 and P4

virus stocks is expected to yield very high % reassortment across nearly all levels of % HA positive cells. In other words, when parameterized in this way, the model did not match the data. We therefore evaluated the outcomes when P_P was set to 1.0 for all segments and P_I to those measured for P3 and P4 virus stocks (Fig. 12E-H). Although the model gave a range of predictions depending on the value assigned to DIX, the results obtained with $P_P = 1.0$ (or $P_P = 0.9$; S2 Fig.) for the DI-containing viruses were consistent with those observed following P3 and P4 virus co-infections. One explanation for this result is that short, DI, segments may be packaged (or delivered to the site of infection) more efficiently than standard segments.

To further explore the inter-relationships among P_P, P_I and DIX, we tested a range of theoretical settings for each parameter within the model and show 12 representative results for % HA positive cells vs. % reassortment in S3 Fig. The theoretical outcomes displayed indicate that there is a complex interplay among P_P, P_I and DIX in determining reassortment levels. Importantly, the presence of mildly interfering DI segments (i.e. those with DIX near to 0.5) in virus populations is predicted to enhance reassortment under all P_P conditions tested. This result indicates that a combined effect of missing segments and mildly interfering DI segments could lead to reassortment levels comparable to those observed experimentally with our standard Pan/99wt and Pan/99var virus stocks. As shown in Fig. 9D, however, inclusion of DI segments but not missing segments in the theoretical virus populations is insufficient to account for the experimental reassortment data.

Discussion

The results of both simulated and experimental IAV co-infections indicate that the presence of incomplete particles in parental virus populations enhances the frequency with which reassortant progeny viruses emerge. Our results suggest that both non-interfering, semi-infectious particles and classical defective interfering particles can act to enhance reassortment above that expected for theoretical virus populations that carry only intact genomes. The extent to which DI particles can enhance reassortment is limited, however, by the interference with infectious progeny production imposed by DI segments. As a consequence of this interference, DI particles suppress reassortment relative to that seen with standard, biological, virus stocks.

Higher average reassortment levels seen with SI particles are not due to increased efficiency of reassortment within individual co-infected cells, but rather are brought about by an increase in the proportion of productively infected cells that are co-infected when SI particles are present. This mechanism differentiates reassortment outcomes between virus populations containing and lacking SI particles even when the total number of particles entering each cell is unchanged. In addition, if instead of holding MOI constant one considers a constant number of infected cells, the particle number required to reach a given level of infection will be higher for parental viruses carrying SI particles. In this situation, the resultant increase in MOI will lead to more co-infection and more reassortment. Thus, SI particles could enhance reassortment by two mechanisms in an infected host. The former mechanism will be more important if the total number of virus particles that can be produced in an infected tissue is limiting, while the latter would be more important if the total number of cells that can be infected is limiting.

The results of Brooke et al. indicate that IAV of diverse strain backgrounds and grown under a range of culture conditions (including in vivo) carry a high proportion of SI particles [18,27]. These results were based on the expression of an incomplete set of viral proteins in cells infected at low multiplicity. Herein, we confirm the presence of SI particles in an additional strain background (Pan/99) and using a distinct methodology (tracking reassortment) to detect SI particles. Our analyses yielded a range of possible values for the probability of a segment being present and, while our results clearly show that P_P is not equivalent among the segments, they do not allow more precise definition of P_P. Nevertheless, our results are consistent with the average P_P value for all eight segments estimated by Brooke et al. for an influenza A/Puerto Rico/8/34 (H1N1) virus (average P_P of Brooke et al. = 0.781; averages among our 28 best P_P settings ranged from 0.65 to 0.78). Coupled with the finding reported herein that SI particles enhance reassortment efficiency, their detection in diverse strain backgrounds suggests that these incomplete virions play a significant role in the evolution of influenza viruses.

Reassortment among variants within a viral population is expected to act like sexual reproduction of cellular organisms in that it allows the combination of multiple adaptive mutations within a single genome, as well as separation of lethal or fitness decreasing changes in one segment from adaptive changes in another segment. In these ways, reassortment is predicted to increase the rate of evolution of a diverse viral population under selection pressure [12,46]. Of course, in the context of a host co-infected with multiple influenza viruses of distinct lineages, reassortment also facilitates genetic exchange that gives rise to large shifts in viral genotype and phenotypes. These instances of genetic shift can very rapidly advance adaptation of an influenza virus to a new

environment, including a new host species [4-6,8,12]. For these reasons, the potential for SI particles to increase reassortment efficiency suggests that these virions may accelerate the evolution of IAV.

Defective interfering particles were found experimentally to suppress reassortment relative to that seen with standard virus stocks, but to yield higher levels of reassortment than those predicted for theoretical "perfect" virus stocks that carry only complete genomes. DI particles are similar to SI particles in that they require complementation for infectious progeny production. In addition, DI particles are well known to decrease the production of fully infectious progeny from co-infected cells [17,20,39,42,47]. Thus, DI segments are expected to enhance reassortment by increasing the proportion of productively infected cells that are co-infected, but suppress reassortment by reducing the number of infectious progeny emerging from those cells. Our experimental data obtained with Pan/99-based P3 and P4 viruses suggests that the latter, suppressive, effect of DIs may be most important from a biological standpoint: reassortment levels characteristic of standard virus stocks (that have non-zero baseline levels of SI particles) are lowered by the emergence of DI particles.

Mathematical modeling allowed us to explore whether similar outcomes are expected when the prevalence and/or the potency of interference of the DI segments is varied. The interfering effect of a DI segment arises due to segment-specific competition between a DI and the corresponding standard segment: if a DI PB2 is packaged into a virion, for example, the full length PB2 will not be [45,48]. The accumulation of DI particles over multiple passages indicates that DI segments carrying internal deletions are furthermore more likely to win this competition than are the full-length segments. The mechanism

that leads to favoring of influenza virus DI segments over standard segments is not fully resolved, but likely occurs at the level of genome replication and/or packaging and may be related to segment length [44,45,48-50]. Importantly, differing DI segments interfere more or less potently [44]. We found that defective segments that interfere mildly are expected to enhance reassortment relative to the presence of only complete genomes. In contrast, if a DI segment has a strong competitive advantage over the corresponding standard segment, leading to a 10-100 fold reduction in progeny, the presence of DI particles can suppress reassortment. Thus, whether DI particles have a positive or negative impact on reassortment is determined mainly by the potency with which DI segments interfere with infectious progeny production. Our experiments show that, in the context of biological virus populations, the overall impact of all types of DI particles is to suppress reassortment.

Modeling also revealed an additional layer of complexity governing the behavior of DI particles: the presence of SI particles in a virus population can change the expected impact of DI particles on reassortment, presumably by increasing the requirement for complementation. Comparison of experimental data obtained with P3 and P4 viruses to the model suggests, however, that SI particles do not comprise a large fraction of these virus stocks. In this way, the data suggest that, compared to standard segments, DI segments are less likely to be missing. This finding fits well with reports indicating that DI segments are incorporated into virions more efficiently than their full-length counterparts [45,48,51]. Since the behavior of DI particles is complex, it is important to highlight that modeling of segments that compete equally to, or with an advantage over, full-length segments in computational virus populations cannot alone account for the

levels of reassortment observed experimentally. Rather, the inclusion in the model of virions that fail to deliver one or more segments to the site of replication is needed to match the experimental data.

We report the effects of SI and DI particles on reassortment in the context of a cell culture model where replication is limited to one cycle. One important difference between this experimental system and infection in an animal host, where IAV will undergo multiple rounds of replication, is in the multiplicity of infection. By tracking reassortment in co-infected guinea pigs, we have seen that MOI increases with viral load in vivo and, at the time of peak shedding, is sufficient to support the production of reassortant viruses at a frequency of about 70% [52,53]. Similar results were obtained whether mixed infection was achieved by intranasal inoculation or through dual transmission events. Thus, MOIs achieved in vivo are sufficiently high to allow complementation of SI or DI particles. The impact of these particles most likely varies with the time after infection, however, since MOI changes as infection spreads in the target tissue. A second important difference between our cell culture model and an animal host is the potential for multiple rounds of replication. DI particles may have a stronger positive effect on reassortment in vivo, since reassortant DI viruses would have the opportunity to be complemented through co-infection in subsequent rounds of replication. Another important consequence of multi-cycle replication in vivo is the potential for rare reassortant viruses to be amplified. If certain reassortant genotypes confer higher fitness than the parental genotypes in the host where they arise, even low overall levels of reassortment can lead to major biological changes.

Our data, and those of Brooke et al., suggest that SI particles outnumber fully infectious particles in a typical IAV population. We have furthermore attributed important biological activities to these particles [18,27]. Nevertheless, the precise nature of SI particles remains unclear. SI particles may lack one or more gene segments due to a failure to package all eight vRNAs during assembly. This possibility is substantiated by lower rates of detection of NA vRNA in a mutant virus population that was shown to have increased SI particle content relative to the wild type strain [54]. A failure to package some segments is not, however, supported by recent fluorescence in situ hybridization data that show a high percentage of virus particles contain eight different viral RNAs [55]. Although not quantitative, electron microscopic analyses of RNPs within IAV virions also show the presence of eight segments arranged in an ordered fashion [56,57]. The possibility that SI particles carry eight fully functional vRNA molecules but fail to deliver one or more to the nucleus is feasible but weakened by FISH analysis of IAV genomes in infected cells, which suggests that the segments remain associated prior to nuclear import [58]. Direct visualization of IAV ribonucleoproteins allowed identification of the polymerase complex bound to the 3’ and 5’ termini of the RNA, but also revealed some segments that did not appear to be associated with a polymerase [59]. Thus, SI particles might carry one or more segments that are not bound by a polymerase complex and are therefore not copied during primary transcription and may be more susceptible to exonuclease activity. While the data presented herein are informative regarding the potential biological implications of SI particles, they do not elucidate the physical nature of these particles, nor narrow down the possibilities listed above.

In summary, our data show that the presence of semi-infectious particles in an influenza virus population increases the potential for genetic diversification through reassortment. This activity of semi-infectious particles is due to an increase in the proportion of productively infected cells that are co-infected, which in turn reflects the need for complementation in order for cells infected with SI particles to produce progeny. Similar to SI particles, the presence of DI particles increases the proportion of infected cells that are co-infected; however, since DI segments inhibit the production of infectious progeny viruses, their overall effect is to decrease rather than increase levels of reassortment relative to those seen with standard virus stocks. We conclude that IAV particles that are not fully infectious may have an important role in influenza virus biology through their effects on reassortment and, in turn, adaptive evolution of the virus.

Materials and Methods

Computational methods

Simulation setup and MOI variation. We performed computational simulations to monitor levels of infection, co-infection, and reassortment, as a function of a varying multiplicity of infection (MOI). As indicated in the table below, the MOI was varied dynamically from $1x10^{-5}$ to 15 particles per cell in (approximately) log-linear steps. This approach was used to minimize stochastic variations at low MOI and increase computational speed for otherwise slow simulation steps at high MOI that do not suffer from stochastic variations.

No. virions per type	No. cells	MOI per type
10	1000000	1.000e-5
40	1000000	4.000e-5
158	1000000	1.580e-4

631	1000000	6.310e-4
2512	1000000	2.512e-3
10000	1000000	1.000e-2
39811	1000000	3.981e-2
100000	1000000	1.000e-1
100000	794328	1.259e-1
100000	630957	1.585e-1
100000	501187	1.995e-1
100000	398107	2.512e-1
100000	316228	3.162e-1
100000	251189	3.981e-1
100000	199526	5.012e-1
100000	158489	6.310e-1
100000	125893	7.943e-1
100000	100000	1.000
125893	100000	1.259
158489	100000	1.585
199526	100000	1.995
251189	100000	2.512
316228	100000	3.162
398107	100000	3.981
501187	100000	5.012
630957	100000	6.310
1000000	100000	10
1500000	100000	15

Each row indicates a run. For example, the first run would have 10 virions of type A and 10 virions of type B distributed over 1,000,000 cells, giving an effective MOI of $1x10^{-5}$ for each type and a total MOI of $2x10^{-5}$ virions per cell.

Infection, co-infection and reassortment of complete genomes. Each virion is randomly assigned to a cell. Based on the number of virions of each type assigned to a cell, the % infection (number of cells infected with any virion type, divided by the number of cells) and % co-infection (number of cells infected by both virion types, divided by the number of cells) is calculated. The expected reassortment level for a cell infected with N_A virions of type A and N_B virions of type B is:

$$1-(N_A/(N_A+N_B))^8-(N_B/(N_A+N_B))^8$$

The % reassortment is calculated as an average of the expected reassortment level across all infected cells.

Modeling semi-infectious virions. We defined the likelihood for a segment to be present in a virion and copied upon infection as P_P. Therefore the likelihood that a virion carries and copies all 8 segments is the product of the P_P of all eight segments. The model above was modified to account for missing segments as follows. The number of virions that have a given segment, N_P, was calculated by multiplying the number of virions by the likelihood P_P for that segment. From the full set of virions, we selected a random subset of size N_P, and these virions have the given segment. This process was repeated for all 8 segments, thereby producing a registry of which segments are present for each original virion, after it has been assigned to a cell. This process of assigning segments to virions can give rise to virions with no segments, but this situation is expected to occur at a relevant frequency only with low values of P_P for all 8 segments (e.g. with P_P=0.25 for all 8 segments, the chance for a random virion to have 0 segments is 0.75^8=0.100).

For a cell to express HA of a given type, the HA segment of that type needs to be present and, in addition, at least one of each segment NP, PA, PB1 and PB2 needs to be present [1,31,32]. For a cell to be counted as dually HA positive, therefore, both HA of type A and type B are required, as well as at least a single segment of NP, PA, PB1 and PB2.

For a cell to produce progeny, at least one copy of each of the 8 segments is required. Therefore, when semi-infectious virions are present, not all infected and co-infected cells will have progeny. For cells producing progeny, the expected reassortant frequency is calculated as follows:

expected reassortment=1

$$-\left\{\frac{N_{NA_A}}{N_{NA_A}+N_{NA_B}}*\frac{N_{HA_A}}{N_{HA_A}+N_{HA_B}}*\frac{N_{M_A}}{N_{M_A}+N_{M_B}}*\frac{N_{NS_A}}{N_{NS_A}+N_{NS_B}}\right.$$
$$\left.*\frac{N_{NP_A}}{N_{NP_A}+N_{NP_B}}*\frac{N_{PA_A}}{N_{PA_A}+N_{PA_B}}*\frac{N_{PB1_A}}{N_{PB1_A}+N_{PB1_B}}*\frac{N_{PB2_A}}{N_{PB2_A}+N_{PB2_B}}\right\}$$
$$-\left\{\frac{N_{NA_B}}{N_{NA_A}+N_{NA_B}}*\frac{N_{HA_B}}{N_{HA_A}+N_{HA_B}}*\frac{N_{M_B}}{N_{M_A}+N_{M_B}}*\frac{N_{NS_B}}{N_{NS_A}+N_{NS_B}}\right.$$
$$\left.*\frac{N_{NP_B}}{N_{NP_A}+N_{NP_B}}*\frac{N_{PA_B}}{N_{PA_A}+N_{PA_B}}*\frac{N_{PB1_B}}{N_{PB1_A}+N_{PB1_B}}*\frac{N_{PB2_B}}{N_{PB2_A}+N_{PB2_B}}\right\}$$

Where N_{Y_Z}represents the number of segment Y present for virion type Z (A or B). The expected % reassortment is calculated as the average of the expected reassortant frequencies across all cells producing progeny.

To evaluate which set of P_P values corresponded best to the measured data, P_P was varied between 0.25 and 1.0 in increments of 0.25. We tested all possible combinations, taking into account the redundancy of PB2, PB1, PA and NP as well as that of NA, M and NS. These redundancies arise because the polymerase and nucleoprotein components are each required for an infected cell to be HA positive, and removing any one of these segments therefore has the same impact on HA positivity. Conversely, the presence of NA, M and NS are not required for a cell to be HA positive and, again, removing any one of this group has the same impact on HA positivity. The absence of any segment impacts reassortment, since all eight segments are needed to generate infectious progeny. Thus, for example, P_P=0.25 for PB2 gives the same reassortment and HA positivity outcomes

as P_P=0.25 for PB1. In total, we evaluated the 2800 different combinations of P_P values by comparing them to the measured data.

From the resulting simulations, we interpolated the HA positive, dually HA positive and reassortment values to get 20 values between any original set of two simulation values, in the graphs of % HA positive versus % dually HA positive, % HA positive versus reassortment, and % dually HA positive versus reassortment. From these three now high-resolution data curves, we calculated for each P_P value the sum of distances of the experimental data to the interpolated simulation curves (sum of errors). The optimal P_P settings, which would have the smallest sum of distances between the data and the graphs, were then determined by taking the sum of the three sums of errors from the three graphs. The optimal settings were: P_P(PB2): 0.25; P_P(PB1): 0.5; P_P(PA): 0.75; P_P(HA): 0.75; P_P(NP): 1; P_P(NA): 1; P_P(M): 1; P_P(NS): 1; both virus types A and B had the same setting per segment.

Modeling UV treatment of virions. The probability of UV treatment introducing a lesion in a given segment is directly related to their length [60]. For a given UV dose U_D the proportion present for a specific segment was modified as follows from P_P to $P_{P,UV}$:

$$P_{P,UV} = P_P * (1 - U_D * \frac{L}{13623})$$

Where L is the length of the segment (2341 for PB2 and PB1, 2233 for PA, 1762 for HA, 1566 for NP, 1466 for NA, 1027 for M, 887 for NS). A UV dose of 2 would on average hit two positions per genome with this model.

This value $P_{P,UV}$ was then used instead of P_P to determine which virions had which segments present, as described in "Modeling semi-infectious virions". Using the set of P_P values determined above, we then varied the UV dose between U_D 0 and 5 in steps of 0.05. As described for "determining the P_P value", the sum of the distances of the measured points after UV treatment to the interpolated UV simulation results curves (the sum of errors) were calculated, for % HA positive cells versus % dually HA positive cells, % HA positive cells versus % reassortment, and % dually HA positive cells versus % reassortment. The minimum of the sum of the three error values was found for U_D 2.0 hits per genome, which following the Poisson distribution corresponds to an expected 13.5% of genomes being unaffected by the UV treatment.

Testing the role of MOI in determining the relationship between P_P and reassortment. To better understand the mechanisms underlying changes in reassortment levels seen with changes in P_P, we modeled reassortment and co-infection levels as functions of P_P. For these simulations, we varied the P_P from 0.02 to 1 in steps of 0.02 and performed 20 repeats. Using 10^5 cells, we calculated the number of virions of type A and B needed to achieve a given MOI, e.g. 3000 virions of type A and 3000 of type B for an MOI of 0.03. The average % reassortment was calculated across all progeny-producing cells (i.e. those cells with at least one copy for each of the 8 segments), or all co-infected, progeny-producing cells, as indicated. Of the 10^5 cells, those that were producing progeny were either categorized as co-infected (if containing segments of both type A and B), or singly infected (if only containing segments of one type).

Modeling defective-interfering virions. We defined the probability that a segment is not a DI as the probability intact, P_I. DI particles were then added to the model as follows.

After determining which virions have which segments present (based on P_P), the probability that a segment is intact, P_I, was used to determine the number of virions that have a segment present and intact, according to $N_{PI} = N_P * P_I$. From the virions with the segment present, we selected a random subset of size N_{PI}, and these virions have the given segment present and intact. All the other segments that are present, but not intact, represent defective-interfering segments. We modeled defective interfering segments for PA, PB1 and PB2 of virus types A and B [37,38,44], and allowed all six segments to have different probabilities of being intact. The resulting simulation produced a registry of which segments are present and intact for each original virion, after it has been assigned to a cell.

For cells producing progeny, the expected reassortant frequency is calculated per the formula above, where N_{Y_Z} represents the number of segment Y present and intact for virion type Z (A or B). However, because the DI segments reduce the number of infectious progeny produced, the expected % reassortment is calculated as a *weighted* average of the expected reassortant frequencies across all cells producing progeny, where the weighting factor is calculated as:

$$\text{"weighting factor= "}\ DIX^{\#DI}$$

That is, the factor DIX decreases the progeny produced per DI particle present, as #DI represents the number of DI segments present within that cell.

We evaluated, for three settings of DIX (0.01, 0.1 and 0.45), a series of 125 settings of P_I, where the PB2, PB1 and PA P_I were varied independently from 0.2 to 1.0 in increments of 0.2, while the P_I of all other segments and the P_P for all segments was set to 1.

Additionally, we made a model where DIX was varied from 0.05 to 0.5 in increments of 0.05, the experimentally measured P_I parameters were used (Table 2), and P_P was set to the settings found optimal above (P_P(PB2): 0.25; P_P(PB1): 0.5; P_P(PA): 0.75; P_P(HA): 0.75; P_P(NP): 1; P_P(NA): 1; P_P(M): 1; P_P(NS): 1; same settings for A and B). We then repeated this model with P_P=1 for all segments.

Finally, we evaluated for three settings of DIX (0.01, 0.1 and 0.45), a series of 125 settings of P_I, where the PB2, PB1 and PA P_I were varied independently from 0.2 to 1.0 in increments of 0.2, four different settings of P_P: i) all segments 1; ii) all segments 0.8; iii) all segments 1, except PB2, which is 0.1; iv) the best P_P settings found previously (0.25,0.5,0.75,0.75,1,1,1,1).

Experimental methods

Ethics statement. Embryonated hens' eggs obtained from HyLine International were incubated for 9-11 days and then used to propagate influenza viruses. Animal ethics board approval was not required for this work because the eggs were not allowed to hatch and therefore do not constitute live animals.

Viruses and cells. Madin-Darby Canine Kidney (MDCK) cells were obtained from the ATCC and maintained in minimum essential medium (MEM) supplemented with 10% FBS and penicillin-streptomycin. Infections were carried out in serum-free MEM supplemented with 3% Bovine Serum Albumin and penicillin-streptomycin. Recombinant influenza A/Panama/2007/1999 (H3N2) [rPan/99wt-His] and rPan/99var2-HAtag viruses were described previously [30,61]. Briefly, these viruses were generated by reverse genetics and propagated in 9-11 day old embryonated hens' eggs for one or

two passages. rPan/99var2-HAtag virus contains the following silent mutations relative to rPan/99wt-His virus (nucleotide numbering is from the 5' end of the cRNA): NS C329T, C335T, and A341G; M C413T, C415G and A418C; NA C418G, T421A and A424C; NP C537T, T538A and C539G; HA T308C, C311A, C314T, A464T, C467G and T470A; PA G603A, T604A and C605G; PB1 C364T, T348G and A351G; and PB2 T621C, T622A and C623G. In addition, the two viruses differ in the epitope tags inserted into the HA protein after the signal peptide [30,62], with the wt virus encoding a His tag and the var virus encoding an HA tag. Collectively, these mutations were shown not to attenuate the growth of rPan/99var2-HAtag virus relative to rPan/99wt-His virus in MDCK cells [30].

UV irradiation of virus stocks. Pyrimidine dimers were introduced randomly into the rPan/99wt-HIS and rPan/99var2-HAtag viral genomes by partial UV inactivation. Each virus stock was diluted to $1x10^8$ PFU/ml in PBS and separately placed into a 6-well culture dish (340ul/well). Each culture dish was placed approximately 30cm from a 254nm, 8W, UV light source and exposed for 35 seconds.

Co-infection at a range of MOIs with untreated and UV treated viruses. Untreated and UV treated rPan/99wt-HIS and rPan/99var2-HAtag virus inocula were prepared in parallel, from the same virus stocks. As indicated above, each virus stock was diluted to $1x10^8$ PFU/ml in PBS. One aliquot of each virus was UV treated and a second aliquot of each virus was "mock treated" (placed in a culture dish but not put under the UV lamp). Untreated rPan/99wt-HIS and rPan/99var2-HAtag virus stocks were then mixed in a 1:1 ratio. Similarly, UV-treated rPan/99wt-HIS and rPan/99var2-HAtag virus stocks were mixed in a 1:1 ratio. Each virus mixture was then diluted with PBS to the appropriate titer

for inoculation at MOI 10, 6, 3, 1, 0.6, 0.3 and 0.1 PFU/cell of each virus. These MOIs were based on the viral titers before UV treatment.

Infections were performed in 6-well dishes seeded with $4x10^5$ MDCK cells per well on the previous day. For inoculation, dishes were placed on ice, growth medium removed, and monolayers washed with PBS three times. Each well was inoculated with 250ul volume, on ice, and cells were incubated at 4˚C for one hour to allow virus attachment. The inoculum was aspirated and any unattached virus removed by washing the monolayers three times with PBS. After the addition of virus medium (MEM supplemented with 3% BSA and Penicillin/Streptomycin), cells were transferred to 33˚C. At 3 h post-infection, virus medium was removed from the monolayers and replaced with medium containing NH_4Cl (MEM supplemented with Penicillin/Streptomycin, 20mM NH_4Cl, 50mM HEPES buffer and 0.1% BSA) and returned to 33˚C. At 12 h post-infection, supernatant was collected and stored at -80˚C for subsequent genotyping of released virus. MDCK-infected cells were harvested and prepared for flow cytometry (see below).

Generation of virus stocks with high levels of DI particles. Virus stocks with abundant DI particles were generated by serial passage in MDCK cells at high MOI. For the first passage, Pan/99wt-His and Pan/99var-HAtag viruses were used to infect MDCK cells in a T75 flask at MOI = 5 PFU/cell. Passages 2-5 were performed blindly, using 2 ml undiluted cell culture supernatant from the previous passage as inoculum in each T75 flask. Incubations at each passage were performed at 33^oC for ~48 h. To gauge particle:PFU ratio at each passage, PFU titers were determined in MDCK cells according to standard techniques and RNA was extracted from 140 cell culture supernatant

(QiaAmp Viral RNA Kit), subject to reverse transcription with Univ.F(A) primer and Maxima RT (Fermentas), and analyzed by quantitative PCR using primers specific for NS, M and NA segments with BioRad SsoFast Evagreen Supermix. PCR was run in triplicate and median Ct values were used in further analyses. RNA copy numbers of P1 – P5 (Px) viruses relative to the corresponding progenitor stock (P0wt or P0var) were calculated for each segment according to the equation $2^{(-Ct_{Px})} / 2^{(-Ct_{P0})}$. The average result for all three segments was then calculated to give the relative RNA copy number for each passage. PFU titers of P1 – P5 stocks were also normalized to those of the corresponding P0 stock. Finally, RNA:PFU ratios shown in Fig. 10 were calculated as relative RNA copy number divided by relative PFU titer.

Measurement of relative DI particle content. We used an RT qPCR assay to determine the proportion of gene segments with large internal deletions in the P3 and P4 stocks, relative to our standard stocks (referred to as "P0"). Total RNA was extracted from 140 ul samples of each virus stock using the QiaAmp Viral RNA Kit (Qiagen) and reverse transcribed using the Univ.F(A) primer and Maxima RT, according to the manufacturer's instructions. Viral cDNAs were then subjected to qPCR using SsoFast Evagreen Supermix (BioRad) and a panel of 16 primer pairs. The panel comprised two primer pairs for each segment: the first set bound within 150 nucleotides of the 3' terminus and the second set bound internally, in a region typically deleted within DI segments [37,38] (primer sequences available upon request). The procedure was carried out three times on different days to give three biological replicates and each assay included three technical replicates. The proportion of viral gene segments that were intact (P_I), relative to P0 stocks, was calculated according to the following formula, where "Px" refers to P3 or P4

viruses, "internal" indicates Ct values obtained with primers binding at an internal site and "terminal" indicates Ct values obtained with primers binding within 150 nt of the 3' end of the vRNA.

$P_I = [2^{(-\text{Ct internal})} / 2^{(-\text{Ct terminal})}]_{Px} / [2^{(-\text{Ct internal})} / 2^{(-\text{Ct terminal})}]_{P0}$

This calculation was performed separately for each segment. The median Ct value among the three technical replicates was used for the calculation. The median P_I values determined from three independent experiments are reported in Table 2.

Co-infection at a range of MOIs with P0, P3 and P4 virus stocks.

The RNA:PFU ratios were higher for rPan/99wt-HIS virus than for rPan/99var-HA virus at each passage (Fig. 10). Appropriate volumes of P0 rPan/99wt-HIS virus were therefore spiked into both P3wt and P4wt viruses to yield stocks with RNA:PFU ratios equivalent to their P3var and P4var counterparts. P3wt and P3var virus stocks were then mixed in a 1:1 ratio and P4wt and P4var virus stocks were similarly mixed in a 1:1 ratio. One-to-one mixtures of P0wt and P0var viruses were also prepared. Each virus mixture was diluted with PBS to the appropriate titer for inoculation at MOI 3, 1, 0.3, 0.1, 0.03 and 0.01 PFU/cell of each virus. MOI 3 was not carried out for the P4 viruses due to insufficient titers. PFU values refer to those of the P0 viruses. The amount of P3 and P4 viruses used in each infection was based on the RNA:PFU ratios. Thus, equivalent units of RNA were used for P0, P3 and P4 infections and the amounts of RNA used corresponded to 3 – 0.1 PFU/cell of the P0 viruses. Inoculation of MDCK cells was performed as described above for untreated and UV treated viruses, except that medium was not changed at 3 h post-infection to introduce NH_4Cl. At 16 hours post-infection,

supernatant was collected and stored at -80˚C for subsequent genotyping of released virus. MDCK-infected cells were harvested and prepared for flow cytometry (see below).

Measurement of % infection, % co-infection and % reassortment. Infection and co-infection levels were determined as described previously [30]. Briefly, flow cytometry using commercial antibodies specific for a His tag (Qiagen Penta-HIS Alexa Fluor 647 conjugate, Mouse IgG1 [item# 35370]) and an HA tag (Sigma Aldrich monoclonal anti-HA-FITC, Clone HA-7 [item# H7411]) allowed enumeration of Pan/99wt-His and Pan/99var2-HA virus-infected cells, respectively. Singly and doubly infected cell populations were gated manually using uninfected cells treated with both anti-His and anti-HA antibodies as negative controls.

To calculate % reassortment, virus genotypes were determined by high resolution melt analysis essentially as described previously [30,52]. Briefly, the following steps were performed. 1) Plaque isolates were obtained by plaque assay of MDCK cell supernatants. 2) RNA was extracted from agar plugs using the Zymogen 96 Viral RNA kit, according to the manufacturer's protocol except that 40 ul water was used for elution. 3) Twelve microliters of RNA was reverse transcribed from an IAV-specific "universal" primer (Univ.F(A): 5' GGCCAGCAAAAGCAGG) using Maxima reverse transcriptase (Fermentas) according to the manufacturer's instructions. 4) cDNA was used as template in qPCR reactions with the appropriate primers [30] and Precision Melt Supermix (BioRad) in wells of a white, thin wall, 384 well plate (BioRad). qPCR and melt analyses were carried out in a CFX384 Real-Time PCR Detection System, as per the instructions provided with the Precision Melt Supermix. Data were analysed using Precision Melt Analysis software (BioRad). Viruses were scored as reassortant if the genome comprised

a mixture of wt and var gene segments in any proportion. Occasionally, one or more gene segments gave an ambiguous result in the melt analysis. In these cases, virus isolates were excluded from the analysis if >1 segment could not be typed. Where only one segment could not be assigned as wt or var, the genotype was recorded based on the remaining seven segments.

Acknowledgements

We thank Kara Phipps and Maria White for critical reading of the manuscript.

Bibliography and References Cited

1. Palese P, Shaw ML (2006) Orthomyxoviridae: The Viruses and Their Replication. In: Knipe DMH, P. M., editor. Fields Virology. Philidelphia: Lippincott-Raven. pp. 1647-1690.

2. Palese P (1977) The genes of influenza virus. Cell 10: 1-10.

3. Scholtissek C (1995) Molecular evolution of influenza viruses. Virus Genes 11: 209-215.

4. Steel J, Lowen AC (2014) Influenza A virus reassortment. Curr Top Microbiol Immunol 385: 377-401.

5. Kilbourne ED (2006) Influenza pandemics of the 20th century. Emerg Infect Dis 12: 9-14.

6. Smith GJ, Vijaykrishna D, Bahl J, Lycett SJ, Worobey M, et al. (2009) Origins and evolutionary genomics of the 2009 swine-origin H1N1 influenza A epidemic. Nature 459: 1122-1125.

7. Garten RJ, Davis CT, Russell CA, Shu B, Lindstrom S, et al. (2009) Antigenic and genetic characteristics of swine-origin 2009 A(H1N1) influenza viruses circulating in humans. Science 325: 197-201.

8. Simonsen L, Viboud C, Grenfell BT, Dushoff J, Jennings L, et al. (2007) The genesis and spread of reassortment human influenza A/H3N2 viruses conferring adamantane resistance. Mol Biol Evol 24: 1811-1820.

9. Holmes EC, Ghedin E, Miller N, Taylor J, Bao Y, et al. (2005) Whole-genome analysis of human influenza A virus reveals multiple persistent lineages and reassortment among recent H3N2 viruses. PLoS Biol 3: e300.

10. Westgeest KB, Russell CA, Lin X, Spronken MIJ, Bestebroer TM, et al. (2013) Genome-wide Analysis of Reassortment and Evolution of Human Influenza A(H3N2) Viruses Circulating between 1968 and 2011. Journal of Virology.

11. Nelson MI, Viboud C, Simonsen L, Bennett RT, Griesemer SB, et al. (2008) Multiple reassortment events in the evolutionary history of H1N1 influenza A virus since 1918. PLoS Pathog 4: e1000012.

12. Ince WL, Gueye-Mbaye A, Bennink JR, Yewdell JW (2013) Reassortment complements spontaneous mutation in influenza A virus NP and M1 genes to accelerate adaptation to a new host. J Virol 87: 4330-4338.

13. Wei Z, McEvoy M, Razinkov V, Polozova A, Li E, et al. (2007) Biophysical characterization of influenza virus subpopulations using field flow fractionation and multiangle light scattering: correlation of particle counts, size distribution and infectivity. J Virol Methods 144: 122-132.
14. Enami M, Sharma G, Benham C, Palese P (1991) An influenza virus containing nine different RNA segments. Virology 185: 291-298.

15. Donald HB, Isaacs A (1954) Counts of influenza virus particles. J Gen Microbiol 10: 457-464.

16. Noton SL, Simpson-Holley M, Medcalf E, Wise HM, Hutchinson EC, et al. (2009) Studies of an influenza A virus temperature-sensitive mutant identify a late role for NP in the formation of infectious virions. J Virol 83: 562-571.

17. McLain L, Armstrong SJ, Dimmock NJ (1988) One defective interfering particle per cell prevents influenza virus-mediated cytopathology: an efficient assay system. J Gen Virol 69 (Pt 6): 1415-1419.

18. Brooke CB (2014) Biological activities of 'noninfectious' influenza A virus particles. Future Virol 9: 41-51.

19. Marcus PI, Ngunjiri JM, Sekellick MJ (2009) Dynamics of biologically active subpopulations of influenza virus: plaque-forming, noninfectious cell-killing, and defective interfering particles. J Virol 83: 8122-8130.

20. Nayak DP, Tobita K, Janda JM, Davis AR, De BK (1978) Homologous interference mediated by defective interfering influenza virus derived from a temperature-sensitive mutant of influenza virus. J Virol 28: 375-386.

21. Crumpton WM, Dimmock NJ, Minor PD, Avery RJ (1978) The RNAs of defective-interfering influenza virus. Virology 90: 370-373.

22. Von Magnus P (1951) Propagation of the PR8 strain of influenza A virus in chick embryos. III. Properties of the incomplete virus produced in serial passages of undiluted virus. Acta Pathol Microbiol Scand 29: 157-181.

23. Von Magnus P (1951) Propagation of the PR8 strain of influenza A virus in chick embryos. II. The formation of incomplete virus following inoculation of large doses of seed virus. Acta Pathol Microbiol Scand 28: 278-293.

24. Parvin JD, Moscona A, Pan WT, Leider JM, Palese P (1986) Measurement of the mutation rates of animal viruses: influenza A virus and poliovirus type 1. J Virol 59: 377-383.

25. Drake JW (1993) Rates of spontaneous mutation among RNA viruses. Proc Natl Acad Sci U S A 90: 4171-4175.

26. Hirst GK (1973) Mechanism of influenza recombination. I. Factors influencing recombination rates between temperature-sensitive mutants of strain WSN and the classification of mutants into complementation--recombination groups. Virology 55: 81-93.
27. Brooke CB, Ince WL, Wrammert J, Ahmed R, Wilson PC, et al. (2013) Most influenza a virions fail to express at least one essential viral protein. J Virol 87: 3155-3162.

28. Henle W, Liu OC (1951) Studies on host-virus interactions in the chick embryo-influenza virus system. VI. Evidence for multiplicity reactivation of inactivated virus. J Exp Med 94: 305-322.

29. Hirst GK, Pons MW (1973) Mechanism of influenza recombination. II. Virus aggregation and its effect on plaque formation by so-called noninfective virus. Virology 56: 620-631.

30. Marshall N, Priyamvada L, Ende Z, Steel J, Lowen AC (2013) Influenza virus reassortment occurs with high frequency in the absence of segment mismatch. PLoS Pathog 9: e1003421.

31. Neumann G, Watanabe T, Kawaoka Y (2000) Plasmid-driven formation of influenza virus-like particles. J Virol 74: 547-551.

32. Weber M, Sediri H, Felgenhauer U, Binzen I, Banfer S, et al. (2015) Influenza virus adaptation PB2-627K modulates nucleocapsid inhibition by the pathogen sensor RIG-I. Cell Host Microbe 17: 309-319.

33. Ohkuma S, Poole B (1978) Fluorescence probe measurement of the intralysosomal pH in living cells and the perturbation of pH by various agents. Proc Natl Acad Sci U S A 75: 3327-3331.

34. Condit RC (2013) Principles of Virology. In: Knipe DM, Howley PM, editors. Fields Virology. 6th ed. pp. 21-51.

35. Davis AR, Hiti AL, Nayak DP (1980) Influenza defective interfering viral RNA is formed by internal deletion of genomic RNA. Proc Natl Acad Sci U S A 77: 215-219.

36. Nayak DP, Sivasubramanian N, Davis AR, Cortini R, Sung J (1982) Complete sequence analyses show that two defective interfering influenza viral RNAs contain a single internal deletion of a polymerase gene. Proc Natl Acad Sci U S A 79: 2216-2220.

37. Jonges M, Welkers MR, Jeeninga RE, Meijer A, Schneeberger P, et al. (2014) Emergence of the virulence-associated PB2 E627K substitution in a fatal human

case of highly pathogenic avian influenza virus A(H7N7) infection as determined by Illumina ultra-deep sequencing. J Virol 88: 1694-1702.

38. Saira K, Lin X, DePasse JV, Halpin R, Twaddle A, et al. (2013) Sequence analysis of in vivo defective interfering-like RNA of influenza A H1N1 pandemic virus. J Virol 87: 8064-8074.

39. Janda JM, Nayak DP (1979) Defective influenza viral ribonucleoproteins cause interference. J Virol 32: 697-702.

40. Nayak DP (1980) Defective interfering influenza viruses. Annu Rev Microbiol 34: 619-644.

41. Rott R, Scholtissek C (1963) Investigations About the Formation of Incomplete Forms of Fowl Plague Virus. J Gen Microbiol 33: 303-312.

42. Janda JM, Davis AR, Nayak DP, De BK (1979) Diversity and generation of defective interfering influenza virus particles. Virology 95: 48-58.

43. Von Magnus P (1954) Incomplete forms of influenza virus. Adv Virus Res 2: 59-79.

44. Nayak DP, Chambers TM, Akkina RK (1985) Defective-interfering (DI) RNAs of influenza viruses: origin, structure, expression, and interference. Curr Top Microbiol Immunol 114: 103-151.

45. Duhaut SD, McCauley JW (1996) Defective RNAs inhibit the assembly of influenza virus genome segments in a segment-specific manner. Virology 216: 326-337.

46. Andino R, Domingo E (2015) Viral quasispecies. Virology.

47. Carter MJ, Mahy BW (1982) Incomplete avian influenza A virus displays anomalous interference. Arch Virol 74: 71-76.

48. Odagiri T, Tashiro M (1997) Segment-specific noncoding sequences of the influenza virus genome RNA are involved in the specific competition between defective interfering RNA and its progenitor RNA segment at the virion assembly step. J Virol 71: 2138-2145.

49. Dimmock NJ, Easton AJ (2014) Defective interfering influenza virus RNAs: time to reevaluate their clinical potential as broad-spectrum antivirals? J Virol 88: 5217-5227.

50. Akkina RK, Chambers TM, Nayak DP (1984) Expression of defective-interfering influenza virus-specific transcripts and polypeptides in infected cells. J Virol 51: 395-403.

51. Odagiri T, Tominaga K, Tobita K, Ohta S (1994) An amino acid change in the non-structural NS2 protein of an influenza A virus mutant is responsible for the generation of defective interfering (DI) particles by amplifying DI RNAs and suppressing complementary RNA synthesis. J Gen Virol 75 (Pt 1): 43-53.

52. Tao H, Steel J, Lowen AC (2014) Intra-host dynamics of influenza virus reassortment. J Virol.

53. Tao H, Li L, White MC, Steel J, Lowen AC (2015) Influenza A virus co-infection through transmission can support high levels of reassortment. J Virol.

54. Brooke CB, Ince WL, Wei J, Bennink JR, Yewdell JW (2014) Influenza A virus nucleoprotein selectively decreases neuraminidase gene-segment packaging while enhancing viral fitness and transmissibility. Proc Natl Acad Sci U S A 111: 16854-16859.

55. Chou YY, Vafabakhsh R, Doganay S, Gao Q, Ha T, et al. (2012) One influenza virus particle packages eight unique viral RNAs as shown by FISH analysis. Proc Natl Acad Sci U S A 109: 9101-9106.

56. Noda T, Sagara H, Yen A, Takada A, Kida H, et al. (2006) Architecture of ribonucleoprotein complexes in influenza A virus particles. Nature 439: 490-492.

57. Noda T, Sugita Y, Aoyama K, Hirase A, Kawakami E, et al. (2012) Three-dimensional analysis of ribonucleoprotein complexes in influenza A virus. Nat Commun 3: 639.

58. Chou YY, Heaton NS, Gao Q, Palese P, Singer R, et al. (2013) Colocalization of different influenza viral RNA segments in the cytoplasm before viral budding as shown by single-molecule sensitivity FISH analysis. PLoS Pathog 9: e1003358.

59. Sugita Y, Sagara H, Noda T, Kawaoka Y (2013) Configuration of viral ribonucleoprotein complexes within the influenza A virion. J Virol 87: 12879-12884.

60. Abraham G (1979) The effect of ultraviolet radiation on the primary transcription of influenza virus messenger RNAs. Virology 97: 177-182.

61. Steel J, Lowen AC, Mubareka S, Palese P (2009) Transmission of influenza virus in a mammalian host is increased by PB2 amino acids 627K or 627E/701N. PLoS Pathog 5: e1000252.

62. Langley WA, Bradley KC, Li ZN, Smith ME, Schnell MJ, et al. (2010) Induction of neutralizing antibody responses to anthrax protective antigen by using influenza virus vectors: implications for disparate immune system priming pathways. J Virol 84: 8300-8307.

Figure Legends

Figure 1. Relationships between % infection and % reassortment or % co-infection, as predicted by computational simulation of co-infection with viruses of two types. Viruses of type A and type B were assigned at random to a computational set of cells over a range of MOIs. Cells infected with any virus type were counted as infected and cells infected with both A and B types were counted as co-infected. The proportion of progeny viruses carrying a reassortant genome produced from each infected cell was calculated, taking into account the number type A and type B viruses present in each cell. The average % reassortment for all infected cells is plotted.

Figure 2. Impact on % infection, % co-infection, and % reassortment of introducing semi-infectious particles into the model. The probability that a given segment is present in each virus particle (P_P) was varied from 1.0 to 0.3 within the model. The color scale indicates the value assigned to P_P in each simulation. A) The relationship between % infected and % co-infected cells is not affected by changing P_P. B) The relationship between % HA positive cells and % dually HA positive cells varies with P_P, due to the potential for segments that are required for HA gene expression to be missing from the infecting virus particle(s). C) The relationship between % HA positive cells and expected % reassortment, averaged across all productively infected cells, changes markedly with P_P.

Figure 3. Measurement of HA positive cells, dually HA positive cells and reassortment following co-infection of MDCK cells with Pan/99wt and Pan/99var viruses. Pan/99wt and Pan/99var viruses were mixed in equal proportions and used to inoculate MDCK cells at a range of MOIs. Infection at each MOI was performed in triplicate. Following a single cycle of infection, cell culture supernatants were stored and HA positive and dually HA positive cells were identified by flow cytometry. Clonal viral isolates (n=18-21) derived from each cell culture supernatant were genotyped by high resolution melt analysis to allow calculation of % reassortment. Individual data points, each corresponding to one cell culture dish, are plotted.

Figure 4. Modeled outcomes do not match the observed relationship between HA positive and dually HA positive cells when P_P is constant among the eight segments. Experimental data points, plotted with black circles, are overlaid on colored lines that indicate the predicted relationships between % HA positive cells and % dually HA positive cells given a range of P_P values. In this version of the model, the same P_P value was assigned to all eight segments. The color scale in the legend indicates the value assigned to P_P in each simulation.

Figure 5. Varying P_P by segment yields good fit between modeled and observed relationships among HA positive cells, dually HA positive cells and reassortment. When P_P was allowed to vary among the segments (from 0.25 to 1.0 in increments of 0.25), several combinations of P_P values allowed a good fit between observational and modeled data. Shown here are the modeled results for the 1% of P_P combinations yielding the best fit (i.e. the top 28 of the 2800 settings tested). The 28 lines are colored

from best (red) to worst (blue) fit. Experimental data points, plotted with black circles, are overlaid on these colored lines to allow comparison between experimental and modeled results for % HA positive cells vs. % dually HA positive cells (A) and % HA positive cells vs. % reassortment (B).

Figure 6. Increasing semi-infectious particle content by UV irradiation of virus stocks augments observed % reassortment. Pan/99wt and Pan/99var viruses were exposed to low dose UV light sufficient to reduce viral titers by ~10-fold (white circles) or were mock treated (black circles). Treated wt and var viruses were mixed in equal proportions and mock treated wt and var viruses were mixed in equal proportions. Each mixture was used to inoculate MDCK cells at a range of MOIs, in triplicate. Following a single cycle of infection, cell culture supernatants were stored and HA positive and dually HA positive cells were identified by flow cytometry. Clonal viral isolates (n=18-21) derived from each cell culture supernatant were genotyped by high resolution melt analysis to allow calculation of % reassortment. A) Relationship between % HA positive cells and % dually HA positive cells. B) Relationship between % HA positive cells and % reassortment. Individual data points, each corresponding to one cell culture dish, are plotted. Data from mock treated samples (black circles) are also presented in Figure 3 and are included here to allow direct comparison with data from UV treated samples.

Figure 7. Results observed with UV treated Pan/99wt and Pan/99var viruses match simulated co-infections in which each virus carries an average of 2.0 UV hits per genome. Experimental data points obtained with UV treated virus stocks, plotted with

open circles, are overlaid on a black line indicating the model's predicted relationships for % HA positive cells vs. % dually HA positive cells (A) and % HA positive cells vs. % reassortment (B). Computational viruses carried an average of 2.0 UV hits per genome when P_P settings found to best match the data obtained with untreated virus stocks were used (0.25, 0.5, 075, 0.75, 1, 1, 1, 1 for segments 1-8, respectively).

Figure 8. Semi-infectious particles increase reassortment at a given MOI by increasing the proportion of infected cells that are co-infected. Results of computationally simulated co-infections are shown. In each simulation, multiplicity of infection in terms of total particles/ cell was held constant and is indicated by the color scale inset in panel (A). The same P_P value, plotted on the x-axis, was assigned to all eight segments and was varied from 0.3 to 1.0 in increments of 0.1. Twenty replicates were run, and the mean of these 20 runs is shown. In (A), the average % reassortment expected under each condition is plotted. Fully infectious progeny viruses generated from all infected cells are considered in this analysis. The results show that, at each MOI, the % of viruses that are reassortant increases with decreasing P_P. In (B), the average % reassortment for productively co-infected cells is plotted for each MOI condition. Here, only those fully infectious viruses generated in productively co-infected cells are considered. The results show that, regardless of MOI and P_P, the vast majority of fully infectious viruses emerging from co-infected cells have a reassortant genotype. In (C), the ratio of co-infected cells to singly infected cells is plotted on a log 10 scale. This plot shows that, at MOIs less than 3 particles/cell, this ratio increases with decreasing P_P. In

other words, where P_P is lower, a greater proportion of cells are potential vessels for reassortment. A log 10 scale was used to allow visualization of all lines on one graph.

Figure 9. Impact on % reassortment of introducing defective interfering particles into the model. DI particles were introduced into the model by varying P_I values of PB2, PB1 and PA independently from 0.2 – 1.0 in increments of 0.2. Thus, 125 different settings for the prevalence of DI segments were tested. Computational virus populations A and B were assigned the same P_I values in each simulation. For each of the 125 settings, the potency with which the DI segments interfere with infectious virus production, DIX, was set to 0.01 (A), 0.1 (B) and 0.45 (C and D). In each panel, the color assigned to each of the 125 P_I settings reflects the product of P_I(PB2), P_I(PB1) and P_I(PA), with the highest product (0.75) in red and the lowest product (0.008) in blue. In addition, the line representing results obtained with P_I=1.0 for all segments is shown in black for reference. (D) Experimental data obtained with standard virus stocks are plotted with black circles and overlaid on the modeled results for DIX = 0.45. This comparison indicates that, although the presence of mildly interfering DI segments enhances reassortment, this effect is not sufficient to account for the levels of reassortment observed with Pan/99wt and Pan/99var viruses.

Figure 10. Production of virus stocks with high levels of DI particles: ratio of RNA copy number to PFU increases with serial passage at high MOI. Pan/99wt and Pan/99var viruses were passaged five times in MDCK cells. The first passage was performed at an MOI = 5 PFU/cell and subsequent passages were performed with

undiluted cell culture supernatants. RNA copy numbers relative to egg-grown progenitor ("P0") stocks were determined based on the average of NS, M and NA segments. Plaque assays were performed in triplicate. Error bars indicate standard deviation.

Figure 11. Virus populations dominated by DI particles give rise to a higher proportion of dually HA positive cells but a lower proportion of reassortant progeny viruses compared to virus populations with low DI content. Pan/99wt and Pan/99var viruses with matched passage histories were mixed in equal proportions (P0wt + P0var, P3wt + P3var and P4wt + P4var). Each mixture was used to inoculate MDCK cells at a range of MOIs, in triplicate. MOIs of P3 and P4 virus infections were calculated based on RNA equivalents relative to P0, such that comparable numbers of particles/cell were used in each case. A) Relationship between % HA positive cells and % dually HA positive cells. B) Relationship between % HA positive cells and % reassortment. C) Relationship between the proportion of HA positive cells that are dually HA positive and % reassortment. Results from two independent experiments are shown: data labeled as P0a were obtained in parallel with those for P3 and data labeled as P0b were obtained in parallel with those for P4.

Figure 12. Comparison of modeled and experimentally determined relationships among % HA positive cells, % dually HA positive cells and % reassortment. To allow comparison between experimental and theoretical results obtained with DI particles in the virus populations, P_I parameters measured for the P3 (panels A, C, E and G) and P4

(panels B, D, F and H) viruses stocks were input into the model. DIX was varied from 0.05 to 0.5 in increments of 0.05 and is shown with a color scale in each panel, where blue represents DIX=0.05 and orange is DIX=0.5. In panels A-D, P_P values of 0.25, 0.5, 0.75, 0.75, 1.0, 1.0, 1.0, 1.0 for segments 1-8, respectively, were used. In panels E-G, P_P was set to 1.0 for all eight segments.

Figure 13. Theoretical interplay among P_P, P_I and DIX in determining reassortment outcomes. To capture the inter-relationships among P_P, P_I and DIX in determining reassortment levels, we evaluated in the model four representative P_P settings (shown above each column for segments 1 through 8), three disparate DIX values (shown to the left of each row, and 125 different PI settings in which values for PB2, PB1 and PA were varied independently from 0.2 – 1.0 in increments of 0.2 (shown within each panel with colored lines). The color assigned to each of the 125 P_I settings reflects the product of P_I(PB2), P_I(PB1) and P_I(PA), with the highest product (1.0) in red and the lowest product (0.008) in blue.

Table 1. Terminology used herein to identify different types of infected cells and virus particles.

Term	Definition
Infected cell	A cell into which any virus has entered
Co-infected cell	A cell into which at least one virus type A and at least one virus type B has entered
Singly infected cell	A cell into which only one type of virus (A or B) has entered
Productively infected cell	A cell that produces viral progeny
Productively co-infected cell	A cell that has genes of viruses type A and B in any combination and produces viral progeny
Productively singly infected cell	A cell which produces viral progeny of only one type (A or B)
HA positive cell	An infected cell that expresses the HA protein on its surface (in the model, such a cell must have at least one functional copy of each of PB2, PB1, PA, NP and HA)
Dually HA positive cell	A co-infected cell that expresses type A and type B HA proteins on its surface (in the model, such a cell must have at least one functional copy of each of PB2, PB1, PA, NP and HA_A and HA_B)
Reassortant virus	A virus carrying genes of type A and type B in any combination
Multiplicity of infection (MOI)	The average number of virus particles that enter one cell
P_P	The probability that a given segment is present in a virion and copied following infection. Based on their biological properties, segments with nonsense or frameshift mutations or with large internal deletions (DI segments) are treated as present.
P_I	The probability that a segment which is present is also intact and functional
DIX	The factor by which a single DI segment delivered to a productively infected cell changes the output of infectious progeny from that cell.
Fully infectious virus	A virus that can initiate a productive infection in the absence of co-infection
Semi-infectious virus	A virus that delivers fewer than eight segments to the site of replication in the cell. An SI particle cannot complete the viral life cycle in the absence of complementation but does not interfere with infectious progeny production.
Defective-interfering virus	A virus that delivers one or more defective gene segments to a cell. A DI particle cannot complete the viral life cycle in the absence of complementation and interferes with the production of fully infectious progeny in the context of co-infection.

Table 2. Proportion of polymerase segments intact in P3 and P4 viruses, relative to P0 viruses.

	P_I (95% confidence interval)			
Segment	P3wt	P3var	P4wt	P4var
PB2	0.113 (0.027)	0.672 (0.31)	0.134 (0.078)	0.697 (0.30)
PB1	0.111 (0.016)	0.077 (0.021)	0.0616 (0.012)	0.0495 (0.011)
PA	0.288 (0.062)	0.60 (0.13)	0.223 (0.053)	0.462 (0.19)

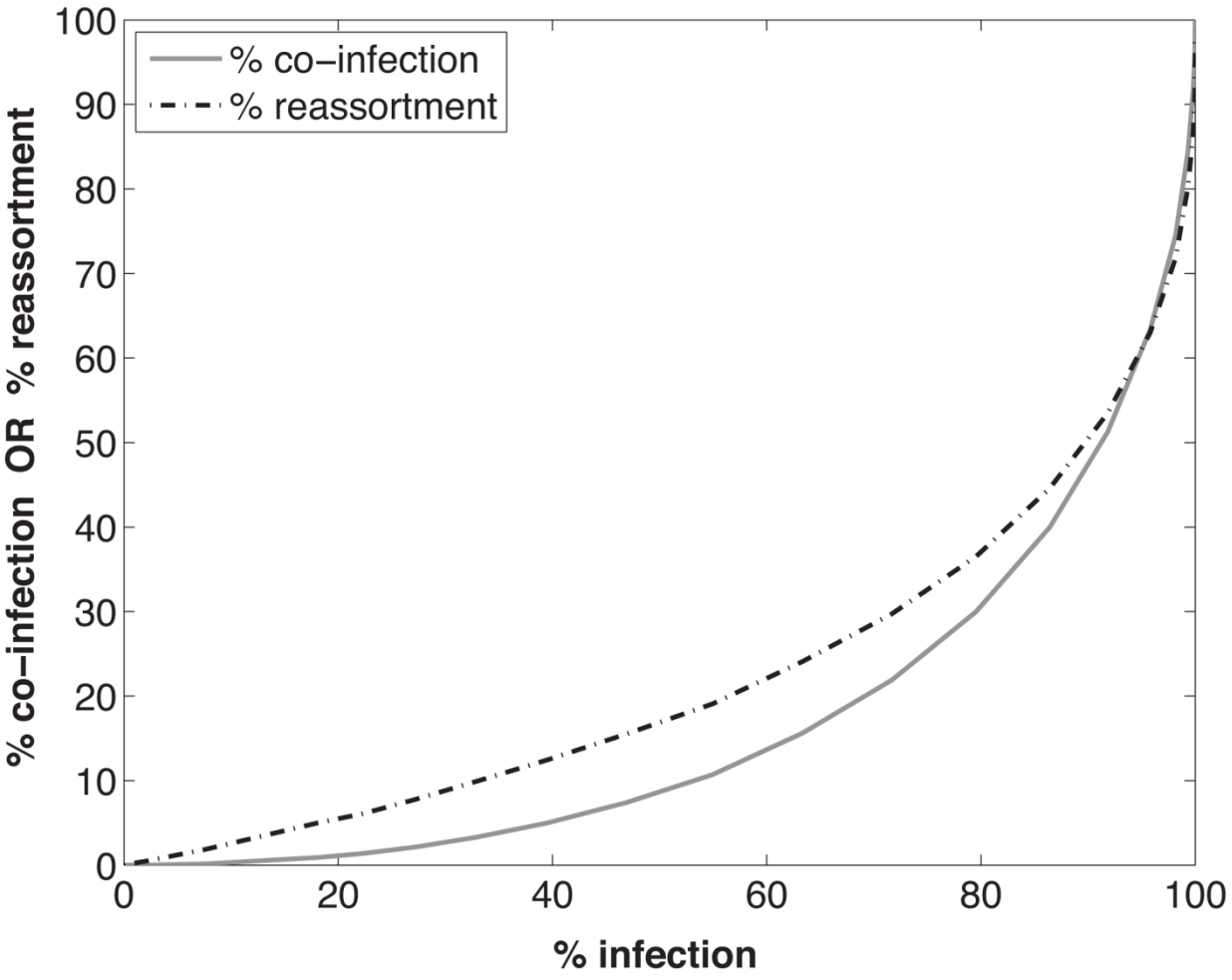
% co–infection
% reassortment
% co–infection OR % reassortment
% infection
0
10
20
30
40
50
60
70
80
90
100
0
20
40
60
80
100

Figure 1

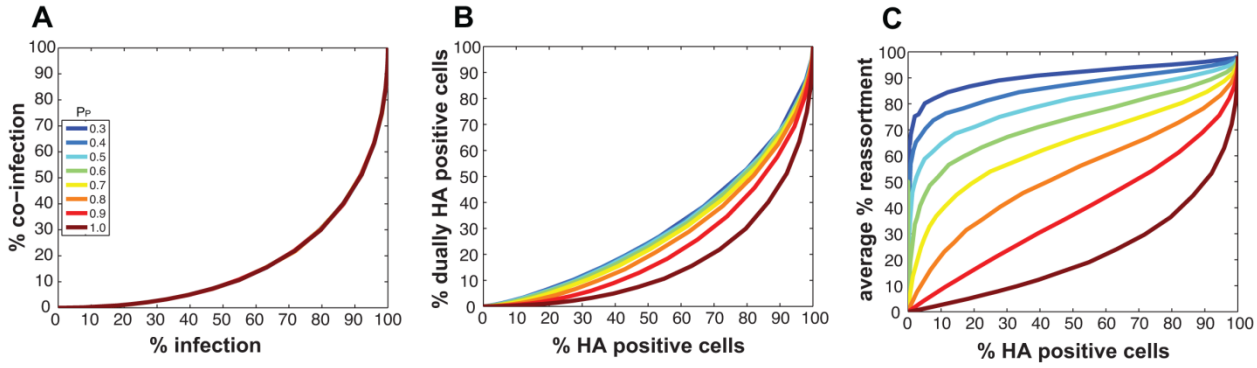
A
% co-infection
% infection
Pp
0.3
0.4
0.5
0.6
0.7
0.8
0.9
1.0
B
% dually HA positive cells
% HA positive cells
C
average % reassortment
% HA positive cells

Figure 2

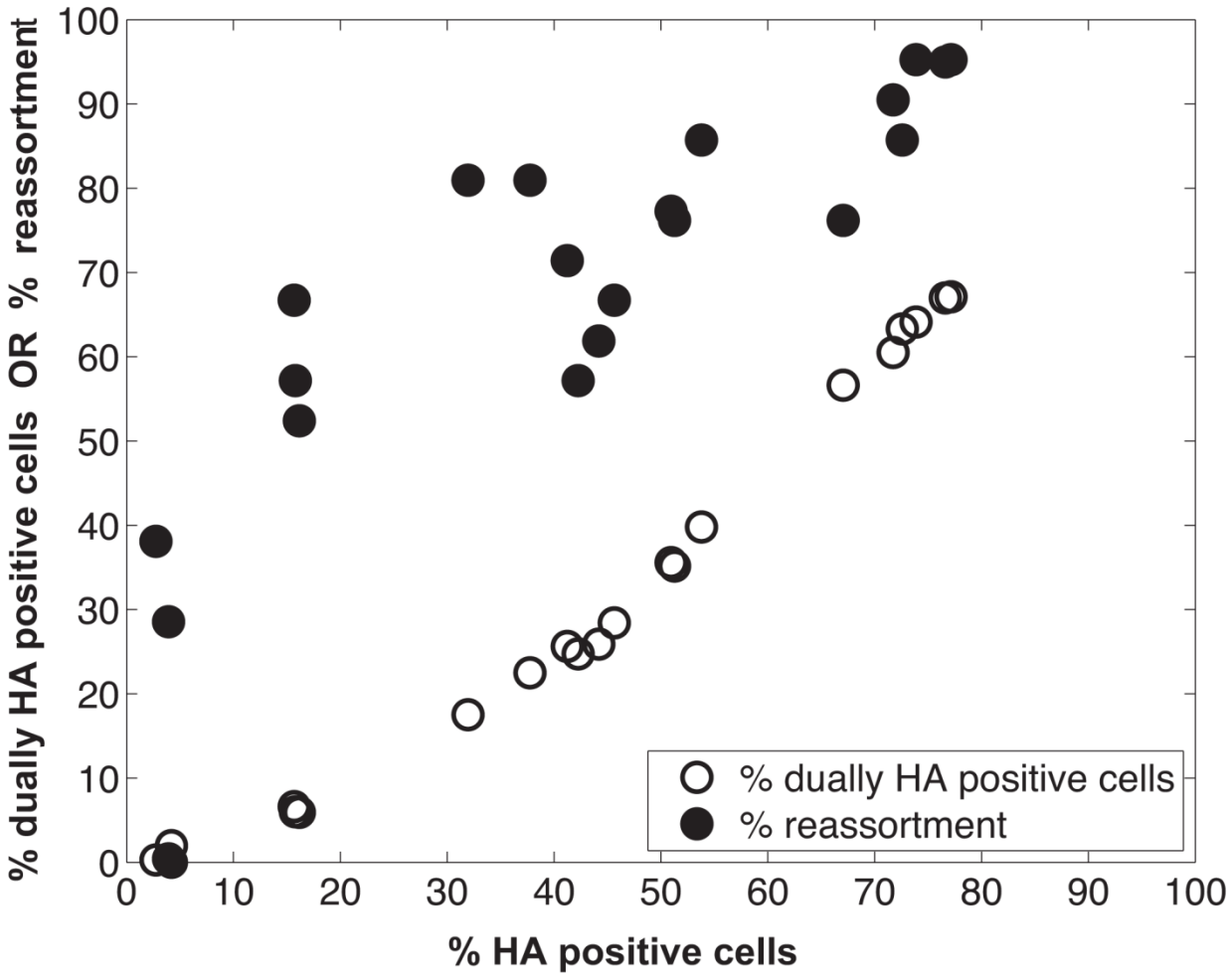
% dually HA positive cells OR % reassortment
% HA positive cells
% dually HA positive cells
% reassortment
0
10
20
30
40
50
60
70
80
90
100

Figure 3

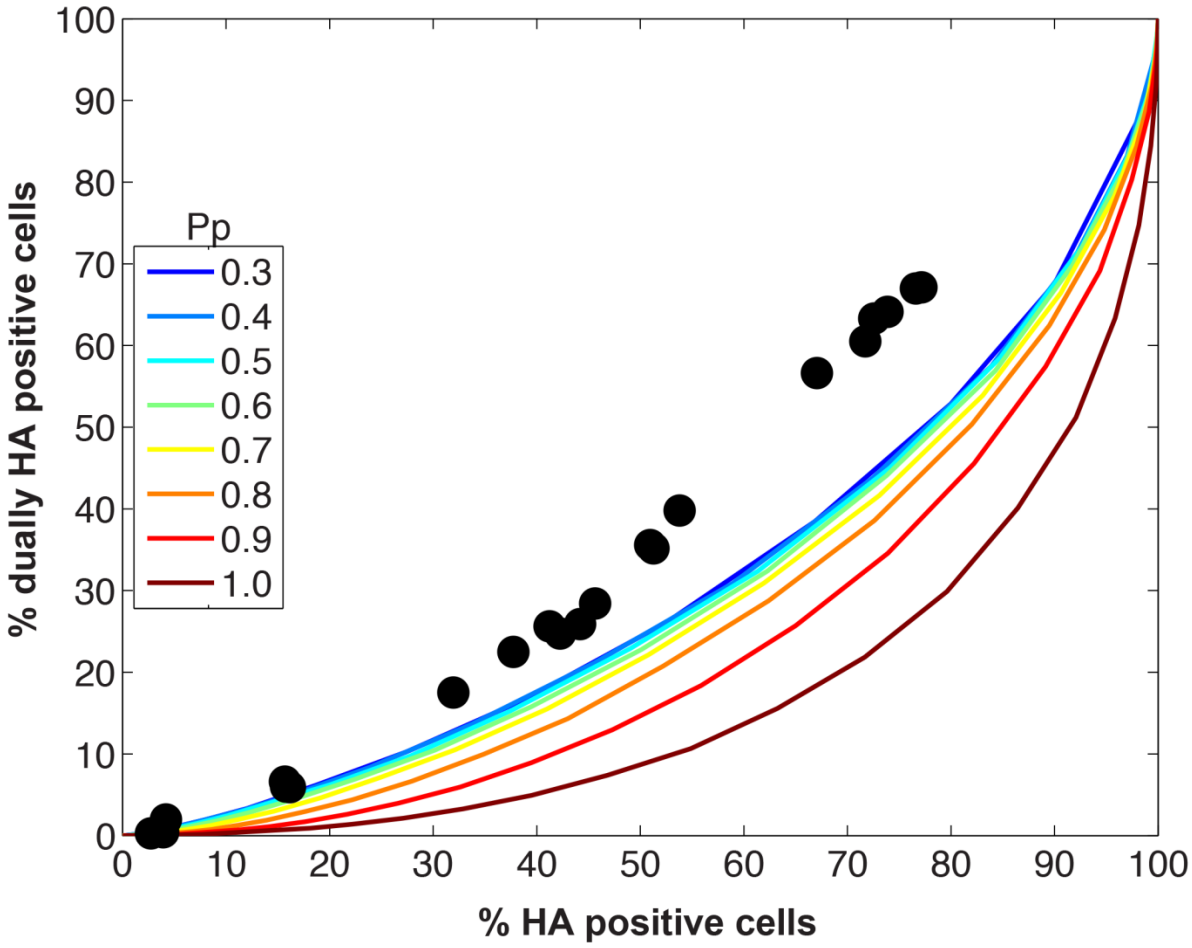
% dually HA positive cells
% HA positive cells
Pp
0.3
0.4
0.5
0.6
0.7
0.8
0.9
1.0
0
10
20
30
40
50
60
70
80
90
100

Figure 4

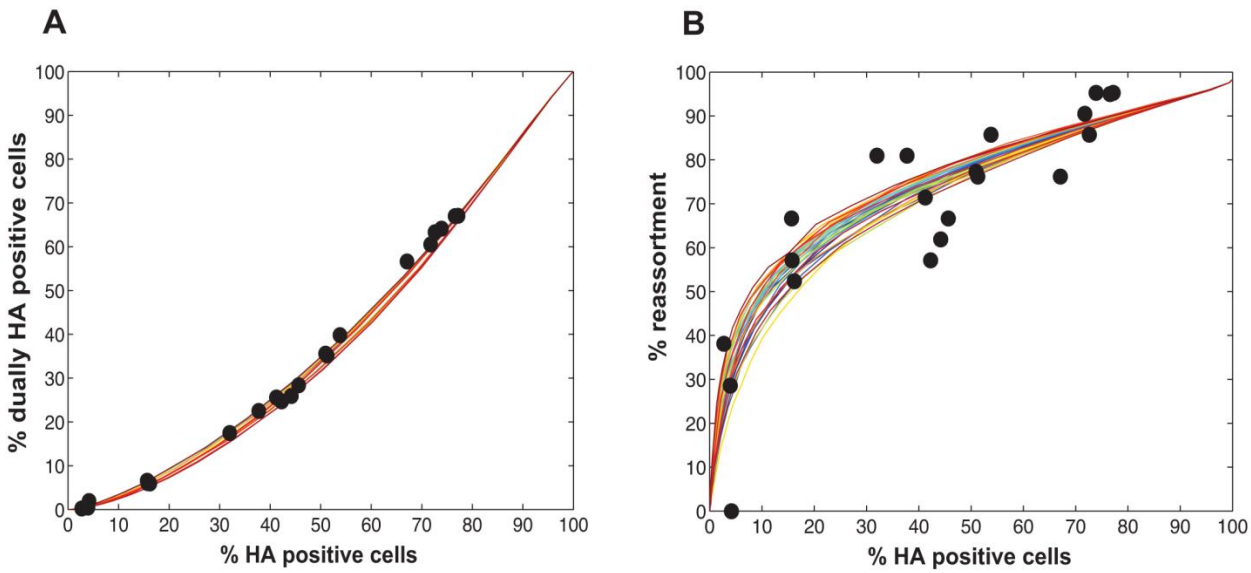
A
% dually HA positive cells
% HA positive cells
B
% reassortment
% HA positive cells

Figure 5

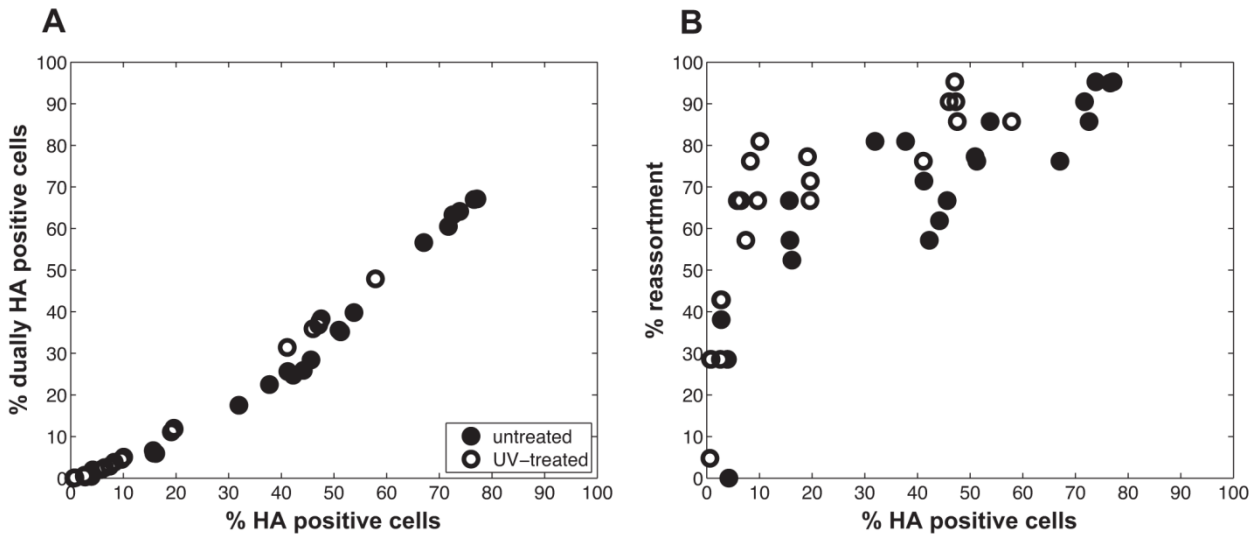
A
% dually HA positive cells
% HA positive cells
untreated
UV–treated
B
% reassortment
% HA positive cells

Figure 6

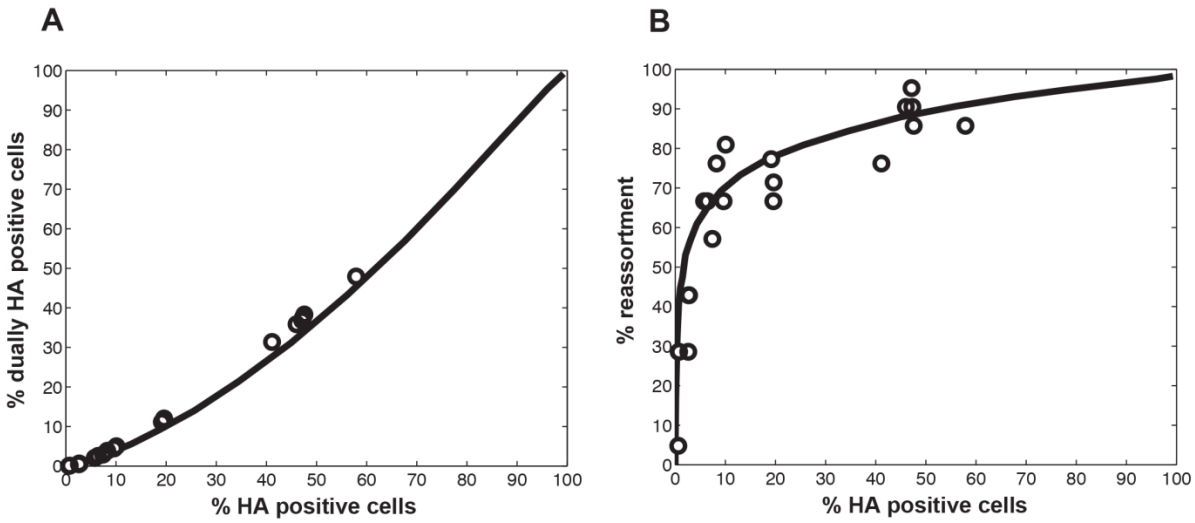
A
% dually HA positive cells
% HA positive cells
B
% reassortment
% HA positive cells

Figure 7

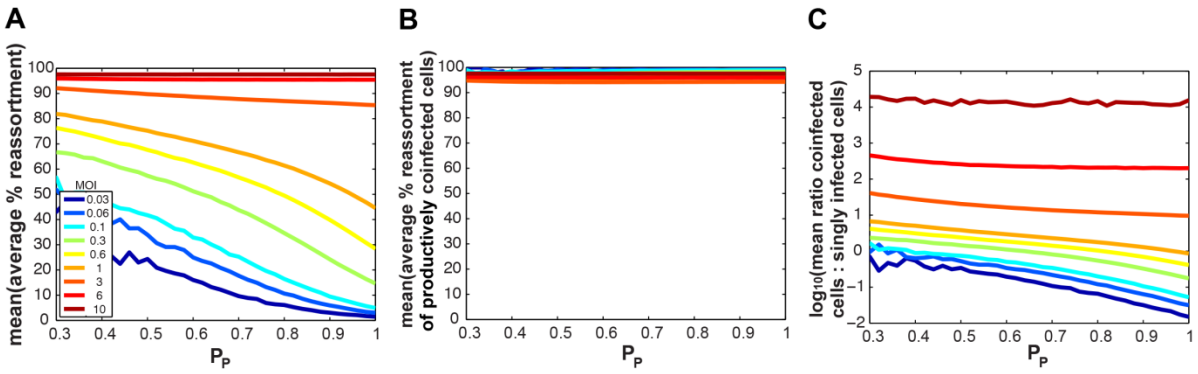
A
B
C
mean(average % reassortment)
mean(average % reassortment of productively coinfected cells)
log10(mean ratio coinfected cells : singly infected cells)
MOI
0.03
0.06
0.1
0.3
0.6
1
3
6
10
PP

Figure 8

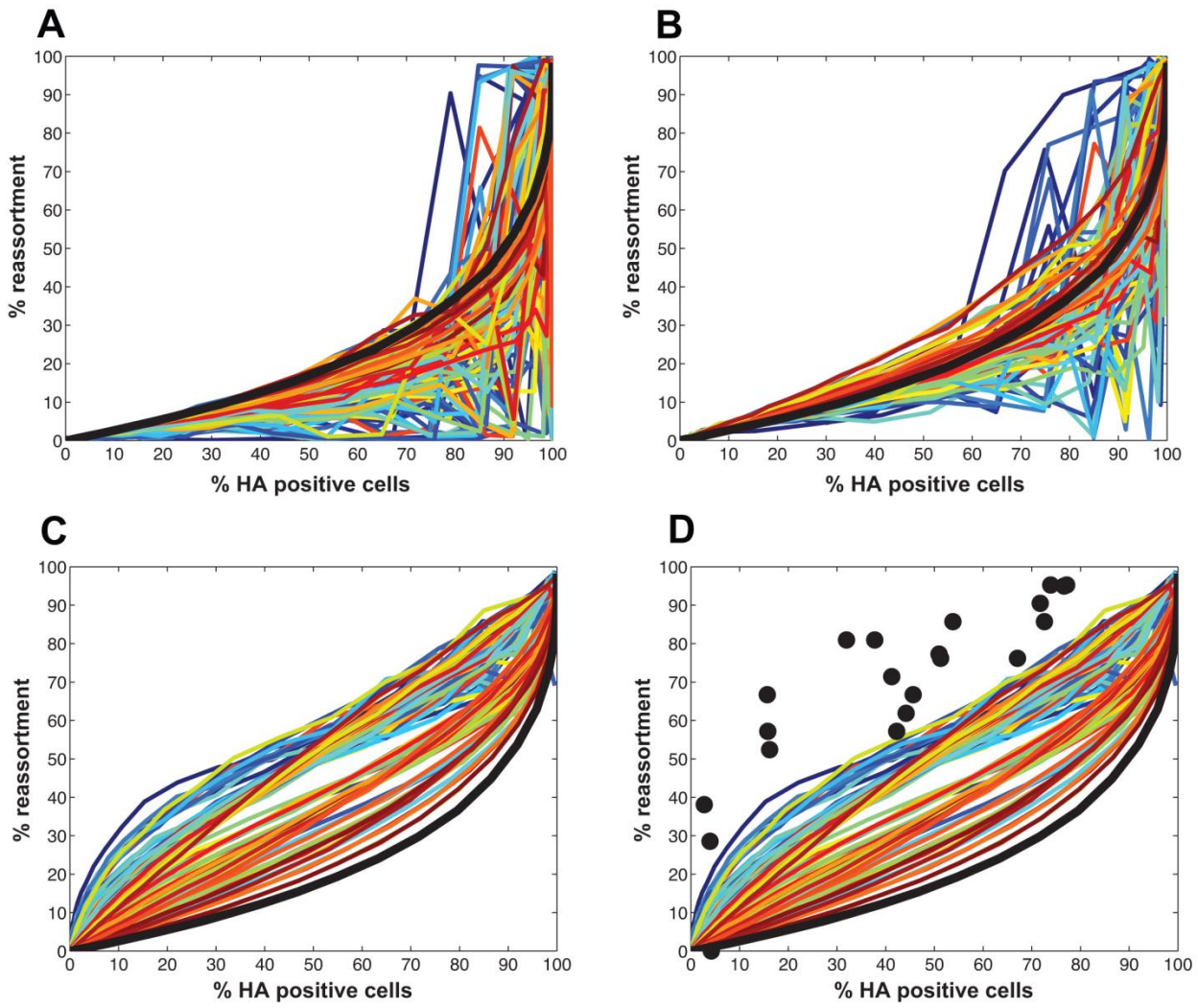
A
B
C
D
% reassortment
% HA positive cells
0
10
20
30
40
50
60
70
80
90
100

Figure 9

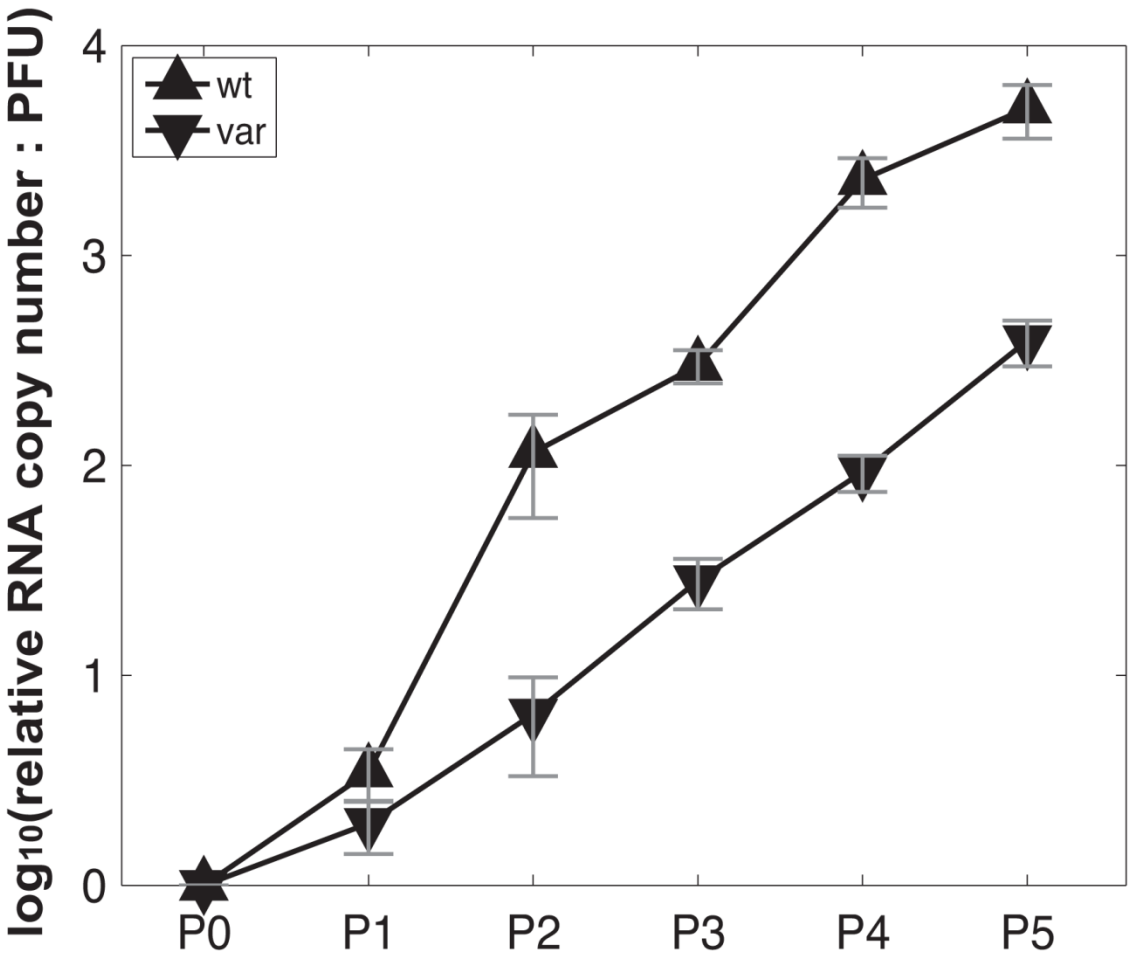
log10(relative RNA copy number : PFU)
4
3
2
1
0
wt
var
P0
P1
P2
P3
P4
P5

Figure 10

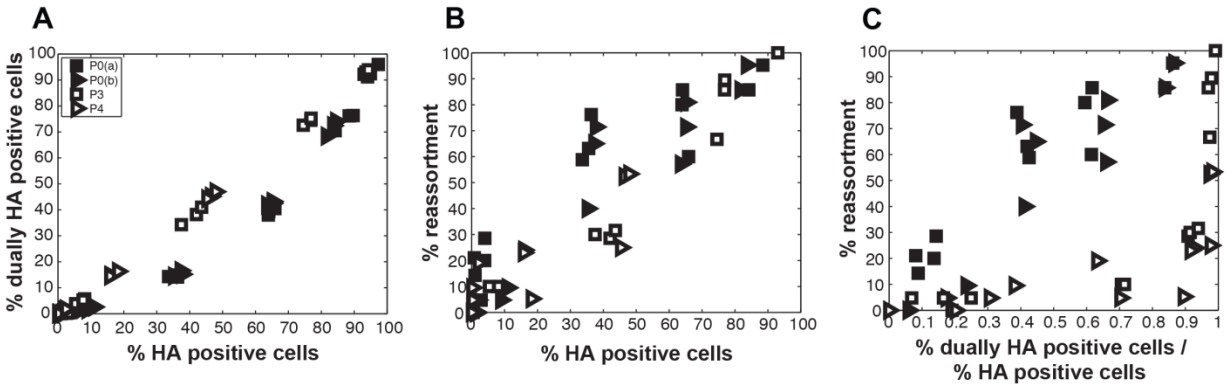
A
B
C
P0(a)
P0(b)
P3
P4
% dually HA positive cells
% HA positive cells
% reassortment
% HA positive cells
% reassortment
% dually HA positive cells /
% HA positive cells

Figure 11

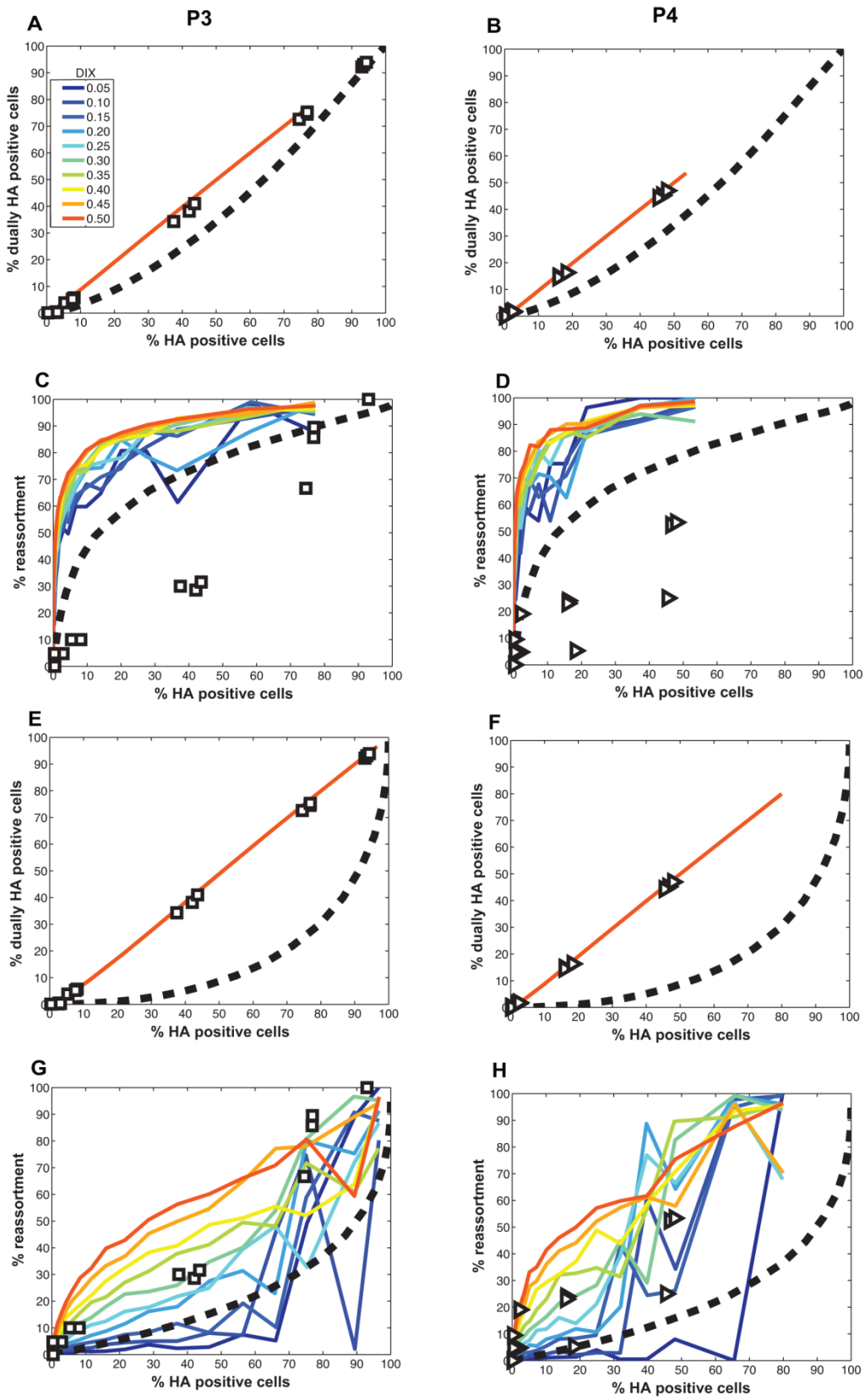
A
P3
B
P4
C
D
E
F
G
H
DIX
0.05
0.10
0.15
0.20
0.25
0.30
0.35
0.40
0.45
0.50
% dually HA positive cells
% reassortment
% HA positive cells

Figure 12

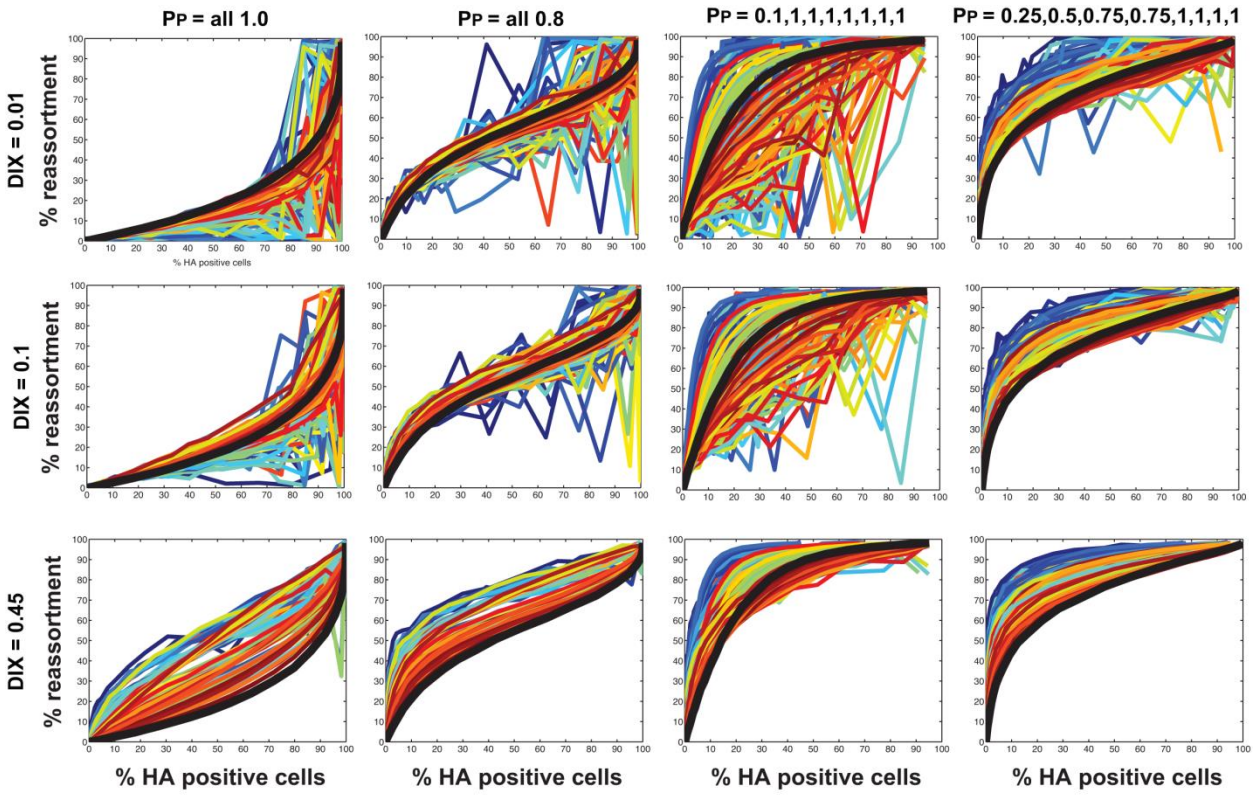
PP = all 1.0
PP = all 0.8
PP = 0.1,1,1,1,1,1,1,1
PP = 0.25,0.5,0.75,0.75,1,1,1,1
DIX = 0.01
DIX = 0.1
DIX = 0.45
% reassortment
% HA positive cells

Figure 13

Chapter 4: Mechanisms of influenza virus super-infection interference

Nicolle Marshall, Debby van Riel, John Steel and Anice C. Lowen

The work of this chapter is in preparation for publication

Abstract

Reassortment plays a significant role in the evolution of influenza A virus and has repeatedly contributed to the emergence pandemics and epidemics. However, many fundamental aspects of reassortment remain poorly understood. Our previous work defined time windows during which influenza virus super-infection must occur to see reassortment in cell culture and in-vivo. We discovered that super-infection interference was the primary mechanism preventing reassortment beyond that time window. Herein, we examined two mechanisms that could underlie the observed super-infection interference: 1) removal of sialic acid receptors by the viral neuraminidase and 2) host innate immune responses. To test the role of sialic acid stripping, we first confirmed that treatment of cells with exogenous neuraminidase was sufficient to decrease infection levels. Next, we compared levels of co-infection and reassortment achieved upon super-infection when initial infections were performed with influenza A/Panama/2007/99 (Pan/99) virus vs. a neuraminidase-deficient Pan/99 virus (Pan/99-NA mut). Late in infection, the number of sialic acid-positive cells was markedly higher when first infecting with Pan/99-NA mut virus. While we observed greater super-infection in cells infected with Pan/99-NA mut virus than in those infected with Pan/99 virus, exclusion of the second virus remained strong following Pan/99-NAmut infection. To evaluate the role of innate immune responses, we assessed whether the kinetics of the IFN-β response were consistent with those of super-infection interference. We found a strong temporal correlation between declining super-infection and increasing IFN-β mRNA. Our results indicate that influenza virus neuraminidase activity can inhibit super-infection and therefore reassortment, but that host antiviral responses appear to play a greater role in

our system. Natural variation in NA activity and viral interferon antagonists may therefore lead to strain differences in the frequency of reassortment.

Introduction

Influenza A virus (IAV) carries an eight-segmented genome. Due to its segmentation, the viral genome can undergo reassortment, or the exchange of gene segments between two or more distinct strains upon co-infection of the same cell. Reassortment can result in progeny viruses that are different from the parental viruses both genotypically and phenotypically. For this reason, reassortment can give rise to viruses with the potential to initiate pandemics and epidemics. For example, the unusually severe epidemics of 1947, 1951 and 2003 were the result of reassortant viruses generated from co-circulating human IAV strains [1, 2]. In addition, reassortant viruses carrying genes from human, avian, and – in 2009 – swine adapted influenza A viruses caused the 1957, 1968 and 2009 influenza pandemics [3-6]. Reassortment has also been shown to underlie other zoonotic events, such as the generation of H5N1 and H7N9 subtype viruses that are currently circulating in poultry in Southeast Asia [7-9]. The potential for reassortment to bring together mutations that modify host range, transmission and/or pathogenicity make it a significant factor in influenza virus evolution.

Many different viruses exhibit super-infection interference: once infection is established within a host cell, that cell is refractory to re-infection with the same or a similar virus. This effect can arise through different mechanisms. For example, several paramyxoviruses prevent super-infection by removal of the oligosaccharide viral receptor from the host cell surface after primary infection [10-13]. Comparably, Human immunodeficiency virus-1 (HIV-1) employs the Env, Vpu and Nef proteins to down-

regulate the CD4 receptor from the host cell surface to resist super-infection [14-16]. The ability of innate immune responses to block primary infections suggests they may also play a role in super-infection exclusion, and limited studies have alluded to such a role of interferon (IFN) responses [17, 18]. This mechanism of interference may take effect at the point of viral entry or replication [19, 20]. Super-infection exclusion could have a significant impact on viral evolution as it reduces the likelihood that two distinct viruses would infect the same cell, a necessary prerequisite for reassortment or recombination. To date, there is limited information on the mechanisms of influenza A virus super-infection interference and their impact on reassortment frequency.

Herein, we examined the contributions of the viral receptor-destroying enzyme, neuraminidase (NA), and host type I IFN responses to inhibition of influenza A virus super-infection. Using lectin staining, we show that a primary infection with A/Panama/2007/99 virus significantly reduced the availability of viral receptors in a time-dependent fashion. In contrast, primary infection with an NA-deficient Pan/99 virus led to minimal stripping of viral receptors throughout the course of infection. Accordingly, when primary infection was performed with the NA deficient virus, a greater number of cells became super-infected at late times post-infection compared to primary infection with the NA competent Pan/99 virus. The level of super-infection observed following Pan/99-NAmut virus infection remained low, however, compared to that achieved early after infection with either Pan/99 virus, suggesting a second mechanism was at play. Examination of the kinetics of IFN-β induction revealed a robust correlation between increased IFN-β mRNA and decreased numbers of co-infected cells, suggesting that cellular innate immune responses play a critical role in super-infection

exclusion. Our data indicate that innate responses are the more potent mechanism of influenza A virus super-infection interference in our system, but that NA activity can also block super-infection.

Materials and Methods

Viruses

A/Panama/2007/99 wild-type and variant viruses were generated by reverse genetics as previously described [21] and propagated in 11-day old embryonated chicken eggs at 37˚C to generate virus stocks. Virus titers were determined by plaque assay on MDCK cells. Four recombinant (r) Pan/99 viruses were used for the experiments described: rPan/99wt-HIS, rPan/99var2-HA, rPan/99var6, and rPan/99var-HA: NA D198N (rPan/99-NA mut). The first three viruses, rPan/99wt-HIS, rPan/99var2-HA and rPan/99var6, have been described previously [22]. Briefly, rPan/99wt-HIS is a reverse-genetics derived version of the wild-type A/Panama/2007/99 virus that encodes a HIS tag C-terminal to the HA signal peptide. The rPan/99var2-HA virus is similar to the rPan/99wt-HIS virus but contains silent mutations in each of the eight gene segments and encodes an HA tag C-terminal to the HA signal peptide. The rPan/99var6 virus carries silent mutations in each of the eight gene segments relative to the wild-type Pan/99 virus (and no epitope tag). The fourth virus, rPan/99-NA mut, is identical to the rPan/99var2-HA virus except for an aspartic acid to asparagine mutation at amino acid position 198 of the NA protein. Influenza A/Netherlands/213/03 (H3N2) virus, which was used in virus histochemistry, is a human isolate grown in MDCK cells.

Cells

Madin-Darby Canine Kidney cells were maintained in minimal essential medium (MEM) supplemented with 10% FBS and penicillin-streptomycin. 293T cells were maintained in Dulbecco's MEM supplemented with 10% FBS.

Guinea Pigs

Female, Hartley strain guinea pigs weighing 300-350g were obtained from Charles River Laboratories. Prior to intranasal inoculation and euthanization by CO2, guinea pigs were sedated with a mixture of ketamine and xylazine (30mg/kg and 2mg/kg, respectively). Inoculation was performed by instilling a 300 ul volume of virus diluted PBS intranasally, as described previously [23].

Virus preparation, inactivation and labeling for virus histochemistry

A/Netherlands/213/03 virus was grown in MDCK cells. The supernatant was harvested and cleared by low-speed centrifugation. Cleared supernatants were then centrifuged at 85k x g for 2h in a SW28 rotor at 4˚C. The pellet was re-suspended in 2ml of PBS and then placed on a sucrose gradient (20%-60% w/w) and centrifuged overnight at 300k x g in a SW41 rotor at 4˚C. The sucrose was removed by additional centrifugation at 85k x g for 2h in a SW28 rotor at 4˚C. The virus was re-suspended in PBS and inactivated by incubation with 1:1 (v/v) 10% formalin for 1h at room temperature. After inactivation, virus suspensions were dialyzed against PBS. Inactivation was confirmed by inability to passage on MDCK cells. The concentrated virus was labeled by mixing re-suspended viruses with 0.1mg/ml fluorescein isothiocyanate (FITC, Sigma Aldrich) in 0.5mol/L bicarbonate buffer (pH 9.5) for 1h with constant stirring. To remove excess FITC, the

labeled virus was dialyzed against PBS. The hemagglutinin titer was determined after inactivation and labeling to ensure HA activity.

Histochemistry

Guinea pigs (n=3) were inoculated intranasally with 106 PFU of rPan/99var6 virus. At 48h post-infection, nasal turbinates, specifically the respiratory and olfactory epithelia of the upper respiratory tract, were extracted and fixed in 10% formalin and processed within 48h for paraffin embedding. After paraffin-embedding, tissue samples were sectioned at 3μm intervals. Paraffin was removed from the tissues with xylene and hydrated using an alcohol gradient. Duplicate sections were stained for 1) detection of viral antigen and 2) detection of viral attachment. For detection of viral antigen, a primary antibody against the viral nucleoprotein (Mouse-anti-influenza A NP, Clone Hb65, mouse IgG2; R&D) was used as previously described [24] with the following modifications: tissue sections were pre-incubated with 0.1% protease in pre-warmed PBS for 10 minutes at 37˚C. Binding of the primary antibody was detected using a peroxidase-labeled goat-anti-mouse IgG2a secondary antibody (Southern Biotech). Peroxidase was revealed using a 3-amino-9-ethyl-carbazole (AEC, Sigma Chemicals) in 2.5ml N, N-dimethylformamide (DMF), resulting in a red precipitate. For the detection of viral attachment to the tissues, tissues were incubated with the concentrated, labeled A/Netherlands/213/03 (H3N2) virus overnight at 4˚C at a titer of 50-100 hemagglutinin units/50ul. The FITC-label was detected with horseradish peroxidase-labeled rabbit anti-FITC antibody (Dako, Glostrup, Denmark). The signal was amplified with a tyramide signal amplification system (Perkin Elmer) according to the manufacturer's instructions. The peroxidase was revealed with 3-amino-9-ethyl-carbazole, producing a red

precipitate. All tissues were counterstained with hematoxylin and embedded in glycerol gelatin. Viral attachment and antigen is visualized by a red precipitate on the surface of epithelial cells by light microscopy.

Bacterial neuraminidase assay

A 6-well dish of nearly confluent MDCK cells were treated with MEM media, supplemented with 10% FBS, penicillin-streptomycin and varying concentrations (0, 120 or 240 mU/ml) of exogenous bacterial neuraminidase (Clostridium perfringens (C.welchii); Sigma Aldrich) for 24h at 37˚C. rPan/99wt-HIS virus was diluted in PBS to the appropriate titer for inoculation at MOI 10 PFU/cell. Prior to inoculating MDCK cells, the 6-well dish was placed on ice, growth media was removed and monolayers washed three times with cold PBS. Each well was inoculated with a 250ul volume of prepared virus and incubated at 4˚C for one hour to allow virus binding. With the 6-well dishes on ice, inocula were aspirated and monolayers were washed three times with cold PBS to remove any unattached virus. Cells were treated with virus medium (MEM supplemented with 3% BSA, penicillin-streptomycin and 1ug/ml TPCK trypsin) and transferred to 33˚C. At 12h post-infection, MDCK cells were harvested by trypsinizing the monolayer and collected in serum-supplemented media. The cells were prepared for flow cytometry (see below) to determine the number of alpha-2,6 sialic acid positive cells and the number of HIS-positive cells.

Comparison of co-infection and reassortment with NA-competent vs. NA-deficient primary viruses

To examine the effect of viral neuraminidase activity on co-infection and reassortment, primary infections were performed in parallel with rPan/99var2-HA virus or rPan/99-NAmut virus. At a range of time points after primary infection, cells were collected for enumeration of alpha-2,6 sialic acid (2,6-SA) positive MDCK cells or secondary infection was performed with rPan/99wt-His virus. Each infection condition was set up in triplicate. Thus, to evaluate seven time points, seven 6 well plates were set up for detection of 2,6-SA and seven 6 well plates were set up for super-infection. Super-infections were performed as previously described [22]. Briefly, for the "0h" time point, MDCK cells were infected simultaneously with rPan/99wt-HIS virus and either rPan/99var2-HA or rPan/99-NA mut virus at MOI 10 PFU/cell of each virus. For the remaining time points, cells were infected at MOI 10 PFU/cell with either rPan/99var2-HA or rPan/99-NA mut virus at time = 0h and then subsequently (2, 4, 8, 12, 16, or 24h after the primary virus infection) infected with rPan/99wt-HIS virus at MOI 10 PFU/cell. All infections were performed on ice, with attachment at 4˚C for one hour, and subsequent incubation at 33˚C.

Enumeration of co-infected cells

To determine the number of co-infected cells, MDCK cells were harvested 12h post-infection with rPan/99wt-HIS virus and prepared for flow cytometry [22]. Briefly, cells were trypsinized and collected with serum-supplemented media. The cells were washed three times with PBS-2% FBS and incubated with Penta HIS Alexa Fluor 647 conjugated antibody (5ug/ml; Qiagen) and Anti-HA-FITC Clone HA-7 (7ug/ml; Sigma Aldrich) for 45 minutes, on ice, in the dark. The cells were then washed two times with PBS-2% FBS

and re-suspended with PBS-2% FBS and 5ul/sample (0.25ug) of 7-Amino Actinomycin D (7-AAD), a dead cell excluder (BD Biosciences). Flow cytometry was performed using a FACSDiva flow cytometer and analyzed with FlowJo software.

Determination of reassortment frequency

To determine the reassortment frequency, virus genotypes were determined by qPCR and high resolution melt analysis as previously described [22]. In summary, the cell supernatant was used to obtain plaque isolates by plaque assay. RNA was then isolated from the plaque isolates using the Zymogen 96 Viral RNA kit according to the manufacturer's instructions (with the exception of using 40ul of water for elution). Twelve microliters of RNA was reverse transcribed from an IAV-specific "universal" primer (Univ. F(A): 5' GGCCAGCAAAAGCAGG) using Maxima Reverse Transcriptase (Fermentas) according to the manufacturer's protocol. The cDNA was used as a template in qPCR reactions with segment specific primers [22] and Precision Melt Supermix (BioRad) in a white, 384-well, thin-wall plate (BioRad). Both qPCR and high resolution melt analysis were performed using a CFX384 Real-Time PCR Detection System. Data was analyzed using Precision Melt Analysis software (BioRad). Viruses were scored as reassortant if the genome comprised any combination of wt and var gene segments.

Enumeration of alpha-2,6 sialic acid positive MDCK cells

To determine the number of alpha-2,6 sialic acid positive MDCK cells, cells were harvested (as described above for enumeration of co-infected cells) at 2, 4, 8, 12, 16, or 24h post-infection with either rPan/99var2-HA or rPan/99-NA mut virus . The cells were washed three times with PBS-2% BSA and incubated with Fluorescein Sambucus Nigra

(Elderberry) Bark Lectin (20ug/ml; Vector Labs) for 45 minutes, on ice, in the dark. Cells were then washed two times with PBS-2% BSA and re-suspended with PBS-2% BSA and 5ul/sample (0.25ug) of 7-Amino Actinomycin D (7-AAD), a dead cell excluder (BD Biosciences). Flow cytometry was performed using a FACSDiva flow cytometer (Becton Dickinson) and analyzed with FlowJo software.

Comparison of the kinetics of host innate responses and super-infection interference

To investigate the role of host innate responses in preventing super-infection, we monitored levels of IFN-β mRNA and the efficiency of super-infection in parallel. Triplicate MDCK cells in 6 well dishes were infected with rPan/99var2-HA virus at MOI 10 PFU/cell for each time point and for each analysis. Cells were collected from three wells at each time point for quantification of IFN-β mRNA. Super-infections with rPan/99wt-HIS virus were performed with the remaining wells as described above for comparison of NA-competent and NA-deficient viruses.

Determining the amount of IFN-β induction in MDCK cells

To quantify the amount of IFN-β mRNA in MDCK cells at 2, 4, 8, 12, 16, or 24h post-infection with rPan/99var2-HA virus, cell monolayers were collected in 1ml of Qiagen Cell Protect Reagent and stored at -20˚C. Samples were later thawed and centrifuged at 5000 x g for five minutes. The supernatant was discarded and RNA was extracted from the samples using Qiagen RNeasy Plus Mini kit following the manufacturer's instructions, eluting in 35ul of RNase-free water. One microgram of RNA was reverse transcribed from random hexamers (Invitrogen) using Maxima Reverse Transcriptase (Fermentas) according the manufacturer's protocol. The cDNA was used as a template in qPCR reactions with primers specific for canine IFN-β and 18s [25] and SsoFast

EvaGreen Supermix (BioRad) in a white, 384-well, thin-wall PCR plate (BioRad). Levels of IFN-β mRNA relative to those in uninfected cells were calculated as 2^-Ct, using 18s rRNA for data normalization.

Results

Infection with influenza virus inhibits attachment by a second influenza virus ex-vivo

The last step in the influenza virus life cycle is the cleavage of sialic acid receptors on the host cell surface, which is necessary for the release of progeny virus. Because viral binding of sialic acid receptors is a necessary precursor to infection, we decided to test whether a primary influenza virus infection in vivo would influence the attachment of a second influenza virus to epithelial cells of the infected tissues. We first inoculated guinea pigs with rPan/99var6 virus at 10^6 PFU, and at 48h post-infection harvested the olfactory and respiratory epithelia from the upper respiratory tract. The tissues were then embedded, serially sectioned and stained either with an anti-NP antibody to detect influenza virus infected cells, or with a labeled H3N2 subtype influenza virus to evaluate viral attachment. As shown in Figure 1(A), viral infection is seen in patches on the apical surface of epithelial cells, as indicated by the red precipitate. Strikingly, the attachment pattern of virus added ex vivo, shown in Figure 1(B), is reciprocal to the pattern of infection. Viral attachment *ex-vivo* occurs only on uninfected cells, indicating that influenza virus-infected cells are resistant to viral attachment, most likely due to a lack of sialic acid receptors.

Pre-treating with bacterial neuraminidase reduces influenza virus infection MDCK cells

As a direct test of the hypothesis that sialic acid removal by the progeny virus neuraminidase prevents attachment by a second influenza virus, we pre-treated MDCK cells with exogenous bacterial NA (bNA) at varying concentrations. The cells were washed and inoculated, on ice, with rPan/99wt-HIS virus at MOI 10 PFU/cell. Inoculation on ice and a subsequent 1h attachment period at 4˚C was used to inhibit the effects of any residual NA. At 12h post-infection, cells were harvested to determine the percentage of cells infected and the proportion of cells that were positive for 2,6-SAs by flow cytometry. The results show a reduction in the number of alpha-2,6-SA-positive cells with increasing concentrations of bacterial NA (Figure 2). With a concentration of 240mU/ml of bacterial NA, the quantity of 2,6-SA positive cells decreased by approximately 92% compared to 0mU/ml of bNA. This reduction was accompanied by a 55% reduction in the number of infected cells when compared to 0mU/ml, suggesting that stripping of cell surface SAs by the viral neuraminidase could be an important mechanism of super-infection interference.

Neuraminidase deficient virus elicits incomplete super-infection interference

Together, the results from the guinea pig and bacterial neuraminidase experiments strongly suggest that sialic acid stripping has the potential to lead to super-infection interference. To evaluate directly whether viral neuraminidase activity prevents super-infection, we compared the efficiency of super-infection when the first virus applied to cells encoded a mutant NA protein with negligible enzyme activity [26] to the efficiency seen when the first virus encoded a wild-type NA protein. Experiments were performed in which inoculation of MDCK cells with either rPan/99var2-HA or rPan/99-NA mut

virus was followed at a series of time points later by inoculation with rPan/99wt-HIS virus. At 12h post-infection with rPan/99wt-HIS virus, supernatant was collected to genotype released virus and cells were harvested to determine what proportion of cells were co-infected. In parallel, the number of alpha-2,6 sialic acid-positive cells present at the time of super-infection with rPan/99wt-HIS virus was evaluated using a second set of cell cultures. At each time point post-infection with the primary virus (rPan/99var2-HA or rPan/99-NA mut), triplicate wells were harvested for analysis of 2,6-SA positivity by flow cytometry (experimental design is outlined in Figure 3). As seen in Figure 4, late in infection (24h), we observed a marked increase in the number of 2,6-SA positive cells when first infecting with rPan/99-NA mut virus as compared to rPan/99var2-HA virus (79% vs 7%). Correspondingly, during the same time, primary infection with rPan/99-NA mut virus supported higher levels of super-infection relative to rPan/99var2-HA virus (Figure 5 (A)). The proportion of co-infected cells at 24h was 16% when rPan/99-NA mut virus was used for the primary infection, whereas primary infection with rPan/99var2-HA virus only supported 0.84% co-infection. Despite having higher levels of 2,6-SA's and a higher proportion of the cells co-infected when rPan/99-NA mut virus was used for primary infections vs. rPan/99var2-HA virus, higher levels of reassortment were not achieved (Figure 5 (B)). At 24h, with a 72% increase in 2,6-SAs and a 15% increase in the quantity of co-infected cells relative to infection with rPan/99var2-HA virus, rPan/99-NA mut virus only supported a 4.7% increase in the amount of reassortment (9.5% vs 4.8%). Thus, when primary infection is characterized by low NA activity, the potential for productive secondary infection is increased but not rescued completely, and the potential for reassortment is not detectably affected.

A decrease in co-infection correlates temporally with an increase in the host innate immune response

Although we observed a greater amount of co-infected cells at 24h with the rPan/99-NA mut virus, levels were not as high as we had predicted given the significant amount of 2,6-SAs present at the same time point. We therefore hypothesized that an additional mechanism, specifically the host innate immune response, was contributing to super-infection interference. To test this hypothesis, we again evaluated the efficiency of super-infection at a range of time points in MDCK cells and this time measured IFN- β mRNA levels in parallel. For super-infection, cells were inoculated with rPan/99var2-HA and rPan/99wt-HIS viruses simultaneously (0h) or first inoculated with rPan/99var2-HA virus and at a series of time points later (2, 4, 8, 12, 16, or 24h) with rPan/99wt-HIS virus. At 12h post-infection with rPan/99wt-HIS virus, cells were harvested and the number of co-infected cells was determined by flow cytometry. To assess induction of the type I IFN response, triplicate wells set up in parallel with those for super-infection were harvested at each time point and the production of IFN-β mRNA was determined by RT qPCR. We found that, as the amount of IFN-β mRNA in the host cell increased, the number of co-infected cells decreased (Figure 6). At time 0h, a high proportion of co-infected cells was observed (97%), without any IFN-β mRNA detected. However, as the time between infections spread to 8h, there is a significant decrease (76%) in co-infection relative to a simultaneous infection (0h), which is accompanied with an increase in the amount of IFN-β mRNA induced to levels of about 26 times that of mock-infected cells. Finally, at 24h, co-infection decreased to 0.44%, while the quantity of IFN-β mRNA rose to levels of ~1300 times that of mock-infected cells. This striking inverse correlation

between IFN-β expression and super-infection suggests a prominent role for innate immune responses in super-infection exclusion.

Figure Legends

Figure 1. Infection with influenza virus inhibits attachment by a second influenza virus ex-vivo. Guinea pigs were inoculated intranasally with 10^6 PFU of Pan/99var6 virus. Nasal turbinates were harvested 48h p.i. and tissues were embedded, serially sectioned and stained with either anti-influenza NP antibody to determine areas of infection (A) or with labeled A/Netherlands/213/03 (H3N2) virus to determine areas of attachment (B).

Figure 2. Treating with bacterial NA is sufficient to markedly reduce infection of MDCK cells. MDCK cells were treated with varying concentrations of bacterial neuraminidase for 24h before being infected with Pan/99wt-HIS virus (MOI 10). At 12h p.i., cells were harvested and the number of α-2,6 sialic acid positive cells were determined using an SNA lectin and flow cytometry. The number of HIS-positive cells were determined using an anti-HIS antibody and flow cytometry. Error bars represent average value of +/- standard deviation.

Figure 3. Super-infection experimental design. MDCK cells were first inoculated with both rPan/99var2-HA and rPan/99wt-HIS viruses simultaneously (0h) or first with rPan/99var2-HA virus and at a series of time points later (2, 4, 8, 12, 16 or 24h) with rPan/99wt-HIS virus. At 12h post-infection with rPan/99wt-HIS virus, supernatant was collected and reassortant genotypes were assessed by high resolution melt analysis. Cells

were also harvested and the number of co-infected cells was determined by flow cytometry. In addition, at 12h post-infection with the primary virus, cells were harvested and the number of alpha-2,6 sialic acids were determined by flow cytometry. A parallel experiment was performed in which the primary infection was made using rPan/99-NA mut virus.

Figure 4. SA receptors remain intact late after infection with NA mutant virus. MDCK cells were first infected with either Pan/99var2-HA or Pan/99-NA mut virus at MOI 10 PFU/cell. At the times indicated, cells were harvested and the number of α-2,6 sialic acid-positive cells was determined by flow cytometry. Error bars represent average values of +/- standard deviation.

Figure 5. Neuraminidase deficient virus elicits incomplete super-infection interference. MDCK cells were first infected with both Pan/99var2-HA and Pan/99wt-HIS viruses simultaneously (0h) at MOI 10 PFU/cell for each virus, or first with either Pan/99var-2HA or Pan/99-NA mut virus at MOI 10 PFU/cell and then super-infected at the times indicated with Pan/99wt-HIS virus at MOI 10 PFU/cell. At 12h p.i. with Pan/99wt-HIS virus, cells and supernatant were harvested and the % of co-infected cells was determined by flow cytometry (A) and the frequency of reassortment was determined by qPCR and HRM analysis (B). Error bars represent average values of +/- standard deviation.

Figure 6. A decrease in co-infection correlates temporally with an increase in IFN-β induction. MDCK cells were first infected with Pan/99var2-HA virus at MOI 2 PFU/cell. At the times indicated, cells were either harvested and the amount of IFN-β

induction was determined by PCR or the cells were super-infected with Pan/99wt-HIS virus at MOI 2. At 12h p.i. with Pan/99wt-HIS virus, cells were harvested and the number of co-infected cells determined by flow cytometry.

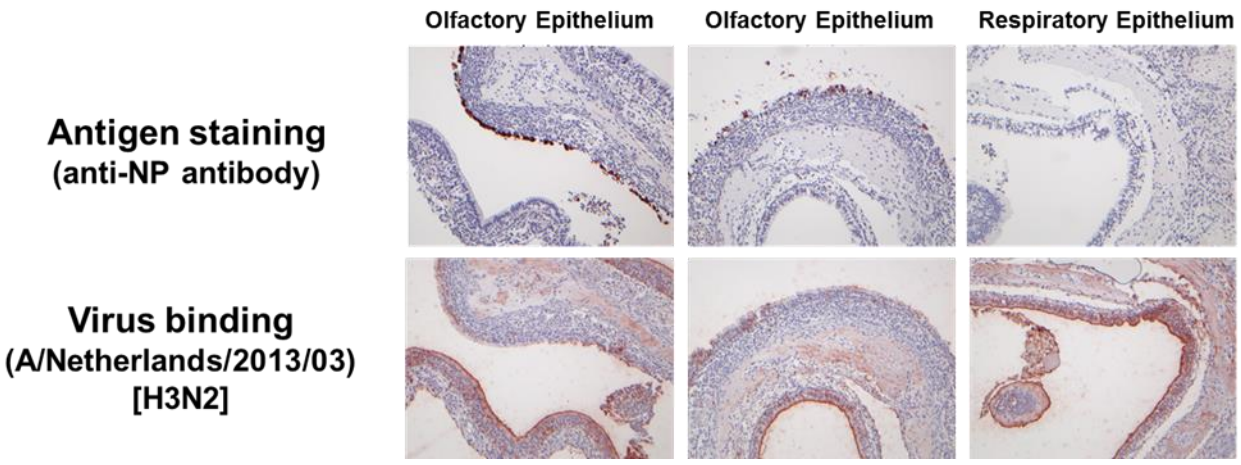
Olfactory Epithelium
Olfactory Epithelium
Respiratory Epithelium
Antigen staining
(anti-NP antibody)
Virus binding
(A/Netherlands/2013/03)
[H3N2]

Figure 1

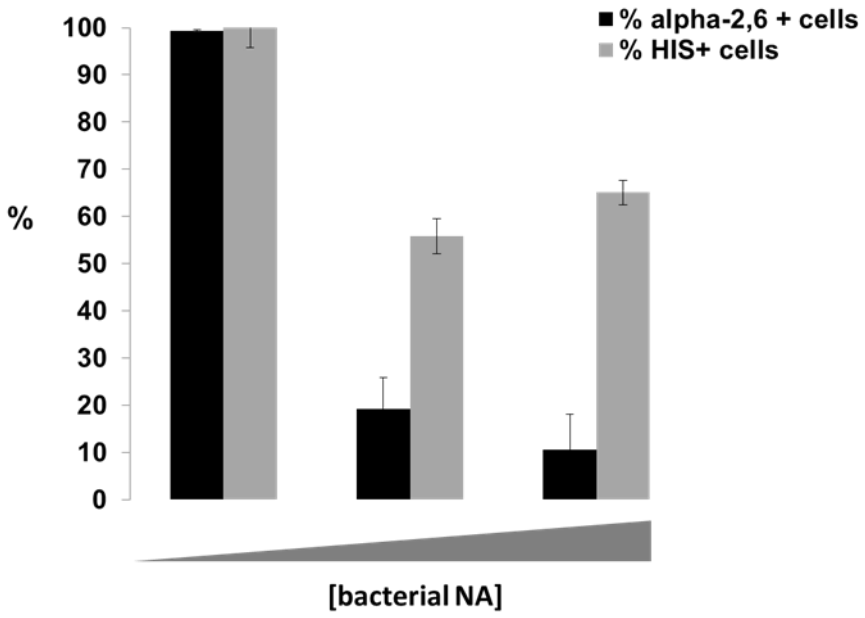
% alpha-2,6 + cells
% HIS+ cells
100
90
80
70
%
60
50
40
30
20
10
0
[bacterial NA]

Figure 2

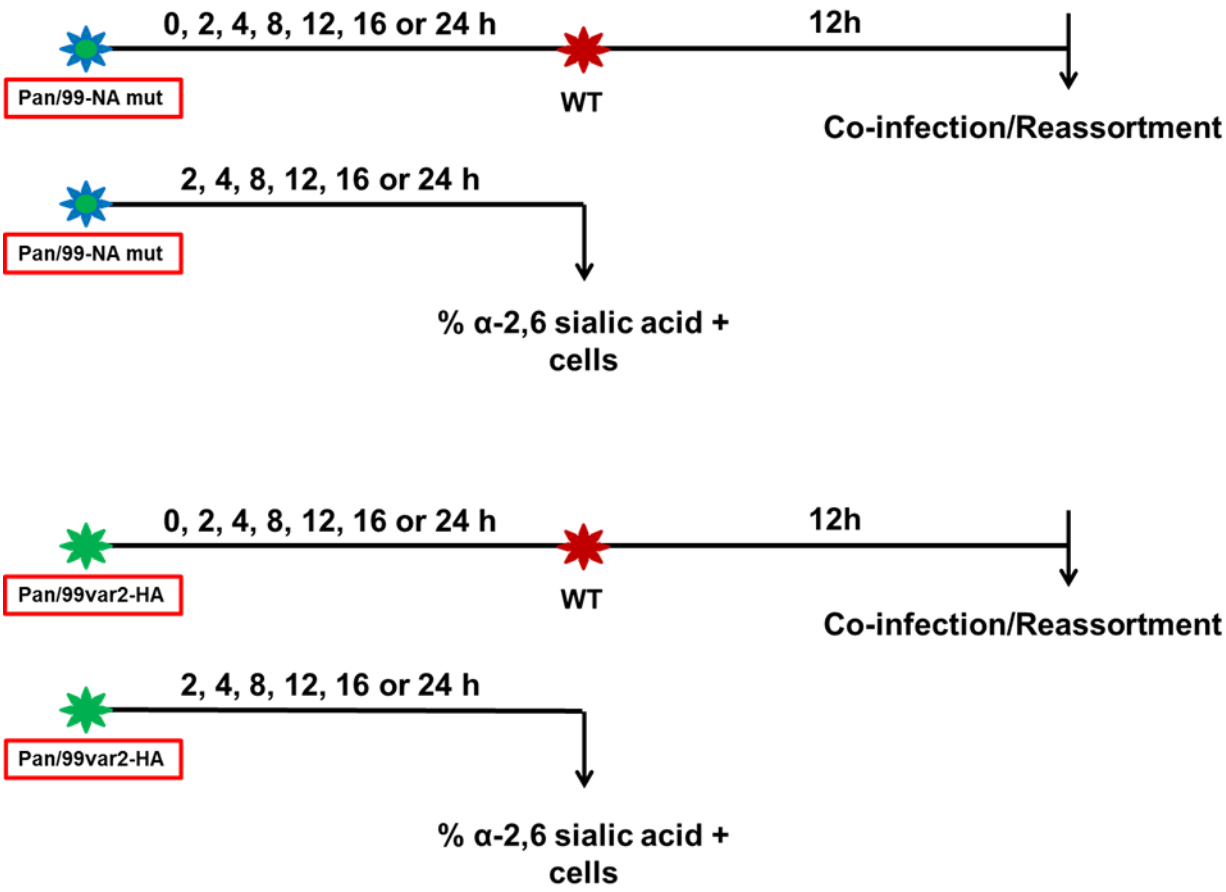
0, 2, 4, 8, 12, 16 or 24 h
12h
Pan/99-NA mut
WT
Co-infection/Reassortment
2, 4, 8, 12, 16 or 24 h
Pan/99-NA mut
% α-2,6 sialic acid + cells
0, 2, 4, 8, 12, 16 or 24 h
12h
Pan/99var2-HA
WT
Co-infection/Reassortment
2, 4, 8, 12, 16 or 24 h
Pan/99var2-HA
% α-2,6 sialic acid + cells

Figure 3

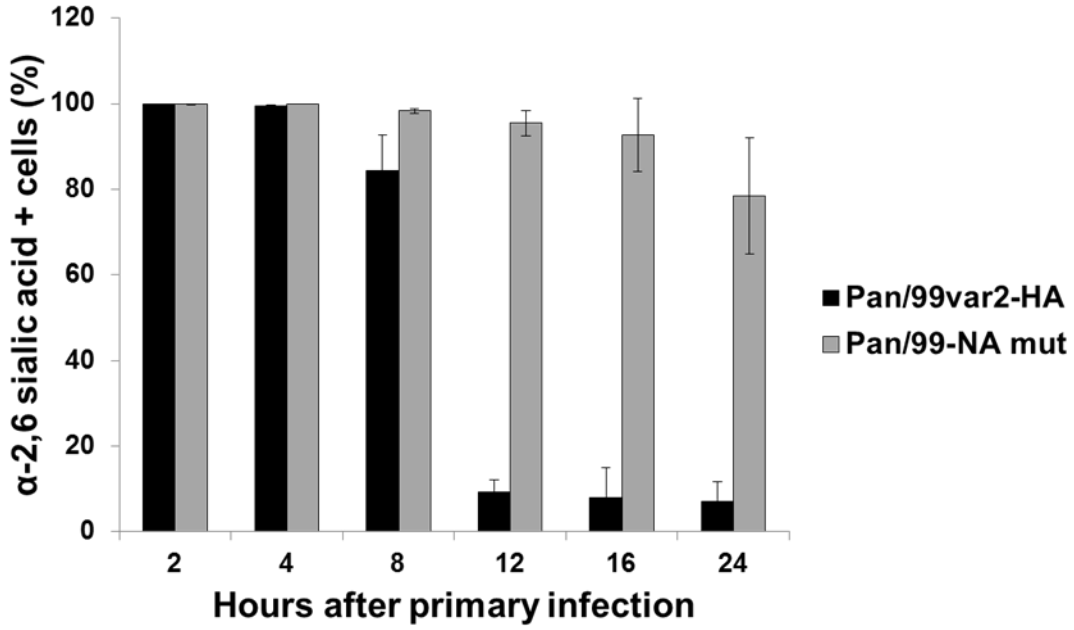
120
100
80
60
40
20
0
α-2,6 sialic acid + cells (%)
2
4
8
12
16
24
Hours after primary infection
Pan/99var2-HA
Pan/99-NA mut

Figure 4

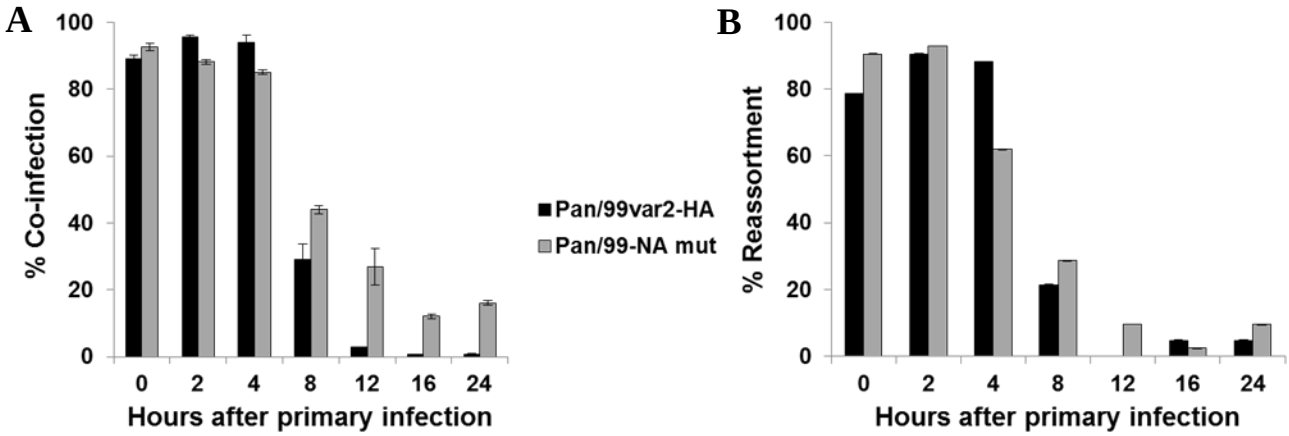
A
100
80
60
40
20
0
% Co-infection
0
2
4
8
12
16
24
Hours after primary infection
Pan/99var2-HA
Pan/99-NA mut
B
100
80
60
40
20
0
% Reassortment
0
2
4
8
12
16
24
Hours after primary infection

Figure 5

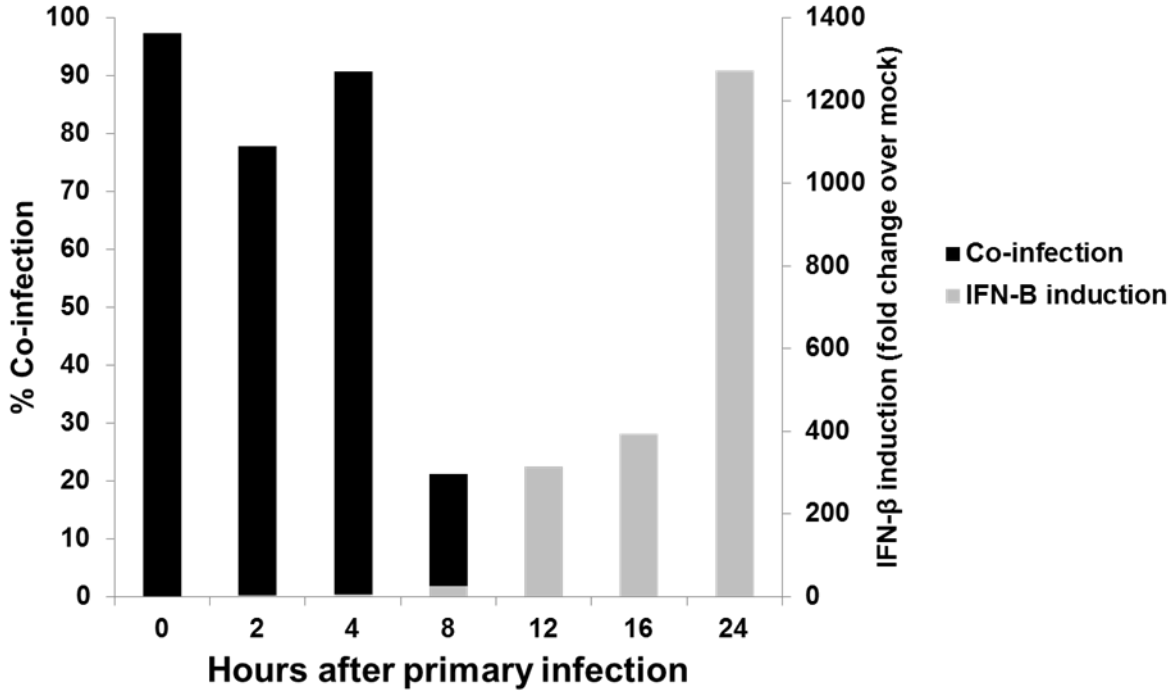
100
90
80
70
60
50
40
30
20
10
0
% Co-infection
1400
1200
1000
800
600
400
200
0
IFN-β induction (fold change over mock)
0
2
4
8
12
16
24
Hours after primary infection
Co-infection
IFN-B induction

Figure 6

Discussion

The phenomenon of super-infection interference was first described in very early research on influenza viruses. In one report, C.H. Andrewes performed super-infection experiments with the Wilson Smith strain of influenza virus and a neurotropic variant (WSN) in cell culture [27]. He determined that when an initial influenza virus infection is given the time to multiply in cell culture, that culture becomes incapable of supporting the growth of another influenza virus strain added successively. The author concluded based on the timing of the interference that it could not be due to the presence of antibody and postulated that some type of cellular diffusible inhibitory substance may prevent infection of the subsequent virus. In another manuscript by Ziegler et al., reciprocal super-infection interference was observed when using human influenza A virus, influenza B virus or a swine influenza A virus in embryonated chicken eggs [28]. The authors concluded that the state of interference was most likely due to some type of alteration of the infected target cells or tissue and that this alteration varied with the dose of the primary virus. The implications of super-infection interference for viral genetic exchange were not recognized at this time but became apparent once the segmented nature of the viral genome and consequent reassortment were described [29-32].

We recently defined the time window both in MDCK cell culture and in-vivo in a guinea pig model in which influenza virus super-infection must occur to achieve robust levels of reassortment [22]. Herein, we investigated the mechanisms underlying influenza virus super-infection interference in MDCK cells. The results suggest that super-infection is suppressed by two distinct mechanisms, sialic acid stripping from host cells by the viral neuraminidase and activation of host innate immune responses.

Our results show that the number of co-infected cells substantially decreased with an 8h delay between infections and is near the limit of detection at 12h, relative to a simultaneous infection in MDCK cells. This observation was accompanied by a dramatic increase in the amount of cellular IFN-β during the same time window. This correlation suggests that if a second influenza virus is introduced prior to robust initiation of the innate immune response it will successfully complete the stages of the lifecycle. Therefore, as long as the window between infection events is short, super-infection can result in high frequencies of both co-infection and reassortment. These results were observed with high MOI infections, and are in accord with a similar experiment we conducted in which cellular IFN-β mRNA was measured at various time points after infection with rPan/99var2-HA virus at a low MOI (0.025 PFU/cell) in MDCK cells. These results showed IFN-β mRNA to be absent in the host cell up to 16h after infection, with only a minimal amount induced at this time point (data not shown). There is abundant evidence that suggests the delay in the host IFN response after influenza virus infection is due to a combination of viral antagonists, such as the PB1-F2 protein, the viral polymerase complex, potentially the M2 protein, and the principal antagonist, the NS1 protein [33-43]. These antagonists counteract the IFN response to allow for efficient replication of the virus. As our results show, the host IFN-β response is ultimately induced, preventing a productive secondary influenza virus infection. Which stage of the viral life cycle that is being affected is unclear, however evidence has shown that interferon-stimulated gene (ISG) products can inhibit influenza virus infection at many different stages of the life cycle, including entry, replication, translation, budding and egress [44-47]. A publication by Seitz et al. showed that treatment of MDCK cells with

IFN did not prevent efficient replication of influenza A virus [25]. The lack of influenza virus suppression was suggested to be due to the failure of the canine Mx protein to inhibit the viral polymerase complex. Our data suggest that the type I IFN response to a primary infection plays an important role in preventing super-infection. Differences in timing and dose of IFN administered to MDCK cells (Seitz et al.) vs. elicited by infection (herein) most likely account for these differing results. While we have not determined the precise mechanism of super-infection interference by elicited by IFN, the data of Seitz et al. suggest that Mx probably does not play a major role; we hypothesize that the actions of several different ISGs combine to render cells refractory to super-infection.

A paper by Huang et al. indicates that the influenza virus NA protein limits influenza virus super-infection [48]. These authors found that non-productive super-infections with two influenza viruses of differing subtypes could be rendered productive with the addition of NA inhibitors. Herein, we confirm the role of NA in influenza virus super-infection interference using a NA deficient virus. Our results reveal a higher occurrence of alpha-2,6 sialic acid receptors available on host cell surfaces at later time points when cells were first infected with the NA deficient virus compared to infection with a NA wt virus. We reasoned that the presence of additional receptors would provide an increased opportunity for a second virus to attach and enter. Therefore, we hypothesized that primary infection with the NA mutant virus vs the NA wt virus in super-infection experiments would increase the number of co-infected cells and therefore the frequency of reassortment with a greater delay between infection events. While marginally higher numbers of co-infected cells were seen following rPan/99-NA mut virus infection, reassortment efficiency remained low at later times and was similar to that seen with

primary rPan/99var2 virus infection. We speculate that the large difference in the timing with which the primary and secondary viruses initiate replication leads to low reassortment at later times even when super-infection is achieved. Though there was enough time for the secondary, rPan/99wt, virus to undergo a full cycle of replication prior to sampling (12h), the additional time available for var virus replication presumably underlies the strong predominance of parental var progeny genotypes observed with longer delays between infections.

In summary, we have shown that both viral neuraminidase activity and host innate immune responses can prevent influenza virus super-infection in cell culture. Our results suggest that, in our system, host innate immune responses are the more potent factor; however the relative importance of each mechanism may vary with different virus strains and/or hosts. It is unclear whether prevention of super-infection provides an advantage to the host and/or the virus. The host, by inducing the innate immune response, limits the spread of virus to other cells, containing the infection. Removal of sialic acid receptors by the viral neuraminidase is important for release of progeny generated by the primary infection, but also acts in the context of super-infection to limit full use of the cellular machinery to the primary virus. Both host and viral functions may therefore have evolved due to their roles in the context of primary infection. We have shown in both cases, however, that the resultant interference with super-infection leads to maintenance of the primary viral genome by limiting reassortment.

References

1. Mukherjee, T.R., et al., Full genomic analysis of an influenza A (H1N2) virus identified during 2009 pandemic in Eastern India: evidence of reassortment event between co-circulating A(H1N1)pdm09 and A/Brisbane/10/2007-like H3N2 strains. Virol J, 2012. 9: p. 233.

2. Holmes, E.C., et al., Whole-genome analysis of human influenza A virus reveals multiple persistent lineages and reassortment among recent H3N2 viruses. PLoS Biol, 2005. 3(9): p. e300.

3. Kilbourne, E.D., Influenza pandemics of the 20th century. Emerg Infect Dis, 2006. 12(1): p. 9-14.

4. Watanabe, T., et al., Characterization in vitro and in vivo of pandemic (H1N1) 2009 influenza viruses isolated from patients. J Virol, 2012. 86(17): p. 9361-8.

5. Cox, N.J. and K. Subbarao, Global epidemiology of influenza: past and present. Annu Rev Med, 2000. 51: p. 407-21.

6. Joseph, U., et al., Adaptation of pandemic H2N2 influenza A viruses in humans. J Virol, 2015. 89(4): p. 2442-7.

7. Liu, D., et al., Origin and diversity of novel avian influenza A H7N9 viruses causing human infection: phylogenetic, structural, and coalescent analyses. Lancet, 2013. 381(9881): p. 1926-32.

8. Wu, A., et al., Sequential reassortments underlie diverse influenza H7N9 genotypes in China. Cell Host Microbe, 2013. 14(4): p. 446-52.

9. Li, K.S., et al., Genesis of a highly pathogenic and potentially pandemic H5N1 influenza virus in eastern Asia. Nature, 2004. 430(6996): p. 209-13.

10. Morrison, T.G. and L.W. McGinnes, Avian cells expressing the Newcastle disease virus hemagglutinin-neuraminidase protein are resistant to Newcastle disease virus infection. Virology, 1989. 171(1): p. 10-7.

11. Horga, M.A., et al., Mechanism of interference mediated by human parainfluenza virus type 3 infection. J Virol, 2000. 74(24): p. 11792-9.

12. Bratt, M.A. and H. Rubin, Specific interference among strains of Newcastle disease virus. II. Comparison of interference by active and inactive virus. Virology, 1968. 35(3): p. 381-94.

13. Steck, F.T. and H. Rubin, The mechanism of interference between an avian leukosis virus and Rous sarcoma virus. II. Early steps of infection by RSV of cells under conditions of interference. Virology, 1966. 29(4): p. 642-53.

14. Bour, S., R. Geleziunas, and M.A. Wainberg, The role of CD4 and its downmodulation in establishment and maintenance of HIV-1 infection. Immunol Rev, 1994. 140: p. 147-71.

15. Geleziunas, R., S. Bour, and M.A. Wainberg, Cell surface down-modulation of CD4 after infection by HIV-1. FASEB J, 1994. 8(9): p. 593-600.

16. Lama, J., The physiological relevance of CD4 receptor down-modulation during HIV infection. Curr HIV Res, 2003. 1(2): p. 167-84.

17. Desmyter, J., J.L. Melnick, and W.E. Rawls, Defectiveness of interferon production and of rubella virus interference in a line of African green monkey kidney cells (Vero). J Virol, 1968. 2(10): p. 955-61.

18. Garcin, D., P. Latorre, and D. Kolakofsky, Sendai virus C proteins counteract the interferon-mediated induction of an antiviral state. J Virol, 1999. 73(8): p. 6559-65.

19. Simon, K.O., et al., Cellular mechanisms in the superinfection exclusion of vesicular stomatitis virus. Virology, 1990. 177(1): p. 375-9.

20. Whitaker-Dowling, P., et al., Superinfection exclusion by vesicular stomatitis virus. Virology, 1983. 131(1): p. 137-43.

21. Garcia-Sastre, A., et al., Influenza A virus lacking the NS1 gene replicates in interferon-deficient systems. Virology, 1998. 252(2): p. 324-30.

22. Marshall, N., et al., Influenza virus reassortment occurs with high frequency in the absence of segment mismatch. PLoS Pathog, 2013. 9(6): p. e1003421.

23. Lowen, A.C., et al., The guinea pig as a transmission model for human influenza viruses. Proc Natl Acad Sci U S A, 2006. 103(26): p. 9988-92.

24. Rimmelzwaan, G.F., et al., Pathogenesis of influenza A (H5N1) virus infection in a primate model. J Virol, 2001. 75(14): p. 6687-91.

25. Seitz, C., et al., High yields of influenza A virus in Madin-Darby canine kidney cells are promoted by an insufficient interferon-induced antiviral state. J Gen Virol, 2010. 91(Pt 7): p. 1754-63.

26. Lentz, M.R., R.G. Webster, and G.M. Air, Site-directed mutation of the active site of influenza neuraminidase and implications for the catalytic mechanism. Biochemistry, 1987. 26(17): p. 5351-8.

27. Andrewes, C.H., Interference by one virus with the growth of another in tissue-culture. Brit. J. Exp. Path, 1942. 23.

28. Ziegler, J.E. and F.L. Horsfall, Interference between the Influenza Viruses : I. The Effect of Active Virus Upon the Multiplication of Influenza Viruses in the Chick Embryo. J Exp Med, 1944. 79(4): p. 361-77.

29. Burnet, F.M. and P.E. Lind, A genetic approach to variation in influenza viruses; recombination of characters between the influenza virus A strain NWS and strains of different serological subtypes. J Gen Microbiol, 1951. 5(1): p. 67-82.

30. Burnet, F.M., Structure of influenza virus. Science, 1956. 123(3208): p. 1101-4.

31. Hirst, G.K., Genetic recombination with Newcastle disease virus, polioviruses, and influenza. Cold Spring Harb Symp Quant Biol, 1962. 27: p. 303-9.

32. Young, J.F. and P. Palese, Evolution of human influenza A viruses in nature: recombination contributes to genetic variation of H1N1 strains. Proc Natl Acad Sci U S A, 1979. 76(12): p. 6547-51.

33. Fernandez-Sesma, A., et al., Influenza virus evades innate and adaptive immunity via the NS1 protein. J Virol, 2006. 80(13): p. 6295-304.

34. Ruckle, A., et al., The NS1 protein of influenza A virus blocks RIG-I-mediated activation of the noncanonical NF-kappaB pathway and p52/RelB-dependent gene expression in lung epithelial cells. J Virol, 2012. 86(18): p. 10211-7.

35. Gao, S., et al., Influenza A virus-encoded NS1 virulence factor protein inhibits innate immune response by targeting IKK. Cell Microbiol, 2012. 14(12): p. 1849-66.

36. Dudek, S.E., et al., The influenza virus PB1-F2 protein has interferon antagonistic activity. Biol Chem, 2011. 392(12): p. 1135-44.

37. Varga, Z.T., et al., The influenza virus protein PB1-F2 inhibits the induction of type I interferon at the level of the MAVS adaptor protein. PLoS Pathog, 2011. 7(6): p. e1002067.

38. Graef, K.M., et al., The PB2 subunit of the influenza virus RNA polymerase affects virulence by interacting with the mitochondrial antiviral signaling protein and inhibiting expression of beta interferon. J Virol, 2010. 84(17): p. 8433-45.

39. Marcus, P.I., J.M. Rojek, and M.J. Sekellick, Interferon induction and/or production and its suppression by influenza A viruses. J Virol, 2005. 79(5): p. 2880-90.

40. Schmolke, M. and A. Garcia-Sastre, Evasion of innate and adaptive immune responses by influenza A virus. Cell Microbiol, 2010. 12(7): p. 873-80.

41. Gannage, M., et al., Matrix protein 2 of influenza A virus blocks autophagosome fusion with lysosomes. Cell Host Microbe, 2009. 6(4): p. 367-80.

42. Hale, B.G., et al., Structural insights into phosphoinositide 3-kinase activation by the influenza A virus NS1 protein. Proc Natl Acad Sci U S A, 2010. 107(5): p. 1954-9.

43. Li, S., et al., Binding of the influenza A virus NS1 protein to PKR mediates the inhibition of its activation by either PACT or double-stranded RNA. Virology, 2006. 349(1): p. 13-21.

44. Iwasaki, A. and P.S. Pillai, Innate immunity to influenza virus infection. Nat Rev Immunol, 2014. 14(5): p. 315-28.

45. Desai, T.M., et al., IFITM3 restricts influenza A virus entry by blocking the formation of fusion pores following virus-endosome hemifusion. PLoS Pathog, 2014. 10(4): p. e1004048

46. Wang, X., E.R. Hinson, and P. Cresswell, The interferon-inducible protein viperin inhibits influenza virus release by perturbing lipid rafts. Cell Host Microbe, 2007. 2(2): p. 96-105.

47. Schoggins, J.W. and C.M. Rice, Interferon-stimulated genes and their antiviral effector functions. Curr Opin Virol, 2011. 1(6): p. 519-25.

48. Huang, I.C., et al., Influenza A virus neuraminidase limits viral superinfection. J Virol, 2008. 82(10): p. 4834-43.

Chapter 5: Discussion

In the previous chapters, we examined underlying factors contributing to reassortment efficiency in the absence of genetic incompatibility. Through our work we have found that, when fitness differences between the parental and progeny strains are eliminated, high levels of reassortment are achieved both in cell culture and in an animal host. Furthermore, we established, in both systems, that the frequency of reassortment was directly dependent on the number of co-infected cells, or dosage. These results indicate that the genomes of the different IAV are able to mix freely during at least one stage in the viral life cycle and that appreciable numbers of co-infected cells occur in vivo. This latter point is somewhat counter-intuitive given the large surface area of respiratory tissues: our data show that reassortment occurs with unexpectedly high efficiency in an intact host. We propose that our subsequent finding that semi-infectious particles enhance reassortment may account for this phenomenon.

Recently, evidence has shown that a significant proportion of a viral population consists of semi-infectious particles [153]. We have determined that the presence of semi-infectious particles increases reassortment frequency by increasing the proportion of productively infected cells that are co-infected. Thus, in nature, SI particles are more likely to be important after the first round of replication has occurred and progeny SI particles have been generated that then have the opportunity to co-infect adjacent cells. If the spread of the virus is relatively localized, SI particles will increase MOI. If the number of virions is limiting (low MOI), fewer productive infections will be initiated when a portion of these virions are SI particles, however of those cells that are productively infected, a greater number will be co-infected.

Additionally, biological aspects of the host respiratory tract could promote a high multiplicity of infection. The presence of mucins and surfactants in the respiratory tract have the potential to bind or cluster IAVs together, resulting in >1 particle initially entering a cell, even early after inoculation. In this context, SI particles have an increased chance of being complemented and contributing to infectious, reassortant progeny. Finally, a recent report by Tao et al. demonstrated that viral spread following initial IAV infection *in-vivo* leads to increased reassortment later in infection [180]. Cells singly infected with SI particles would not be productively infected and therefore SI particles would not have any influence on reassortment; however an initial low transmission dose could eventually reach MOI levels high enough to allow complementation of SI particles, thereby increasing the frequency of reassortment. By increasing reassortment, SI particles are expected to accelerate the evolution of IAV in nature.

Though we found reassortment to be highly efficient with simultaneous co-infections in our system, we also determined that introducing a time window between the primary and secondary infection greatly reduced reassortment efficiency. While a short delay between infections (12h) increased reassortment, a longer delay (>18h) after a primary infection resulted in a considerably lower amount of reassortment *in-vivo*. These results are particularly interesting considering most co-infections likely result from sequential infections, rather than simultaneous infections, in nature. Recent work has tested the prevalence of reassortment when co-infection is achieved through transmission and the results show that similar levels of reassortment were attained whether co-infection was achieved by intranasal co-inoculation with two different viruses (simultaneous co-infection) or by exposure to two different guinea pigs, each infected with a different virus

(two independent infection events) [180, 181]. However, the work was performed under optimal transmission conditions, which are not always present in the field. Thus, it seems likely that reassortment frequency would decrease with independent transmission events in nature, with the degree of reduction being dependent on the time between events. We concluded that the reduction in reassortment observed with a delay between infections could be attributed to super-infection interference, and hypothesized that removal of the cellular receptor by the progeny viral neuraminidase and the host IFN-β response were mechanisms responsible for the interference. Our results show that, while both mechanisms are important in the exclusion of super-infection, the host IFN-β response seems to play a more prominent role.

Because transmission can occur through contact, as well as small or large respiratory droplets, it is possible for timing to play a role in simultaneous co-infections as well. During a co-infection event, distinct IAVs transmitted via different modes may infect different areas of the host respiratory tract. If the regions are in close proximity, the viruses would have time to replicate and spread to the adjacent areas, super-infecting cells before the mechanisms of super-infection interference are induced. However, if the sites are more distant, a localized host innate immune response may develop before progeny viruses spread to areas infected with the alternate virus, precluding co-infection and reassortment.

These considerations illustrate the substantial effect that timing can have on reassortment frequency. Because of the limited window of opportunity, co-infection between two distinct IAV strains is most likely rare in nature. Conversely, our data suggest that reassortment among related IAV variants, within a viral population, is most likely

occurring within every infected host. Reassortment within a quasi-species is expected to contribute to viral evolution on a larger time scale because it has the potential to bring together multiple adaptive mutations into one genome. In this context, one would expect reassortment efficiencies to mimic those observed after a simultaneous co-infection of rPan/99wt and var viruses.

In sum, our results demonstrate that, when fitness differences between parental and progeny viruses are eliminated, IAV reassortment is highly efficient and directly dependent on both dosage and time. We have determined that an IAV population contains a population of SI particles which outnumber fully infectious particles and these SI particles increase the potential for viral evolution through reassortment. Finally, we have shown that the timing of infection events plays a critical role in reassortment frequency due to the induction of super-infection interference mechanisms by both the host and the virus.

References

1. Hause, B.M., et al., *Characterization of a novel influenza virus in cattle and Swine: proposal for a new genus in the Orthomyxoviridae family.* MBio, 2014. **5**(2): p. e00031-14.
2. Yoon, S.W., R.J. Webby, and R.G. Webster, *Evolution and ecology of influenza A viruses.* Curr Top Microbiol Immunol, 2014. **385**: p. 359-75.
3. Tong, S., et al., *A distinct lineage of influenza A virus from bats.* Proc Natl Acad Sci U S A, 2012. **109**(11): p. 4269-74.
4. Tong, S., et al., *New world bats harbor diverse influenza A viruses.* PLoS Pathog, 2013. **9**(10): p. e1003657.
5. Garcia-Sastre, A., *The neuraminidase of bat influenza viruses is not a neuraminidase.* Proc Natl Acad Sci U S A, 2012. **109**(46): p. 18635-6.
6. Nelson, M.I., et al., *Introductions and evolution of human-origin seasonal influenza a viruses in multinational swine populations.* J Virol, 2014. **88**(17): p. 10110-9.
7. Fouchier, R.A., et al., *Avian influenza A virus (H7N7) associated with human conjunctivitis and a fatal case of acute respiratory distress syndrome.* Proc Natl Acad Sci U S A, 2004. **101**(5): p. 1356-61.
8. Skehel, J.J. and D.C. Wiley, *Receptor binding and membrane fusion in virus entry: the influenza hemagglutinin.* Annu Rev Biochem, 2000. **69**: p. 531-69.
9. Luo, M., *Influenza virus entry.* Adv Exp Med Biol, 2012. **726**: p. 201-21.
10. Yang, H., et al., *Structure and receptor binding preferences of recombinant hemagglutinins from avian and human H6 and H10 influenza A virus subtypes.* J Virol, 2015. **89**(8): p. 4612-23.
11. de Graaf, M. and R.A. Fouchier, *Role of receptor binding specificity in influenza A virus transmission and pathogenesis.* EMBO J, 2014. **33**(8): p. 823-41.
12. Shi, Y., et al., *Structures and receptor binding of hemagglutinins from human-infecting H7N9 influenza viruses.* Science, 2013. **342**(6155): p. 243-7.

13. Ma, W., R.E. Kahn, and J.A. Richt, *The pig as a mixing vessel for influenza viruses: Human and veterinary implications.* J Mol Genet Med, 2008. **3**(1): p. 158-66.
14. Kida, H., et al., *Potential for transmission of avian influenza viruses to pigs.* J Gen Virol, 1994. **75 (Pt 9)**: p. 2183-8.
15. de Vries, E., et al., *Dissection of the influenza A virus endocytic routes reveals macropinocytosis as an alternative entry pathway.* PLoS Pathog, 2011. **7**(3): p. e1001329.
16. Dourmashkin, R.R. and D.A. Tyrrell, *Electron microscopic observations on the entry of influenza virus into susceptible cells.* J Gen Virol, 1974. **24**(1): p. 129-41.
17. Matlin, K.S., et al., *Infectious entry pathway of influenza virus in a canine kidney cell line.* J Cell Biol, 1981. **91**(3 Pt 1): p. 601-13.
18. Rust, M.J., et al., *Assembly of endocytic machinery around individual influenza viruses during viral entry.* Nat Struct Mol Biol, 2004. **11**(6): p. 567-73.
19. Rossman, J.S., G.P. Leser, and R.A. Lamb, *Filamentous influenza virus enters cells via macropinocytosis.* J Virol, 2012. **86**(20): p. 10950-60.
20. Sieczkarski, S.B. and G.R. Whittaker, *Influenza virus can enter and infect cells in the absence of clathrin-mediated endocytosis.* J Virol, 2002. **76**(20): p. 10455-64.
21. Bui, M., et al., *Role of the influenza virus M1 protein in nuclear export of viral ribonucleoproteins.* J Virol, 2000. **74**(4): p. 1781-6.
22. Martin, K. and A. Helenius, *Nuclear transport of influenza virus ribonucleoproteins: the viral matrix protein (M1) promotes export and inhibits import.* Cell, 1991. **67**(1): p. 117-30.
23. Pinto, L.H., L.J. Holsinger, and R.A. Lamb, *Influenza virus M2 protein has ion channel activity.* Cell, 1992. **69**(3): p. 517-28.
24. Bui, M., G. Whittaker, and A. Helenius, *Effect of M1 protein and low pH on nuclear transport of influenza virus ribonucleoproteins.* J Virol, 1996. **70**(12): p. 8391-401.
25. Li, S., et al., *pH-Controlled two-step uncoating of influenza virus.* Biophys J, 2014. **106**(7): p. 1447-56.

26. Hamilton, B.S., G.R. Whittaker, and S. Daniel, *Influenza virus-mediated membrane fusion: determinants of hemagglutinin fusogenic activity and experimental aPproaches for assessing virus fusion.* Viruses, 2012. **4**(7): p. 1144-68.
27. Boulo, S., et al., *Human importin alpha and RNA do not compete for binding to influenza A virus nucleoprotein.* Virology, 2011. **409**(1): p. 84-90.
28. Cros, J.F., A. Garcia-Sastre, and P. Palese, *An unconventional NLS is critical for the nuclear import of the influenza A virus nucleoprotein and ribonucleoprotein.* Traffic, 2005. **6**(3): p. 205-13.
29. Ketha, K.M. and C.D. Atreya, *APplication of bioinformatics-coupled experimental analysis reveals a new transport-competent nuclear localization signal in the nucleoprotein of influenza A virus strain.* BMC Cell Biol, 2008. **9**: p. 22.
30. Mukaigawa, J. and D.P. Nayak, *Two signals mediate nuclear localization of influenza virus (A/WSN/33) polymerase basic protein 2.* J Virol, 1991. **65**(1): p. 245-53.
31. Gabriel, G., et al., *Differential use of importin-alpha isoforms governs cell tropism and host adaptation of influenza virus.* Nat Commun, 2011. **2**: p. 156.
32. Krug, R.M., et al., *Transcription and replication of influenza virion RNA in the nucleus of infected cells.* Cold Spring Harb Symp Quant Biol, 1987. **52**: p. 353-8.
33. Herz, C., et al., *Influenza virus, an RNA virus, synthesizes its messenger RNA in the nucleus of infected cells.* Cell, 1981. **26**(3 Pt 1): p. 391-400.
34. Jackson, D.A., et al., *Influenza virus RNA is synthesized at fixed sites in the nucleus.* Nature, 1982. **296**(5855): p. 366-8.
35. Vreede, F.T., T.E. Jung, and G.G. Brownlee, *Model suggesting that replication of influenza virus is regulated by stabilization of replicative intermediates.* J Virol, 2004. **78**(17): p. 9568-72.
36. Vreede, F.T., H. Gifford, and G.G. Brownlee, *Role of initiating nucleoside triphosphate concentrations in the regulation of influenza virus replication and transcription.* J Virol, 2008. **82**(14): p. 6902-10.

37. Shapiro, G.I. and R.M. Krug, *Influenza virus RNA replication in vitro: synthesis of viral template RNAs and virion RNAs in the absence of an added primer.* J Virol, 1988. **62**(7): p. 2285-90.
38. Jorba, N., R. Coloma, and J. Ortin, *Genetic trans-complementation establishes a new model for influenza virus RNA transcription and replication.* PLoS Pathog, 2009. **5**(5): p. e1000462.
39. Perez, J.T., et al., *Influenza A virus-generated small RNAs regulate the switch from transcription to replication.* Proc Natl Acad Sci U S A, 2010. **107**(25): p. 11525-30.
40. Dias, A., et al., *The cap-snatching endonuclease of influenza virus polymerase resides in the PA subunit.* Nature, 2009. **458**(7240): p. 914-8.
41. Plotch, S.J., et al., *A unique cap(m7GPppXm)-dependent influenza virion endonuclease cleaves caPped RNAs to generate the primers that initiate viral RNA transcription.* Cell, 1981. **23**(3): p. 847-58.
42. Guilligay, D., et al., *The structural basis for cap binding by influenza virus polymerase subunit PB2.* Nat Struct Mol Biol, 2008. **15**(5): p. 500-6.
43. Yuan, P., et al., *Crystal structure of an avian influenza polymerase PA(N) reveals an endonuclease active site.* Nature, 2009. **458**(7240): p. 909-13.
44. Ulmanen, I., B.A. Broni, and R.M. Krug, *Role of two of the influenza virus core P proteins in recognizing cap 1 structures (m7GPppNm) on RNAs and in initiating viral RNA transcription.* Proc Natl Acad Sci U S A, 1981. **78**(12): p. 7355-9.
45. Bouloy, M., S.J. Plotch, and R.M. Krug, *Globin mRNAs are primers for the transcription of influenza viral RNA in vitro.* Proc Natl Acad Sci U S A, 1978. **75**(10): p. 4886-90.
46. Poch, O., et al., *Identification of four conserved motifs among the RNA-dependent polymerase encoding elements.* EMBO J, 1989. **8**(12): p. 3867-74.
47. Braam, J., I. Ulmanen, and R.M. Krug, *Molecular model of a eucaryotic transcription complex: functions and movements of influenza P proteins during caPped RNA-primed transcription.* Cell, 1983. **34**(2): p. 609-18.

48. Poon, L.L., et al., *Direct evidence that the poly(A) tail of influenza A virus mRNA is synthesized by reiterative copying of a U track in the virion RNA template.* J Virol, 1999. **73**(4): p. 3473-6.
49. Neumann, G., M.T. Hughes, and Y. Kawaoka, *Influenza A virus NS2 protein mediates vRNP nuclear export through NES-independent interaction with hCRM1.* EMBO J, 2000. **19**(24): p. 6751-8.
50. Brunotte, L., et al., *The nuclear export protein of H5N1 influenza A viruses recruits Matrix 1 (M1) protein to the viral ribonucleoprotein to mediate nuclear export.* J Biol Chem, 2014. **289**(29): p. 20067-77.
51. Iwatsuki-Horimoto, K., et al., *Generation of influenza A virus NS2 (NEP) mutants with an altered nuclear export signal sequence.* J Virol, 2004. **78**(18): p. 10149-55.
52. Whittaker, G., M. Bui, and A. Helenius, *Nuclear trafficking of influenza virus ribonuleoproteins in heterokaryons.* J Virol, 1996. **70**(5): p. 2743-56.
53. Jo, S., et al., *Involvement of vesicular trafficking system in membrane targeting of the progeny influenza virus genome.* Microbes Infect, 2010. **12**(12-13): p. 1079-84.
54. Momose, F., et al., *Apical transport of influenza A virus ribonucleoprotein requires Rab11-positive recycling endosome.* PLoS One, 2011. **6**(6): p. e21123.
55. Amorim, M.J., et al., *A Rab11- and microtubule-dependent mechanism for cytoplasmic transport of influenza A virus viral RNA.* J Virol, 2011. **85**(9): p. 4143-56.
56. Avilov, S.V., et al., *Influenza A virus progeny vRNP trafficking in live infected cells studied with the virus-encoded fluorescently tagged PB2 protein.* Vaccine, 2012. **30**(51): p. 7411-7.
57. Chen, B.J., et al., *The influenza virus M2 protein cytoplasmic tail interacts with the M1 protein and influences virus assembly at the site of virus budding.* J Virol, 2008. **82**(20): p. 10059-70.
58. Enami, M. and K. Enami, *Influenza virus hemagglutinin and neuraminidase glycoproteins stimulate the membrane association of the matrix protein.* J Virol, 1996. **70**(10): p. 6653-7.

59. Ali, A., et al., *Influenza virus assembly: effect of influenza virus glycoproteins on the membrane association of M1 protein.* J Virol, 2000. **74**(18): p. 8709-19.
60. Ohkura, T., et al., *Influenza A virus hemagglutinin and neuraminidase mutually accelerate their apical targeting through clustering of lipid rafts.* J Virol, 2014. **88**(17): p. 10039-55.
61. Scheiffele, P., M.G. Roth, and K. Simons, *Interaction of influenza virus haemagglutinin with sphingolipid-cholesterol membrane domains via its transmembrane domain.* EMBO J, 1997. **16**(18): p. 5501-8.
62. Roberts, K.L., et al., *The amphipathic helix of influenza A virus M2 protein is required for filamentous bud formation and scission of filamentous and spherical particles.* J Virol, 2013. **87**(18): p. 9973-82.
63. Rossman, J.S., et al., *Influenza virus M2 protein mediates ESCRT-independent membrane scission.* Cell, 2010. **142**(6): p. 902-13.
64. Schmidt, N.W., et al., *Influenza virus A M2 protein generates negative Gaussian membrane curvature necessary for budding and scission.* J Am Chem Soc, 2013. **135**(37): p. 13710-9.
65. Leser, G.P. and R.A. Lamb, *Influenza virus assembly and budding in raft-derived microdomains: a quantitative analysis of the surface distribution of HA, NA and M2 proteins.* Virology, 2005. **342**(2): p. 215-27.
66. Chen, B.J., et al., *Influenza virus hemagglutinin and neuraminidase, but not the matrix protein, are required for assembly and budding of plasmid-derived virus-like particles.* J Virol, 2007. **81**(13): p. 7111-23.
67. Lai, J.C., et al., *Formation of virus-like particles from human cell lines exclusively expressing influenza neuraminidase.* J Gen Virol, 2010. **91**(Pt 9): p. 2322-30.
68. Gomez-Puertas, P., et al., *Influenza virus matrix protein is the major driving force in virus budding.* J Virol, 2000. **74**(24): p. 11538-47.
69. Calder, L.J., et al., *Structural organization of a filamentous influenza A virus.* Proc Natl Acad Sci U S A, 2010. **107**(23): p. 10685-90.
70. Noda, T., et al., *Architecture of ribonucleoprotein complexes in influenza A virus particles.* Nature, 2006. **439**(7075): p. 490-2.

71. Gack, M.U., et al., *Influenza A virus NS1 targets the ubiquitin ligase TRIM25 to evade recognition by the host viral RNA sensor RIG-I.* Cell Host Microbe, 2009. **5**(5): p. 439-49.
72. Liedmann, S., et al., *Viral suPpressors of the RIG-I-mediated interferon response are pre-packaged in influenza virions.* Nat Commun, 2014. **5**: p. 5645.
73. Killip, M.J., E. Fodor, and R.E. Randall, *Influenza virus activation of the interferon system.* Virus Res, 2015.
74. Sovinova, O., et al., *Isolation of a virus causing respiratory disease in horses.* Acta Virol, 1958. **2**(1): p. 52-61.
75. Crawford, P.C., et al., *Transmission of equine influenza virus to dogs.* Science, 2005. **310**(5747): p. 482-5.
76. Geraci, J.R., et al., *Mass mortality of harbor seals: pneumonia associated with influenza A virus.* Science, 1982. **215**(4536): p. 1129-31.
77. Hinshaw, V.S., et al., *Characterization of two influenza A viruses from a pilot whale.* J Virol, 1986. **58**(2): p. 655-6.
78. Keawcharoen, J., et al., *Avian influenza H5N1 in tigers and leopards.* Emerg Infect Dis, 2004. **10**(12): p. 2189-91.
79. Klingeborn, B., et al., *An avian influenza A virus killing a mammalian species--the mink. Brief report.* Arch Virol, 1985. **86**(3-4): p. 347-51.
80. Paniker, C.K. and C.M. Nair, *Infection with A2 Hong Kong influenza virus in domestic cats.* Bull World Health Organ, 1970. **43**(6): p. 859-62.
81. Schulman, J.L., *The use of an animal model to study transmission of influenza virus infection.* Am J Public Health Nations Health, 1968. **58**(11): p. 2092-6.
82. Schulman, J.L. and E.D. Kilbourne, *Experimental Transmission of Influenza Virus Infection in Mice. Ii. Some Factors Affecting the Incidence of Transmitted Infection.* J Exp Med, 1963. **118**: p. 267-75.
83. Thangavel, R.R. and N.M. Bouvier, *Animal models for influenza virus pathogenesis, transmission, and immunology.* J Immunol Methods, 2014. **410**: p. 60-79.
84. Bouvier, N.M., *Animal models for influenza virus transmission studies: a historical perspective.* Curr Opin Virol, 2015. **13**: p. 101-108.

85. van Riel, D., et al., *Human and avian influenza viruses target different cells in the lower respiratory tract of humans and other mammals.* Am J Pathol, 2007. **171**(4): p. 1215-23.
86. Margine, I. and F. Krammer, *Animal models for influenza viruses: implications for universal vaccine development.* Pathogens, 2014. **3**(4): p. 845-74.
87. Treanor, J., *Inlfuenza viruses, including avian influenza and swine influenza.*, in *Mandell, Douglas and Bennett's principles and practices of infectious diseases*, B.J. Mandell GL, Dolin R, Editor. 2010, Philadelphia: Elsevier.
88. Zeng, H., et al., *Tropism and infectivity of influenza virus, including highly pathogenic avian H5N1 virus, in ferret tracheal differentiated primary epithelial cell cultures.* J Virol, 2013. **87**(5): p. 2597-607.
89. van der Laan, J.W., et al., *Animal models in influenza vaccine testing.* Expert Rev Vaccines, 2008. **7**(6): p. 783-93.
90. Klepser, M.E., *Socioeconomic impact of seasonal (epidemic) influenza and the role of over-the-counter medicines.* Drugs, 2014. **74**(13): p. 1467-79.
91. Eccles, R., *Understanding the symptoms of the common cold and influenza.* Lancet Infect Dis, 2005. **5**(11): p. 718-25.
92. Martin, C.M., et al., *Asian influenza A in Boston, 1957-1958. II. Severe staphylococcal pneumonia complicating influenza.* AMA Arch Intern Med, 1959. **103**(4): p. 532-42.
93. Gerber, G.J., W.C. Farmer, and L.L. Fulkerson, *Beta-hemolytic streptococcal pneumonia following influenza.* JAMA, 1978. **240**(3): p. 242-3.
94. Fukuyama, S. and Y. Kawaoka, *The pathogenesis of influenza virus infections: the contributions of virus and host factors.* Curr Opin Immunol, 2011. **23**(4): p. 481-6.
95. Taubenberger, J.K. and D.M. Morens, *The pathology of influenza virus infections.* Annu Rev Pathol, 2008. **3**: p. 499-522.
96. Worobey, M., G.Z. Han, and A. Rambaut, *A synchronized global sweep of the internal genes of modern avian influenza virus.* Nature, 2014. **508**(7495): p. 254-7.

97. Watanabe, T., et al., *Characterization in vitro and in vivo of pandemic (H1N1) 2009 influenza viruses isolated from patients.* J Virol, 2012. **86**(17): p. 9361-8.

98. Johnson, N.P. and J. Mueller, *Updating the accounts: global mortality of the 1918-1920 "Spanish" influenza pandemic.* Bull Hist Med, 2002. **76**(1): p. 105-15.

99. Morens, D.M. and A.S. Fauci, *The 1918 influenza pandemic: insights for the 21st century.* J Infect Dis, 2007. **195**(7): p. 1018-28.

100. Joseph, U., et al., *Adaptation of pandemic H2N2 influenza A viruses in humans.* J Virol, 2015. **89**(4): p. 2442-7.

101. Cox, N.J. and K. Subbarao, *Global epidemiology of influenza: past and present.* Annu Rev Med, 2000. **51**: p. 407-21.

102. Kilbourne, E.D., *Influenza pandemics of the 20th century.* Emerg Infect Dis, 2006. **12**(1): p. 9-14.

103. Dawood, F.S., et al., *Estimated global mortality associated with the first 12 months of 2009 pandemic influenza A H1N1 virus circulation: a modelling study.* Lancet Infect Dis, 2012. **12**(9): p. 687-95.

104. Cheng, V.C., et al., *Two years after pandemic influenza A/2009/H1N1: what have we learned?* Clin Microbiol Rev, 2012. **25**(2): p. 223-63.

105. Vijaykrishna, D., et al., *Reassortment of pandemic H1N1/2009 influenza A virus in swine.* Science, 2010. **328**(5985): p. 1529.

106. Molinari, N.A., et al., *The annual impact of seasonal influenza in the US: measuring disease burden and costs.* Vaccine, 2007. **25**(27): p. 5086-96.

107. Lowen, A.C., et al., *Influenza virus transmission is dependent on relative humidity and temperature.* PLoS Pathog, 2007. **3**(10): p. 1470-6.

108. Pica, N. and N.M. Bouvier, *Environmental factors affecting the transmission of respiratory viruses.* Curr Opin Virol, 2012. **2**(1): p. 90-5.

109. Wright PF, N.G., Kawaoka Y., *Orthomyxoviruses: Evolution of Influenza Viruses*, in *Fields Virology*, H.P. Knipe DM, Editor. 2013, LiPpincott, Williams and Wilkins: Philadelphia, PA.

110. Nelson, M.I., et al., *Multiple reassortment events in the evolutionary history of H1N1 influenza A virus since 1918.* PLoS Pathog, 2008. **4**(2): p. e1000012.

111. Viboud, C., et al., *1951 influenza epidemic, England and Wales, Canada, and the United States.* Emerg Infect Dis, 2006. **12**(4): p. 661-8.
112. Holmes, E.C., et al., *Whole-genome analysis of human influenza A virus reveals multiple persistent lineages and reassortment among recent H3N2 viruses.* PLoS Biol, 2005. **3**(9): p. e300.
113. Alexander, D.J., *A review of avian influenza in different bird species.* Vet Microbiol, 2000. **74**(1-2): p. 3-13.
114. Gutierrez, R.A., et al., *A(H5N1) Virus Evolution in South East Asia.* Viruses, 2009. **1**(3): p. 335-61.
115. Millman, A.J., et al., *Detecting Spread of Avian Influenza A(H7N9) Virus Beyond China.* Emerg Infect Dis, 2015. **21**(5): p. 741-9.
116. Liu, D., et al., *Origin and diversity of novel avian influenza A H7N9 viruses causing human infection: phylogenetic, structural, and coalescent analyses.* Lancet, 2013. **381**(9881): p. 1926-32.
117. Compans, R.W. and M.B.A. Oldstone, *Influenza pathogenesis and control. Volume I Volume I*. 2014, Cham: Springer.
118. Tellier, R., *Review of aerosol transmission of influenza A virus.* Emerg Infect Dis, 2006. **12**(11): p. 1657-62.
119. Belser, J.A., et al., *Influenza A virus transmission: contributing factors and clinical implications.* Expert Rev Mol Med, 2010. **12**: p. e39.
120. Reperant, L.A., T. Kuiken, and A.D. Osterhaus, *Adaptive pathways of zoonotic influenza viruses: from exposure to establishment in humans.* Vaccine, 2012. **30**(30): p. 4419-34.
121. Kuiken, T., et al., *Host species barriers to influenza virus infections.* Science, 2006. **312**(5772): p. 394-7.
122. Lin, Y.P., et al., *Avian-to-human transmission of H9N2 subtype influenza A viruses: relationship between H9N2 and H5N1 human isolates.* Proc Natl Acad Sci U S A, 2000. **97**(17): p. 9654-8.
123. Shinya, K., et al., *Avian flu: influenza virus receptors in the human airway.* Nature, 2006. **440**(7083): p. 435-6.

124. Glaser, L., et al., *A single amino acid substitution in 1918 influenza virus hemagglutinin changes receptor binding specificity.* J Virol, 2005. **79**(17): p. 11533-6.

125. Gao, Y., et al., *Identification of amino acids in HA and PB2 critical for the transmission of H5N1 avian influenza viruses in a mammalian host.* PLoS Pathog, 2009. **5**(12): p. e1000709.

126. Yamada, S., et al., *Haemagglutinin mutations responsible for the binding of H5N1 influenza A viruses to human-type receptors.* Nature, 2006. **444**(7117): p. 378-82.

127. Bateman, A.C., et al., *Amino acid 226 in the hemagglutinin of H4N6 influenza virus determines binding affinity for alpha2,6-linked sialic acid and infectivity levels in primary swine and human respiratory epithelial cells.* J Virol, 2008. **82**(16): p. 8204-9.

128. Herfst, S., et al., *Airborne transmission of influenza A/H5N1 virus between ferrets.* Science, 2012. **336**(6088): p. 1534-41.

129. Chen, L.M., et al., *In vitro evolution of H5N1 avian influenza virus toward human-type receptor specificity.* Virology, 2012. **422**(1): p. 105-13.

130. Imai, M., et al., *Experimental adaptation of an influenza H5 HA confers respiratory droplet transmission to a reassortant H5 HA/H1N1 virus in ferrets.* Nature, 2012. **486**(7403): p. 420-8.

131. Yen, H.L., et al., *Hemagglutinin-neuraminidase balance confers respiratory-droplet transmissibility of the pandemic H1N1 influenza virus in ferrets.* Proc Natl Acad Sci U S A, 2011. **108**(34): p. 14264-9.

132. Bouvier, N.M., A.C. Lowen, and P. Palese, *Oseltamivir-resistant influenza A viruses are transmitted efficiently among guinea pigs by direct contact but not by aerosol.* J Virol, 2008. **82**(20): p. 10052-8.

133. Lakdawala, S.S., et al., *Eurasian-origin gene segments contribute to the transmissibility, aerosol release, and morphology of the 2009 pandemic H1N1 influenza virus.* PLoS Pathog, 2011. **7**(12): p. e1002443.

134. Ma, W., et al., *The neuraminidase and matrix genes of the 2009 pandemic influenza H1N1 virus cooperate functionally to facilitate efficient replication and transmissibility in pigs.* J Gen Virol, 2012. **93**(Pt 6): p. 1261-8.

135. Bussey, K.A., et al., *PB2 residue 271 plays a key role in enhanced polymerase activity of influenza A viruses in mammalian host cells.* J Virol, 2010. **84**(9): p. 4395-406.

136. Gabriel, G., et al., *The viral polymerase mediates adaptation of an avian influenza virus to a mammalian host.* Proc Natl Acad Sci U S A, 2005. **102**(51): p. 18590-5.

137. Maines, T.R., et al., *Avian influenza (H5N1) viruses isolated from humans in Asia in 2004 exhibit increased virulence in mammals.* J Virol, 2005. **79**(18): p. 11788-800.

138. Mehle, A. and J.A. Doudna, *Adaptive strategies of the influenza virus polymerase for replication in humans.* Proc Natl Acad Sci U S A, 2009. **106**(50): p. 21312-6.

139. Steel, J., et al., *Transmission of influenza virus in a mammalian host is increased by PB2 amino acids 627K or 627E/701N.* PLoS Pathog, 2009. **5**(1): p. e1000252.

140. Campbell, P.J., et al., *The M segment of the 2009 pandemic influenza virus confers increased neuraminidase activity, filamentous morphology, and efficient contact transmissibility to A/Puerto Rico/8/1934-based reassortant viruses.* J Virol, 2014. **88**(7): p. 3802-14.

141. Campbell, P.J., et al., *Residue 41 of the Eurasian avian-like swine influenza a virus matrix protein modulates virion filament length and efficiency of contact transmission.* J Virol, 2014. **88**(13): p. 7569-77.

142. Chen, R. and E.C. Holmes, *Avian influenza virus exhibits rapid evolutionary dynamics.* Mol Biol Evol, 2006. **23**(12): p. 2336-41.

143. Nelson, M.I. and E.C. Holmes, *The evolution of epidemic influenza.* Nat Rev Genet, 2007. **8**(3): p. 196-205.

144. Taubenberger, J.K. and J.C. Kash, *Influenza virus evolution, host adaptation, and pandemic formation.* Cell Host Microbe, 2010. **7**(6): p. 440-51.

145. Koel, B.F., et al., *Substitutions near the receptor binding site determine major antigenic change during influenza virus evolution.* Science, 2013. **342**(6161): p. 976-9.

146. Perez-Losada, M., et al., *Recombination in viruses: mechanisms, methods of study, and evolutionary consequences.* Infect Genet Evol, 2015. **30**: p. 296-307.

147. Combe, M. and R. Sanjuan, *Variation in RNA virus mutation rates across host cells.* PLoS Pathog, 2014. **10**(1): p. e1003855.
148. Brooke, C.B., *Biological activities of 'noninfectious' influenza A virus particles.* Future Virol, 2014. **9**(1): p. 41-51.
149. Drake, J.W., *Rates of spontaneous mutation among RNA viruses.* Proc Natl Acad Sci U S A, 1993. **90**(9): p. 4171-5.
150. Parvin, J.D., et al., *Measurement of the mutation rates of animal viruses: influenza A virus and poliovirus type 1.* J Virol, 1986. **59**(2): p. 377-83.
151. de Silva, U.C., et al., *A comprehensive analysis of reassortment in influenza A virus.* Biol Open, 2012. **1**(4): p. 385-90.
152. Steel, J. and A.C. Lowen, *Influenza A virus reassortment.* Curr Top Microbiol Immunol, 2014. **385**: p. 377-401.
153. Brooke, C.B., et al., *Most influenza a virions fail to express at least one essential viral protein.* J Virol, 2013. **87**(6): p. 3155-62.
154. Scholtissek, C., et al., *On the origin of the human influenza virus subtypes H2N2 and H3N2.* Virology, 1978. **87**(1): p. 13-20.
155. Scholtissek, C., *Source for influenza pandemics.* Eur J Epidemiol, 1994. **10**(4): p. 455-8.
156. Trifonov, V., et al., *The origin of the recent swine influenza A(H1N1) virus infecting humans.* Euro Surveill, 2009. **14**(17).
157. Smith, G.J., et al., *Origins and evolutionary genomics of the 2009 swine-origin H1N1 influenza A epidemic.* Nature, 2009. **459**(7250): p. 1122-5.
158. Li, K.S., et al., *Genesis of a highly pathogenic and potentially pandemic H5N1 influenza virus in eastern Asia.* Nature, 2004. **430**(6996): p. 209-13.
159. Neverov, A.D., et al., *Intrasubtype reassortments cause adaptive amino acid replacements in H3N2 influenza genes.* PLoS Genet, 2014. **10**(1): p. e1004037.
160. Simonsen, L., et al., *The genesis and spread of reassortment human influenza A/H3N2 viruses conferring adamantane resistance.* Mol Biol Evol, 2007. **24**(8): p. 1811-20.

161. Nishikawa, F. and T. Sugiyama, *Direct isolation of H1N2 recombinant virus from a throat swab of a patient simultaneously infected with H1N1 and H3N2 influenza A viruses.* J Clin Microbiol, 1983. **18**(2): p. 425-7.

162. Xu, X., et al., *Intercontinental circulation of human influenza A(H1N2) reassortant viruses during the 2001-2002 influenza season.* J Infect Dis, 2002. **186**(10): p. 1490-3.

163. Mukherjee, T.R., et al., *Full genomic analysis of an influenza A (H1N2) virus identified during 2009 pandemic in Eastern India: evidence of reassortment event between co-circulating A(H1N1)pdm09 and A/Brisbane/10/2007-like H3N2 strains.* Virol J, 2012. **9**: p. 233.

164. Ritchey, M.B., P. Palese, and J.L. Schulman, *MaPping of the influenza virus genome. III. Identification of genes coding for nucleoprotein, membrane protein, and nonstructural protein.* J Virol, 1976. **20**(1): p. 307-13.

165. Palese, P. and J.L. Schulman, *MaPping of the influenza virus genome: identification of the hemagglutinin and the neuraminidase genes.* Proc Natl Acad Sci U S A, 1976. **73**(6): p. 2142-6.

166. Banbura, M.W., et al., *Reassortants with equine 1 (H7N7) influenza virus hemagglutinin in an avian influenza virus genetic background are pathogenic in chickens.* Virology, 1991. **184**(1): p. 469-71.

167. Jackson, S., et al., *Reassortment between avian H5N1 and human H3N2 influenza viruses in ferrets: a public health risk assessment.* J Virol, 2009. **83**(16): p. 8131-40.

168. Maines, T.R., et al., *Lack of transmission of H5N1 avian-human reassortant influenza viruses in a ferret model.* Proc Natl Acad Sci U S A, 2006. **103**(32): p. 12121-6.

169. Kilbourne, E.D., *Future influenza vaccines and the use of genetic recombinants.* Bull World Health Organ, 1969. **41**(3): p. 643-5.

170. Baez, M., P. Palese, and E.D. Kilbourne, *Gene composition of high-yielding influenza vaccine strains obtained by recombination.* J Infect Dis, 1980. **141**(3): p. 362-5.

171. Fulvini, A.A., et al., *Gene constellation of influenza A virus reassortants with high growth phenotype prepared as seed candidates for vaccine production.* PLoS One, 2011. **6**(6): p. e20823.

172. Lubeck, M.D., P. Palese, and J.L. Schulman, *Nonrandom association of parental genes in influenza A virus recombinants.* Virology, 1979. **95**(1): p. 269-74.

173. Scholtissek C, R.R., Orlich M, Harms E, and W. Rohde, *Correlation of Pathogenicity and Gene Constellation of an Influenza A Virus (Fowl Plague).* Virology, 1977. **81**: p. 74-80.

174. Marsh, G.A., R. Hatami, and P. Palese, *Specific residues of the influenza A virus hemagglutinin viral RNA are important for efficient packaging into budding virions.* J Virol, 2007. **81**(18): p. 9727-36.

175. Essere, B., et al., *Critical role of segment-specific packaging signals in genetic reassortment of influenza A viruses.* Proc Natl Acad Sci U S A, 2013. **110**(40): p. E3840-8.

176. Goto, H., et al., *The genome-packaging signal of the influenza A virus genome comprises a genome incorporation signal and a genome-bundling signal.* J Virol, 2013. **87**(21): p. 11316-22.

177. Fujii, K., et al., *Importance of both the coding and the segment-specific noncoding regions of the influenza A virus NS segment for its efficient incorporation into virions.* J Virol, 2005. **79**(6): p. 3766-74.

178. Li, C., et al., *Reassortment between avian H5N1 and human H3N2 influenza viruses creates hybrid viruses with substantial virulence.* Proc Natl Acad Sci U S A, 2010. **107**(10): p. 4687-92.

179. Rudneva, I.A., et al., *Influenza A virus reassortants with surface glycoprotein genes of the avian parent viruses: effects of HA and NA gene combinations on virus aggregation.* Arch Virol, 1993. **133**(3-4): p. 437-50.

180. Tao, H., J. Steel, and A.C. Lowen, *Intrahost dynamics of influenza virus reassortment.* J Virol, 2014. **88**(13): p. 7485-92.

181. Tao, H., et al., *Influenza A Virus Coinfection through Transmission Can SuPport High Levels of Reassortment.* J Virol, 2015. **89**(16): p. 8453-61.